# Development of an *in vitro* thrombosis model to assess endothelial regulation of thrombus formation.

**R Riley**

**PhD 2022**

# Development of an *in vitro* thrombosis model to assess endothelial regulation of thrombus formation.

**Ryan Riley**

**A thesis submitted in partial fulfilment of the requirements of Manchester Metropolitan University for the degree of Doctor of Philosophy**

**Department of Life Sciences**

**Manchester Metropolitan University**

**2022**

# COVID-19 IMPACT STATEMENT

The progress of this PhD project was significantly affected by the covid-19 pandemic, upon the announcement of the national lockdown in March of 2020 my university closed the campus, including research labs, to all staff and students. With the easing of the restrictions in August of 2020 my university began to gradual re-open and welcome back staff and students. Several restrictions were put in place to mitigate any risks to people attending the university, these extended to the research labs. These restrictions included the labs operating at a 50% occupancy and students being advised to attend up to three days a week. Furthermore, blood work was not allowed until October of 2020, which significantly affected the progression of my project. When a second lockdown was announced in January of 2021, blood work was once again halted for up to 12 weeks, impeding my experiments and my ability to generate data for my thesis. This all had a negative impact on the project and restricted the number of experiments that could be performed before the end of the study.

## Acknowledgements

I would like to thank my supervisory team for all the help, support and guidance they have provided me with during the course of this project. I would like to especially thank Dr Stephen White for the way he responded to the pandemic and lockdown that followed. Dr White ensured regular virtual meetings were still held which helped to maintain a sense of normality in the uncertain times.

A massive thank you to Rhys and Rob who have made the last four years an enjoyable and rewarding experience. I thoroughly enjoyed our talks in the labs and winding each other up (remember the rule of two!). One of the saddest parts of finishing my PhD and leaving MMU is no longer being able to work with such amazing colleagues and more importantly friends.

I would also like to thank the amazing technical team at MMU, In particular Dr Liam Hanson and Dr Stuart Fielding who were always happy to offer a helping hand and in my opinion often went above and beyond when providing support and guidance. In particular thank you for all the times I desperately couldn't find essential reagents only for one of you to reveal a secret stash, or that they had been moved to a different cupboard!

A special thank you to my wife Samantha who has had the patience of a saint these last four years. Thank you for always being there for me and supporting me and in particular for all the times you offered to listen to me practice presentations, you must be sick of hearing about platelets! Finally I would like to dedicate this thesis to my son Sebastian, you are my whole world and I love you.

## Abstract

Arterial thrombosis culminating in myocardial infarction and stroke remains one of the leading causes of death and disability in the western world. Both *in vitro* and *in vivo* thrombosis models have been beneficial tools in furthering our understanding of arterial thrombosis. However, these models are not without limitations, as a result there is not currently a gold standard thrombosis model. Endothelial cells play a key role in regulating platelet activation and thrombus formation, through the activity of endothelial derived platelet inhibitors such as nitric oxide, prostacyclin and CD39. Despite the clear role of endothelial cells in thrombus formation many *in vitro* thrombosis models lack endothelial cells. These models therefore do not consider the role of the endothelium and endothelial dysfunction in thrombus formation which in turn, inhibits their ability to accurately model atherothrombosis.

The aim of this project was to develop a model which incorporates endothelial cells and allows for the assessment of endothelial cell regulation of thrombus formation. Utilising a basic microfluidic model set up, it was successfully demonstrated that incubation of endothelial derived platelet mediators in human whole blood had significant effect on thrombus formation on exposed collagen.

Next, endothelial cells were incorporated into the model, the endothelialised model consisted of two separate compartments one lined with endothelial cells, upstream of a second compartment coated with collagen. This novel model setup allowed for the assessment of the effects of endothelial derived mediators on thrombus formation. Incorporation of endothelial cells into the model significantly reduced thrombus formation, thus supporting the hypothesis that endothelial cells should be incorporated into thrombosis models.

Accurate replication of the proinflammatory atherothrombotic vessel environment observed in cardiovascular disease was also a key component that needed to be incorporated into the model. TNF-alpha stimulation resulted in an increase in cell adhesion molecules, in addition to a decrease in endothelial nitric oxide synthase phosphorylation. Furthermore, TNF-alpha stimulation of endothelial cells incorporated into the model lead to the abolishment of the previous anti-thrombotic

effects observed with endothelial cell incorporation. This confirmed the sensitivity of the model to changes in the endothelial cell compartment, in addition to showing TNF-alpha stimulation could achieve a prothrombotic environment.

Optimisation of the model was important to enable a higher throughput and to allow multiple experimental conditions to be modelled simultaneously. The utilisation of a six-syringe pump enabled this optimisation step and enabled the assessment of anti-platelet drug efficacy in the presence of healthy and activated endothelial cells. Further optimisation compared differences between endothelial cells from different vessel beds and demonstrated a significant difference in the levels of platelet mediators in venous and arterial endothelial cells.

Finally, the model was used to investigate the ACE2/ANG1-7/MAS signalling axis as a potentially novel anti-thrombotic pathway. The unique dual channel setup, with an endothelial cell channel upstream of a collagen channel, enabled the analysis of the effects of ACE2/ANG1-7/MAS stimulation on endothelial cell regulation of thrombus formation. No significant effects on thrombus formation were observed following ACE2/ANG1-7/MAS stimulation; further studies are required to evaluate the anti-thrombotic effects of this pathway.

In conclusion, an *in vitro* thrombosis model was successfully developed during this project, which included the incorporation of endothelial cells and allowed for the assessment of endothelial cell regulation of platelet activity. It was successfully demonstrated that the model was sensitive to changes in the endothelial compartment both in terms of response to cytokine stimulation and the incorporation of endothelial cells from different vessel beds. In addition, the model's ability to assess anti-platelet drug efficacy, in the presence of a healthy or activated endothelium was also successfully demonstrated.

# Contents

# List of figures

## List of tables

## Presentations

**Poster presented at the British Society for Cardiovascular Research Conference, Manchester, UK, 2018**

**Title:** Development of an *in vitro* Thrombosis Model to Assess Endothelial Regulation of Thrombus Formation

**Poster presented at the Physiology Society experimental models meeting, University of Exeter, UK, 2018**

**Title:** A Novel Endothelialized *in vitro* Model of Human Arterial Thrombosis

**Poster presented at the Platelet Society early career researcher meeting, Manchester Metropolitan University, UK, 2018**

**Title:** Assessment of the Effect of Endothelial Dysfunction on Thrombus Formation Using a Novel *in vitro* Thrombosis Model

**Poster presented at the Platelet Society Conference, University of Cambridge, UK, 2019**

**Title:** Development of an *in vitro* Thrombosis Model to Assess Endothelial Contributions to Thrombus Formation and Antithrombotic Efficacy

**Oral presentation at the Northern Vascular Biology Forum, University of Bradford, UK, 2019**

**Title:** Endothelial Cell Contribution to Thrombus Formation and Antiplatelet Drug Efficacy

**Award:** Second place oral presentation

**Oral presentation at the Platelet Society early career researcher meeting, virtual, 2020**

**Title:** Assessment of Antiplatelet Drug Efficacy Using a Novel Endothelialised Thrombosis Model

## Abbreviations

5-HT – 5-hydroxytryptamine

AA – Arachidonic acid

ACD - Acid citrate dextrose

ACE – Angiotensin converting enzyme

ACE2 – Angiotensin converting enzyme 2

ADP - Adenosine diphosphate

AMP – Adenosine monophosphate

ANG – Angiotensin

ANOVA - Analysis of variance

AT1R – Angiotensin II type 1 receptor

AT2R – Angiotensin II type 2 receptor

ATP - Adenosine triphosphate

BSA - Bovine serum albumin

cAMP – Cyclic adenosine monophosphate

COX - Cyclooxygenase

DAG - 1,2-diacyl-glycerol

DAPT – Dual anti-platelet therapy

$DIOC_6$ - 3,3'-dihexyloxacarbocyanine iodide

DMSO - Dimethyl sulfoxide

DNA – Deoxyribose nucleic acid

DTS – Dense tubular system

ECM -Extracellular matrix

eNOS – Endothelial nitric oxide synthase

EPCR – Endothelial cell protein C receptor

ET - Endothelin

FBS - Fetal bovine serum

FcRγ - Fc receptor γ chain

gDNA – Genomic deoxyribose nucleic acid

GP - glycoprotein

GPCR - G protein coupled receptor

GPVI - Glycoprotein VI

HCAECs – Human coronary artery endothelial cells

HIF-2alpha – Hypoxia-inducible factor 2 alpha

HUVECs – Human umbilical vein endothelial cells

ICAM-1 – Intracellular adhesion molecule 1

iNOS – Inducible nitric oxide synthase

ITAM - Hemi-immunoreceptor tyrosine-based activation motif

IP – Prostacyclin receptor

$IP_3$ - Inositol-1,4,5-trisphosphate

LAT - Linker of Activated T cells

LTA – Light transmission aggregation

LDL – Low-density lipoproteins

L-NNA – Nitroarginine

M – Molar

mg – Milligrams

MMU – Manchester Metropolitan University

MrgD – Mas-related-G-protein-coupled receptor D

NaCl – Sodium chloride

nNOS – Neuronal nitric oxide synthase

NO – Nitric oxide

OCS – Open canalicular system

PAF – Platelet-activating factor

PAH – Pulmonary arterial hypertension

PAI-1 – Plasminogen activator inhibitor-1

PAR – Protease activated receptors

PBA – Plate-based aggregation

PBS - Phosphate buffered saline

PCP – Prolyl carboxypeptidase

PCR – Polymerase chain reaction

PDE – Phosphodiesterase

PECAM-1 - Platelet endothelial cell adhesion molecule-1

PEP – Prolyl oligopeptidase

$PGE_2$ – Prostaglandin $E_2$

$PGI_2$ - Prostacyclin

PI3K - Phosphoinositide 3 -kinase

$PIP_2$ - Phosphoinositide-4,5-bisphosphate

$PIP_3$- Phosphoinositide-3,4,5-trisphosphate PKA- Protein kinase A

PKC - Protein kinase C

PKG – Protein kinase G

PLCγ2 - Phospholipase C gamma 2

PRP - Platelet rich plasma

RBCs – Red blood cells

RIPA buffer - Radioimmunoprecipitation assay buffer

RNA – Ribonucleic acid

SDS – Sodium dodecyl sulphate

SDS-PAGE – Sodium dodecyl sulphate polyacrylamide gel electrophoresis

SEM- Standard error of the mean

SFK – Src family kinase

SH2 - Src homology 2

SH3 - Src homology Syk – spleen tyrosine kinase

SNP – Sodium nitroprusside

STEMI – ST-segment elevation myocardial infarction

T2D – Type 2 diabetes

TBST– Tris buffered saline with tween

TF – Tissue factor

TFPI – Tissue factor pathway inhibtor

TGF-β – Transforming growth factor beta

THOP – Thimet oligopeptidase

TNF-alpha – Tumour necrosis factor alpha

tPA – Tissue plasminogen activator

TXA2 – Thromboxane A2

uPA – Urokinase plasminogen activator

VCAM-1 – Vascular cell adhesion molecule 1

VWF – von Willebrand Factor

# 1. General Introduction

## 1.1 Cardiovascular disease

### 1.1.1 Arterial thrombosis

Arterial thrombosis is the leading cause of myocardial infarction and is accountable as the cause for around 80% of stroke cases. The most common trigger for arterial thrombosis is atherosclerotic plaque rupture resulting in the formation of a platelet rich thrombi (Mackman, 2008). Haemostasis is a process which perseveres the integrity of the vessel wall in addition to preventing excessive blood loss, platelets have a key role in this process, upon vascular injury platelets will adhere and aggregate at the site of damage and form a haemostatic plug (Mackman, 2008; Savage *et al*., 1998). Thrombosis is the pathological form of haemostasis and occurs when various haemostatic pathways involved in haemostasis become strongly activated as a result of atherosclerotic plaque disruption. There are two forms of plaque disruption: plaque rupture and plaque erosion, plaque rupture accounts for two thirds of myocardial infarctions and plaque erosion accounts for the remaining third (White *et al*., 2016).

Atherosclerosis begins with the accumulation of cholesterol rich low-density lipoproteins (LDL) in the tunica intima of the endothelium, this LDL can then become oxidised (Rafieian-Kopaei *et al*., 2014; Tavafi *et al*., 2013). This accumulation of oxidised LDL deposits leads to the activation of endothelial cells, these endothelial cells then begin to express leukocyte adhesion molecules such as intracellular adhesion molecule 1 (ICAM-1) and vascular cell adhesion molecule 1 (VCAM-1) (Rafieian-Kopaei *et al*., 2014). The expression of these adhesion molecules results in the recruitment of immune cells, such as monocytes, to the site of the developing plaque. These monocytes then differentiate into macrophages which can upregulate pattern-recognition receptors that facilitate the uptake of lipoproteins and result in the formation of foam cells. These foam cells promote migration of smooth muscle cells from the tunica media to the tunica intima in addition to promoting smooth muscle cell proliferation (Rafieian-Kopaei *et al*., 2014). The activation of toll like

receptors leads to the release of proinflammatory cytokines, in addition to this, T-lymphocytes, found within the developing plaque, produce and release proinflammatory cytokines thus promoting a local pro-inflammatory environment while also encouraging the growth of the plaque (Nayer *et al*., 2013). The development of the plaque can lead to a restriction in coronary blood flow, reducing the amount of oxygen-rich blood that reaches the heart resulting in a condition known as angina pectoris. However, as the plaque begins to grow the pressure will also begin to increase within the plaque making it more susceptible to rupturing (Rafieian-Kopaei *et al*., 2014).

### 1.1.2 Plaque rupture and plaque erosion

One of the distinguishing features of an atherosclerotic plaque is the formation of a lipid rich intima known as a necrotic core. The development of a lipid rich necrotic core begins with the formation of small pools of lipids under the foam cell layer (Bentzon *et al*., 2014; Chen *et al*., 2016). These lipid pools mature into necrotic cores as macrophages migrate to this layer causing irreversible disruption of the intima layer. Apoptosis of foam cells in addition to smooth muscle cells helps drive the development of the necrotic core. The connective tissue of the plaque also changes with the development of the plaque, shifting from the loose fibrocellular tissue of the arterial intima to a collagen rich fibrous tissue. Rupture of the atherosclerotic lesion is the most common cause of thrombosis, this occurs when the structural integrity of the thin fibrous cap of the plaque is lost, leading to the exposure of the pro-thrombotic contents into the bloodstream leading to the development of a thrombus.

The use of intraluminal imaging techniques such as optical coherence tomography has helped to demonstrate that plaque erosion is a key mechanism contributing to acute coronary syndrome (Vergallo *et al*., 2019). Recent studies have revealed that around one third of cases of ST-segment elevation myocardial infarction (STEMI) are caused by plaque erosion (White *et al*., 2016). In addition, plaque erosion has recently been identified as the predominant mechanism in non-ST-segment elevation myocardial infarction (Fahed., 2021). A plaque prior to erosion is quite distinct to those associated with rupture, with a thick fibrous cap being present in plaque

erosions in contrast to the thin fibrous caps found on plaques susceptible to rupture. The thick fibrous plaques observed in plaque erosion are often smooth muscle cell and extracellular matrix protein rich with small lipid cores (White *et al*., 2016). Alterations in flow patterns on endothelial cells at the site of the plaque has been suggested as a potential contributor to plaque erosion. The flow at the site of a developing plaque shifts from laminar flow to what has been termed disturbed flow, which can drive endothelial cells apoptosis (Thondapu *et al*., 2021; Tricot *et al*., 2000). This leads to the loss of endothelial cells localised to the growing plaque and leads to exposure of the pro-thrombotic contents of the plaque, resulting in the formation of a thrombus (White *et al*., 2016). A further distinction that can be made between plaque rupture and plaque erosion is the associated risk factors and at risk groups. Plaque erosion has been shown to be prevalent in premenopausal women and smokers and showed a lower association with key plaque rupture risk factors such as hypertension and diabetes (Orosz *et al*., 2007; White *et al*., 2016). Regardless of whether it is plaque rupture or erosion, the damage caused to the vascular wall exposes extracellular matrix (ECM) proteins, providing a thrombogenic surface facilitating the adhesion and activation of platelets and the subsequent thrombus generation.

### 1.1.3 Dual anti-platelet therapy

Dual anti-platelet therapy (DAPT) is currently used in the prevention of further ischemic events after experiencing acute coronary syndrome. DAPT utilises the combination of aspirin and a $P2Y_{12}$ inhibitor to reduce the risk of future ischemic events by inhibiting platelet activity. Aspirin exerts anti-platelet effects by inhibiting the cyclooxygenase (COX) enzymes, these enzymes are responsible for the production of the potent platelet activator thromboxane A2 (TXA2). Furthermore, once platelets become activated, they release TXA2, which can then further activate circulating platelets close to the site of injury, recruiting them to the growing thrombus (Smyth, 2010). Therefore, the inhibition of the COX enzymes by aspirin prevents the production of TXA2 which in turn inhibits the formation of large platelet aggregates (Ajjan *et al*., 2009). Clopidogrel is a $P2Y_{12}$ receptor inhibitor, $P2Y_{12}$ is the receptor for the potent platelet activator ADP. A key component of platelet

activation is granule secretion, which includes the release of ADP found in platelet dense granules. This causes a positive feedback loop, through which activated platelets release ADP, which can bind to $P2Y_{12}$ receptors on neighbouring platelets, causing them to also become activated and to release more ADP. This results in the secondary amplification of platelet signalling (Estevez and Du, 2017; Sangkuhl *et al*., 2011). Both of $TXA_2$ and ADP release are important in the secondary signalling amplification observed in the formation of a stable thrombus and therefore inhibition of both would lead to a decrease in thrombus formation. A key application of an *in vitro* thrombosis model may be the assessment of anti-platelet drug efficacy, such as DAPT, in addition to the assessment of novel anti-thrombotic therapies.

## 1.2 Platelets

### 1.2.1 Platelet structure

Platelets are anucleate secretory cells, with a diameter of approximately 2-4μm. A normal platelet count in humans ranges between 150-400 x $10^9$ (Martin *et al*., 1982). The lifespan of a platelet in circulation is approximately seven to ten days (Harker *et al*., 2000). The platelet plasma membrane is a standard lipid bilayer containing a number of glycoproteins (GPs) that act as receptors for soluble agonists (Fritsma, 2015). These GPs play an essential role in the initial adhesion of platelets to the ECM exposed from the damaged endothelium in addition to mediating platelet activation and aggregation through various signalling pathways. Platelets contain a complex intracellular network of membrane bound channels also known as the open canalicular system (OCS) (Figure 1.1) (Fritsma, 2015). The OCS allows additional storage of key haemostatic proteins while also facilitating the transport of substances in and out of the platelet (Selvadurai and Hamilton, 2018). Platelets also contain a second membrane system known as the dense tubular system (DTS) (Figure 1.1). The DTS is responsible for the storage and release of calcium in addition to storing enzymes important in the production of thromboxane A2 (TXA2), an eicosanoid that contributes to platelet activation (Cramer *et al*., 1997; Fritsma, 2015). Platelet mitochondria are responsible for the bulk of energy production in platelets (Whiteheart, 2017). In addition, Electron microscopy studies revealed that platelets

also contain glycogen granules which are thought to act as reservoirs for platelet energy production (Figure 1.1) (Fritsma, 2015).

Platelets contain three types of granules; α-granules, dense granules and lysosomes (Figure 1.1). Lysosomes account for a small amount of the 60-80 granules typically found in platelets, their function is to digest vessel wall matrix components during aggregation (Fritsma, 2015). Alpha granules contain proteins that mediate platelet adhesion and aggregation (von Willebrand factor, fibronectin and fibrinogen), coagulation factors (factor V and factor VIII) and transmembrane adhesion molecules (P-selectin and platelet endothelial cell adhesion molecule 1) and growth factors (platelet derived growth factors and TGF-β) (Blair and Flaumenhaft, 2009; Harrison and Cramer, 1993). Dense granules contain several low molecular weight proteins involved in platelet activation such as serotonin, 5-hydroxytryptamine (5-HT), calcium, adenosine triphosphate (ATP) and adenosine diphosphate (ADP) (McNicol and Israels, 1999). Following platelet activation these granules are released resulting in an amplification of platelet signalling which encourages aggregation.

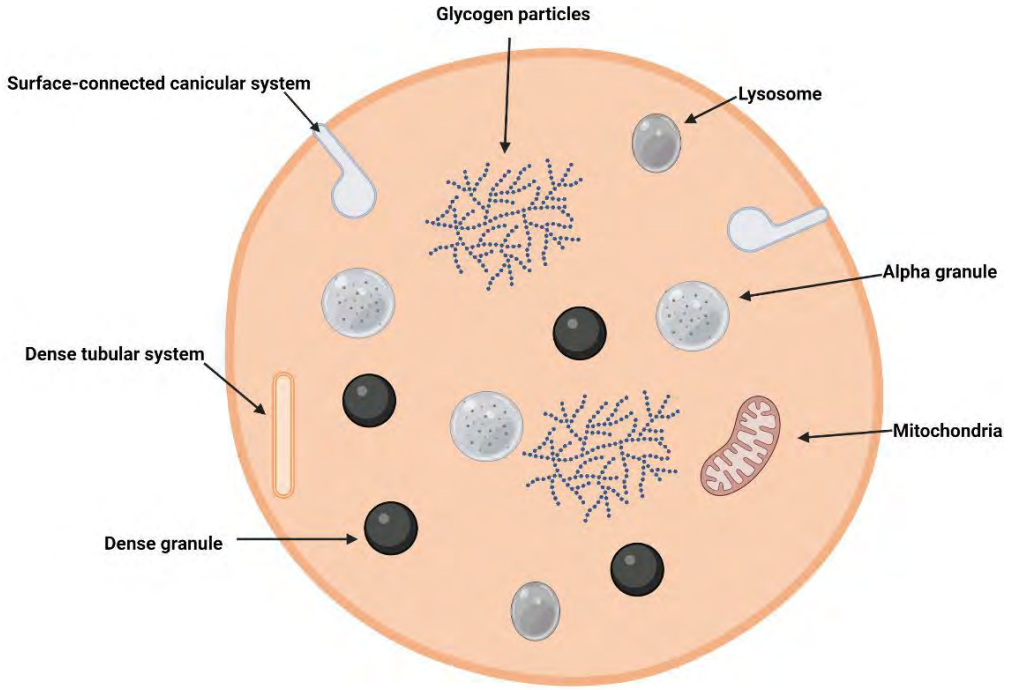


***Figure 1. 1 Diagram portraying the structure of a circulating platelet.***

Platelets are anucleate secretory cells, with a diameter of approximately 2-4µm. Organelles contained in the cell cytoplasm include mitochondria, alpha granules, dense granules and lysosomes. Invaginations are found on the plasma membrane of the platelet and form a complex membrane network known as the surface-connected (open) canicular system (OCS). Granule secretion is thought to be mediated by granule fusion with the plasma membrane or the OCS. Platelets also contain a second membrane system known as the dense tubular system which is responsible for the storage and release of calcium. Figure created using Biorender; adapted from *White JG 1979*.

### 1.2.2 Platelet production

Platelets are formed from one of the largest (50-100μm) cells found in the bone marrow, megakaryocytes (Machlus and Italiano, 2013). Megakaryocytes develop from haematopoietic stem cells, a process regulated by thrombopoietin (also known as megakaryocyte growth and development factor) (Italiano and Shivdasani, 2003; Machlus and Italiano, 2013). Thrombopoietin is produced by the liver and released into the bloodstream, circulating platelets bind to thrombopoietin, preventing it from entering the bone marrow and clearing it from the circulation (Machlus and Italiano, 2013). When there is a decrease in circulating platelet number, the levels of thrombopoietin reaching the bone marrow increases the number of progenitor cells that will commit to megakaryocyte development (Italiano and Shivdasani, 2003). It has been hypothesised that additional, yet to be identified, regulators of platelet development and production must exist as it has previously been demonstrated that mice lacking thrombopoietin can still successfully produce platelets (Bunting *et al*., 1997). In order to produce and release platelets, megakaryocytes undergo endomitosis and become polyploidy, the cytoplasm of the megakaryocytes is then packaged into a series of long branching processes known as proplatelets (Machlus and Italiano, 2013). These proplatelets branches extend into the sinusoidal blood vessels of the bone marrow. The typical megakaryocytes extends between 10 and 20 proplatelets, these proplatelets elongate overtime becoming thin with multiple branches (Thon *et al*., 2010). As the platelets mature organelle and granule contents is transported from the megakaryocyte cell body to the platelets forming at the tips of the proplatelets (Richardson *et al*., 2005). Finally, platelets are shed into the bloodstream from the proplatelet protrusions (Italiano and Shivdasani, 2003; Machlus and Italiano, 2013).

### 1.2.3 Platelets and haemostasis

Platelets circulate the bloodstream and play a key role in haemostasis, achieving cessation of bleeding in a damaged vessel. Under normal circumstances, platelets circulate the blood in a quiescent state and do not adhere to the endothelium lining the vessel wall (Holinstat, 2017). There are two distinct mechanisms by which platelets prevent excessive blood loss following vascular injury, the first mechanism can be categorised into three stages: adhesion, activation and aggregation (Holinstat, 2017). Upon vascular injury the anti-thrombotic endothelium lining is lost thus compromising vessel integrity and exposing sub-ECM proteins such as collagen (Chistiakov *et al*., 2013; Katsuda and Kaji, 2003). This enables the binding of von Willebrand factor (VWF) to the exposed collagen the VWF fibres are then stretched by the vessel shear stress (Peyvandi *et al*., 2011). Circulating platelets begin to adhere to the exposed collagen directly, in addition to binding to VWF fibres, this binding is facilitated by glycoprotein receptors on the surface of platelets (Holinstat, 2017; Peyvandi *et al*., 2011). Platelet adhesion leads to shape change and platelet activation, initiating various responses including granule secretion, calcium mobilisation and activation of platelet integrins (Holinstat, 2017). The bound activated platelets begin to form a thrombus and start to attract platelets from the circulation causing these to adhere to the developing thrombus. These platelets are weakly activated and require positive feedback signalling achieved by the release of platelet activating molecules from granule secretion (Hou, 2015). These granules contain potent platelet activators leading to signalling amplification and the recruitment of additional platelets from the circulation to the thrombus. The activation of platelet integrins allows interactions between integrins $\alpha_{IIb}\beta_3$ and fibrinogen, which is essential for achieving platelet aggregation (Bye *et al*., 2016; Holinstat, 2017). Fibrinogen is able to bind $\alpha_{IIb}\beta_3$ on two platelets thus allowing the formation of cross-links between adjacent activated platelets and promoting platelet aggregation at the site of injury (Bennett, 2006; Bye *et al*., 2016).

The second mechanism by which platelets inhibit blood loss is via the activation of the coagulation cascade (Hoffman, 2000). Upon platelet activation phosphatidylserine, a component of the platelet membrane, flips from the inside of

the cell and is exposed on the outside of the cell (Gale, 2011; Palta *et al*., 2014). This exposure of phosphatidylserine provides a charged phospholipid surface for coagulation enzymes, this leads to an increase in thrombin generation. In addition to being a potent platelet activator, thrombin also plays a key role in the stabilisation of the thrombus by converting fibrinogen into fibrin. Fibrin then forms a mesh over the platelets resulting in a stable platelet plug (Palta *et al*., 2014).

## 1.3 Platelet receptors and agonists

### 1.3.1 Cell adhesion receptors

There are two types of receptors that are key to mediating platelets response to the vessel environment: cell adhesion receptors and soluble agonist receptors. VWF becomes unravelled by the arterial shear rate of the vessel, this allows VWF to bind to exposed collagen at the site of vascular injury and mediate indirect platelet interaction with collagen by binding GPIb-V-IX (Peyvandi *et al*., 2011). This allows platelets to begin to tether to the site of injury and also reduces platelet velocity, enabling direct interactions between collagen and collagen specific receptors on the surface of the platelets (Sangkuhl *et al*., 2011). The first collagen receptor to be identified in platelets was integrin $\alpha_2\beta_1$. The physiological importance of integrin $\alpha_2\beta_1$, in regard to platelet activity in response to collagen was highlighted in 1986. Nieuwenhuis *et al* found that in a patient with only 20% of the normal amount of integrin $\alpha_2\beta_1$ their response to collagen was ablated. However, despite integrin $\alpha_2\beta_1$ facilitating platelet adhesion to collagen, this interaction does not stimulate sufficient tyrosine kinase-dependent signalling to enable collagen induced platelet activation (Hers *et al*., 2000). This led to researchers proposing the existence of a secondary collagen receptor that works in combination with integrin $\alpha_2\beta_1$ achieved collagen platelet activation (Santoro *et al*., 1991). In the proposed model it was suggested that integrin $\alpha_2\beta_1$ would stabilise the interaction with collagen and the second receptor would activate tyrosine kinase signalling pathways (Santoro *et al*., 1991). Glycoprotein (GP) VI was identified as the second receptor; GPVI was first identified using gel electrophoresis by *Phillips and Agin* in 1977. Later it was demonstrated that the platelets of patients deficient in GPVI did not aggregate in response to collagen

despite aggregating in response to other agonists (Moroi *et al*., 1989). These findings confirmed GPVI as the predominant mediator of collagen-induced platelet activation and the downstream signalling pathways has since been well characterized (section 1.4.3).

### 1.3.2 Soluble platelet agonists

Following initial cell adhesion receptor mediated binding to the site of injury, outside-in signalling stimulates platelet activation and the release of soluble platelet agonists, which are key to the formation of a stable thrombus (Estevez and Du, 2017; Li *et al*., 2010). Three of these key platelet agonists are thrombin, TXA2 and ADP. All three are potent platelet activators, which stimulate G-protein coupled receptors (GPCRs) on the platelet surface to reinforce platelet activation and amplify the thrombotic response through the recruitment of additional platelets from the circulation, facilitating the development of a platelet rich aggregate (Estevez and Du, 2017; Li *et al*., 2010). There are also a number of secondary platelet agonists, which are weaker but play an important role in priming the platelets, these weak agonists include: thrombospondin, adrenaline and 5-HT (Ardlie *et al*., 1985; Cerrito *et al*., 1993; Tulasne *et al*., 2001).

### 1.3.3 PAR receptors and thrombin

Thrombin is a serine protease produced by the coagulation cascade at the site of vessel wall injury. Prothrombin (coagulation factor II) is cleaved by factor Xa to yield thrombin, thrombin then converts fibrinogen into fibrin which are required in order to form a stable clot (Palta *et al*., 2014). In addition to its role in the coagulation cascade thrombin is also a potent platelet activator. Thrombin mediated platelet activation is initiated through protease activated receptors (PARs) (De Candia, 2012). PARs are a family of GPCRs, four receptor sub-types have been described PAR1, PAR3 and PAR4 all of which are cleaved and activated by thrombin (De Candia, 2012; Kahn *et al*., 1998). In contrast PAR2 is not activated by thrombin and has been shown to be activated by trypsin and trypsin-like proteases (Heuberger and Schuepbach, 2019). Receptor expression variability exists between species, PAR1 and PAR4 are present in human platelets whereas rat and mouse platelets express PAR3 and PAR4 (Kahn *et*

*al*., 1998). PAR1 is a high affinity receptor which can be activated by low concentrations of thrombin. The activation of PAR1 is a two-step process, first thrombin cleaves the N-terminal exodomain at a specific site on the extracellular loop of the receptor, between residues Arg 41 and Ser 42 (De Candia, 2012). This cleavage unmasks a new N-terminus sequence which acts as a tethered ligand, intramolecular rearrangement enables receptor moieties to interact, stimulating receptor activation and subsequent intracellular signalling pathways in platelets (De Candia, 2012; Franchi *et al*., 2015; Coughlin, 2005).

### 1.3.4 $P2Y_{12}$ receptors and ADP

ADP was identified as the first low molecular weight platelet agonist, initial experiments demonstrated that ADP was derived from red blood cells (RBCs) and induced platelet adhesion on glass (Hellem, 1960; Puri and Colman, 1997). Later Born was able to demonstrate ADP induced platelet aggregation *in vitro,* these findings in addition to the large amounts of ADP present in platelets suggested that ADP held a key role in both physiological haemostasis and pathological thrombosis (Born, 1962; Maffrand *et al*., 1988). ADP is stored in platelet dense granules and is released upon activation and is responsible for the secondary wave of platelet signalling. In 2001 it was identified that members of the P2 receptor family were responsible for mediating ADP platelet activation (Gachet, 2001; Hollopeter *et al*., 2001). There are two classes of P2 receptors; P2X receptors which are ligand gated ion channels and P2Y receptors which are GPCRs. ADP platelet activation is mediated via the $P2Y_1$ and $P2Y_{12}$ receptors on the surface of platelets (Kunapuli *et al*., 2003). $P2Y_1$ receptor expression on platelets is low (150 binding sites per platelet) compared to other receptors for example the thrombin receptor PAR1 has 1000-2000 binding sites per platelet (Gachet, 2006). The receptor is coupled to the $G_q$ class of G-proteins, $P2Y_1$ activation initiates inositol phosphate formation via phospholipase C activation leading to intracellular calcium mobilisation and platelet shape change (Jin *et al*., 1998; Kim and Kunapuli, 2011). Studies using murine models with $P2Y_1$ deficient platelets demonstrated that these platelets failed to undergo shape change and did not aggregate in response to ADP, although partial aggregation could be achieved at high ADP concentrations (Fabre *et al*., 1999). The $P2Y_{12}$ receptor has very limited

tissue distribution and is selectively expressed in platelets and brain tissue (Hollopeter *et al*., 2001). $P2Y_{12}$ is coupled to the $G_i$ class of G-proteins, activation of the $P2Y_{12}$ receptor by ADP leads to signalling amplification and stabilisation of the aggregation response (Jin *et al*., 1998).

### 1.3.5 Thromboxane $A_2$

Prostaglandins are produced by the metabolism of arachidonic acid (AA) a reaction catalysed by the cyclooxygenase (COX) enzymes (Rouzer and Marnett, 2009). TXA2 is the predominant prostaglandin produced by platelets, phospholipases such as phospholipase $A_2$ and diacylglycerol lipase mobilise AA from the platelet membrane (Paul *et al*., 1999; Smyth *et al*., 2001). AA is then converted to prostaglandin $H_2$ by COX enzymes, which is then in turn converted into TXA2 by thromboxane synthase (Paul *et al*., 1999; Smyth *et al*., 2001). The COX enzymes are expressed in two isoforms, COX-1 and COX-2, with COX-1 being highly expressed in platelets (Rouzer and Marnett, 2009). TXA2 is not stored in platelets nor is it produced without stimulation, instead TXA2 is rapidly produced and released by platelets upon activation. TXA2 is released from platelets by diffusing across the plasma membrane, allowing TXA2 to interact with receptors on nearby platelets, in addition to stimulating thromboxane receptors on the surface of the platelet it was released from (Smyth, 2010a). TXA2 acts on a GPCRs found on the surface of platelets, known as the TP receptor. Two isoforms of the TP receptor exist, termed α and β, most tissues express both isoforms, however TPα is the isoform predominantly expressed by platelets (Paul *et al*., 1999; Smyth, 2010a). The TP receptor can be coupled with multiple G proteins, with $G_q$ and $G_{12/13}$ being identified as two G proteins important for mediating TP receptor function (Offermanns *et al*., 1994). Activation of the TP receptor on platelets stimulates numerous intracellular responses including an increase in intracellular calcium, protein kinase C activation, an increased turnover of inositol phosphate and G protein signalling with downstream effectors described later (Paul *et al*., 1999; Smyth, 2010a).

## 1.4 Platelet signalling pathways

### 1.4.1 GPIb signalling

The high shear rates present in arteries and small arterioles means platelet adhesion to collagen alone is not enough to form a stable thrombus. In these high shear vessels VWF is essential for facilitating initial collagen-platelet binding via the platelet GPIb-V-IX complex (Clemetson and Clemetson, 2007; Kauskot and Hoylaerts, 2012). This interaction leads to platelet signalling, granule secretion and upregulation of integrin $\alpha_{IIb}\beta_3$ affinity, a platelet receptor that facilitates thrombus formation by binding VWF and fibrinogen (Clemetson and Clemetson, 2007). VWF binding has a fast off rate and as a result other platelet-collagen receptors, such as integrin $\alpha_2\beta_1$ and GPVI, are essential for the formation of a stable platelet plug. The platelet receptor GPIb should not be thought solely as a collagen receptor, the extracellular domain of GPIb contains binding sites for P-selectin, Mac-1 and VWF (Clemetson and Clemetson, 2007). In addition, GPIb can also function as a receptor for several coagulation factors, including factor XII, XI and thrombin, demonstrating how GPIb functions as a key link between primary and secondary haemostasis (Bradford *et al*., 2000; Kauskot and Hoylaerts, 2012).

### **1.4.2** α2β1 signalling

Integrin $\alpha_2\beta_1$ is comprised of a 150-kDa $\alpha_2$ chain and a 130-kDa $\beta_1$ chain, over 1000 copies of the integrin are present on the surface of platelets (Kauskot and Hoylaerts, 2012). The first indication that integrin $\alpha_2\beta_1$ was a physiological relevant collagen receptor was the discovery of a patient with only a fifth of the normal level of $\alpha_2$ integrin who had no reactivity to collagen. Integrin $\alpha_2\beta_1$ was incorrectly thought of as a purely adhesion receptor, however it was later shown that $\alpha_2\beta_1$ activation leads to the stimulation of intracellular signalling in platelets. The task of identifying signalling pathways that can be attributed to $\alpha_2\beta_1$ alone can be a challenging one as its main agonist is collagen, which also activates signalling via GPVI. This issue was overcome by using $\alpha_2\beta_1$ specific ligands such as GFOGER, a recognition sequence found in collagen I and III (Inoue *et al*., 2003; Siljander *et al*., 2004). Binding of α2β1 to GFOGER leads to platelet spreading this is caused by the activation of SFKs, in addition to Syk

family kinases which in turn leads to tyrosine phosphyrylation of phospholipase C γ2 (Obergfell *et al*., 2002; Wonerow *et al*., 2002). Studies have shown that α2β1 signalling may be an important component of thrombosis, with α2β1 mediated signalling being an important aspect of thrombus stabilisation (Kuijipers 2003).

### 1.4.3 GPVI signalling

The potential role of GPVI as a collagen receptor was first identified when a patient presented with a mild bleeding issue and was found to have platelets deficient in GPVI (Sugiyama *et al*., 1987; Moroi *et al*., 1989). It was later shown that over 9000 copies of the GPVI receptor are present on the surface of platelets and that GPVI plays a major role in triggering platelet activation following initial adhesion to ECM proteins (Burkhart *et al*., 2012). The GPVI receptor belongs to the immunoglobulin receptor superfamily and is associated with the Fc receptor γ chain (FcRγ) (Kauskot and Hoylaerts, 2012). This FcRγ chain is a covalent-linked homodimer, with each chain containing an immunoreceptor tyrosine-based activation motif (ITAM) (Reth,. 1989). GPVI on the surface of platelets can be present in both monomer and dimer forms (Miura *et al*., 2002), with the monomeric form having low affinity for collagen binding (Jung *et al*., 2012). In contrast, the dimeric form of GPVI has a unique conformation which has a high affinity for collagen binding (Horii *et al*., 2006). GPVI-collagen binding leads to GPVI receptor clustering which facilitates the phosphorylation of tyrosine residues found in the ITAM of the FcRγ chain by Src family kinases (SFKs), Fyn and Lyn (Figure 1.2) (Ezumi *et al*., 1998.; Quek *et al*., 2000). This then leads to a signalling cascade with phosphorylated ITAM recruiting Syk which is then phosphorylated and activated by SFKs before undergoing autophosphorylation at position Y525/6 (Kurosaki *et al*,. 1994) leading to the phosphorylation and activation of linker of activated T cells (LAT). LAT then acts as a docking site for other proteins including PI3K which then facilitates the recruitment of phospholipase C γ2 (PLCγ2), leading to the generation of inositol 1, 4, 5 triphosphate ($IP_3$) and diacyl glycerol (DAG) via the hydrolysis of phosphotydalinositol 4, 5, biphosphate ($PIP_2$) (Figure 1.2) (Pasquet *et al*., 1999; Watanabe *et al*., 2001). This cascade eventually leads to the mobilisation of calcium and protein kinase C activation, both of which

are essential components of platelet activation (Gibbins, 2004). GPVI has been identified as a key contributor to arterial thrombosis (Massberg *et al*., 2002), studies using mouse models have demonstrated that GPVI null mice have significantly reduced thrombus formation on collagen (Kato *et al*., 2003). Furthermore, studies using GPVI antibodies have demonstrated that stable aggregates are unable to form on collagen when the GPVI receptor is blocked (Moroi *et al*., 1996), suggesting that GPVI is essential for the formation of stable aggregates on collagen under high shear conditions.

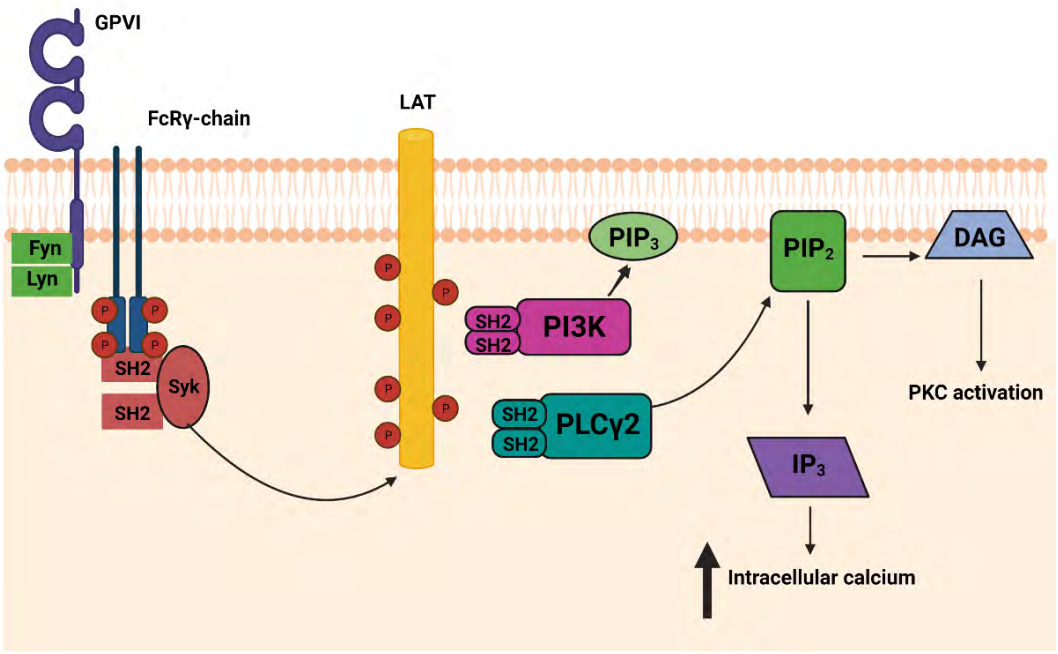


**Figure 1. 2 GPVI signalling pathway**

The binding of collagen to GPVI leads to receptor clustering, this leads to activation of members of Src-family of tyrosine kinases, Lyn and Fyn, which phosphorylate the immunoreceptor tyrosine-based activation motif (ITAM) of the FcRγ chain. phosphorylated ITAM then recruits Syk which binds to the FcRγ chain through Src-homology (SH2) domains. This leads to the phosphorylation and activation of linker for activation of T-cells (LAT). LAT then acts as a docking site for other proteins including PI3K which then facilitates the recruitment of phospholipase C γ2 (PLCγ2), leading to the generation of inositol 1, 4, 5 triphosphate ($IP_3$) and diacyl glycerol (DAG) via the hydrolysis of phosphotydalinositol 4, 5, biphosphate ($PIP_2$).

### 1.4.4 Integrin αIIbβ signalling

Integrin αIIbβ3 is one of the most abundant cell surface proteins found on platelets with 60,000–80,000 copies (Burkhart *et al*., 2012). Platelets also have an internal pool of αIIbβ3, with the integrin being observed on the membrane of the open canicular system, in addition to the internal face of alpha granule membranes (Cramer *et al*., 1990). The integrin is present on the surface of resting platelets in a closed confirmation, which has low binding affinity. Platelet activation leads to the unclipping of the intracellular domain of the integrin by talin and other cytoskeletal proteins which results in a confirmation change and the transformation of the integrin into a high affinity binding state (Petrich *et al*., 2007).

Integrin αIIbβ3 plays a key role in platelet aggregation as upon activation the receptor can facilitate the formation of bridges between platelets (Bledzka *et al*., 2013). Fibrinogen and VWF are two αIIbβ3 ligands that can crosslink bridges between platelets by binding to αIIbβ3 on adjacent platelets and thus supporting platelet aggregation and the formation of a stable platelet plug (Bledzka *et al*., 2013). Ligand binding also leads to integrin clustering and stimulation of outside in signalling (Huang *et al*., 2019). Outside-signalling promotes growth of the forming thrombus by initiating a cascade of signalling which facilitate platelet adhesion, spreading and clot retraction (Huang *et al*., 2019).

### 1.4.5 The coagulation cascade

The coagulation cascade is responsible for the production of thrombin and subsequently the generation of fibrin (Figure 1.3). Fibrin plays a key role in secondary haemostasis, fibrin forms a mesh, which is then incorporated into the haemostatic plug and helps to strengthen and stabilize the clot. The extrinsic pathway has been found to be the primary pathway for the initiation of blood coagulation, the pathway releases thrombin, a key constituent of the coagulation cascade (Palta *et al*., 2014). The pathway is initiated by the release of tissue factor (TF) from activated endothelial cells (Yau *et al*., 2015). TF binds to factor VIIa forming a TF-FVIIa complex, this complex then activates factor IX and factor X. Next factor Xa binds to factor II (prothrombin) resulting in the formation of thrombin (IIa) (Palta *et al*., 2014). The

extrinsic pathway does not produce a large amount of thrombin meaning it can be stopped by tissue factor pathway inhibitor, therefore amplification via positive feedback loops is essential (Geddings and Mackman, 2014). The thrombin produced activates factor XI, which activates factor IX, thrombin also activates factor V and factor VIII which accelerates the activation of factor II by factor Xa (Palta *et al*., 2014).

The intrinsic pathway (Figure 1.3) is a secondary pathway for the formation of thrombin, it begins with the activation of factor XII which activates factor XI, which then activates factor IX, factor IX forms a tenase complex with factor VIII which activates factor X (Geddings and Mackman, 2014; Palta *et al*., 2014). The bridge that connects both pathways, also described as the beginning of the common pathway, is the activation of factor X. Once factor X is activated it forms the prothrombinase complex, which converts prothrombin (II) into thrombin (IIa) (Palta *et al*., 2014) The main role of thrombin is the cleavage of fibrinogen to produce fibrin and the activation of fibrin stabilizing factor (factor XIII). Factor XIII covalently crosslinks fibrin polymers, which are then incorporated into the haemostatic plug strengthening and stabilizing the clot (Gale, 2011). The formation and stabilization of the haemostatic plug is key to achieving cessation of bleeding and maintaining vascular integrity, however it is important that the size of the plug is regulated as a large plug my result in vessel occlusion (Gale, 2011).

In healthy vessels the endothelium inhibits the activation of the coagulation cascade by several anticoagulant mechanisms. The endothelium inhibits the extrinsic pathway by releasing tissue factor pathway inhibitor (TFPI), a protein with two inhibitor domains, which allows it to bind and inactivate factor VIIIa and Xa (Hackeng *et al*., 2006). The endothelium produces heparan sulphate proteoglycans, which activate anti-thrombin III, which in turn inactivates thrombin and factor Xa (van Hinsbergh, 2001). Thrombomodulin is a receptor found on endothelial cells which binds thrombin and is responsible for preventing clot formation by catalysing the activation of protein C (Ishii *et al*., 1986). Activated protein C inhibits the coagulation cascade by inactivating two of the co-factors; Factor Va and VIIIa (Geddings and Mackman, 2014; van Hinsbergh, 2001).

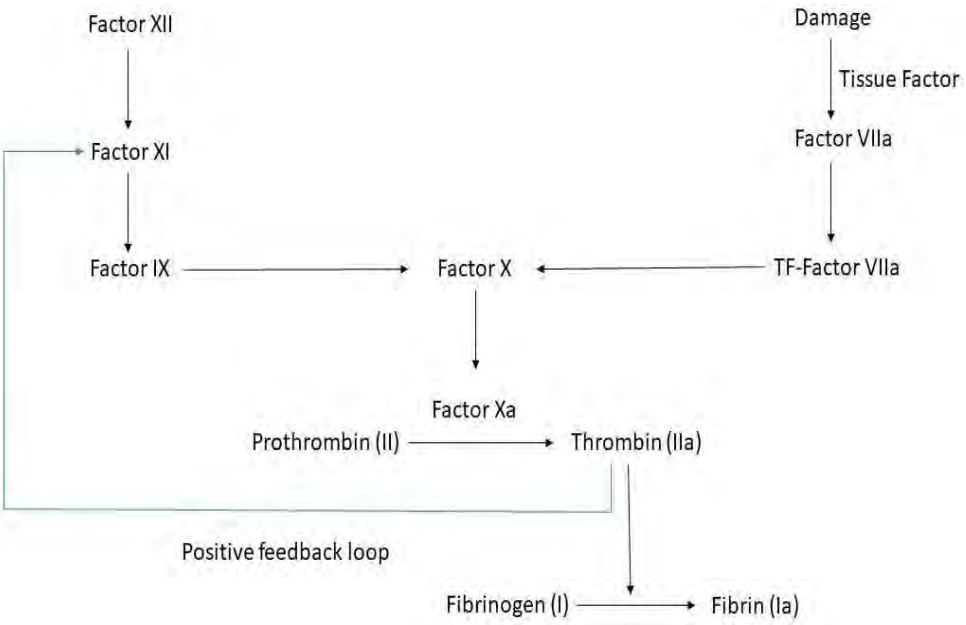


**Figure 1. 5 Overview of coagulation cascade**

The extrinsic pathway is initiated by tissue factor at the site of injury leading to the formation of thrombin. The intrinsic pathway begins with factor XII and results in the formation of thrombus, the bridge between both pathways, often termed the common pathway, is factor X. The positive feedback loop amplifies the coagulation cascade through the activation of factor XI by thrombin.

## 1.5 Endothelial cells

### 1.5.1 Endothelial function and development

Endothelial cells line the blood vessels and form a one cell thick layer known as the endothelium. The endothelium provides a physical barrier between the blood and the surrounding tissues. The endothelium should not be thought of as a passive organ but instead a dynamic organ which plays a role in many key processes such as maintaining blood fluidity and regulating vascular tone. In addition, the endothelium also is essential in regulating immune responses, angiogenesis and platelet adhesion (figure 1.4; figure 1.5) (Yau *et al*., 2015). Although it is important that blood remains within the blood vessels substances, such as macromolecules and ions must be able to move in and out of the blood stream (Roumenina *et al*., 2016). The endothelium regulates this movement of substances from the blood to the surrounding tissues via the tight junction complex and adherens. The endothelium plays a key role in ensuring that a haemostatic balance is maintained and in turn prevents thrombosis via anti-coagulant and anti-platelet mechanisms (Figure 1.4) (van Hinsbergh, 2012).

Endothelial cells and hematopoietic cells are derived from the same precursor, the hemangioblast. During development structures form known as blood islands, the inner cells differentiate and become hematopoietic cells while the outer cells flatten and give rise to the endothelium (Dyer and Patterson, 2010). During their development endothelial cells undergo differentiation, this allows them to meet the specified needs required in their final vessel environment, either venous or arterial. As a result, the overall phenotype of an endothelial cell can differ significantly depending on vascular bed location (Dyer and Patterson, 2010).

The endothelium plays a key role in ensuring that a haemostatic balance is maintained and in turn maintains blood fluidity via activation of fibrinolysis, in addition to anti-coagulant and anti-platelet mechanisms (van Hinsbergh, 2001). The endothelium inhibits platelet adhesion and activation by releasing negative regulators of platelet signalling such as $PGI_2$ and Nitric oxide (NO), which regulate intracellular cyclic nucleotide levels and suppress platelet activation. In addition to this endothelial CD39 facilitates the conversion of the platelet activator ADP to AMP.

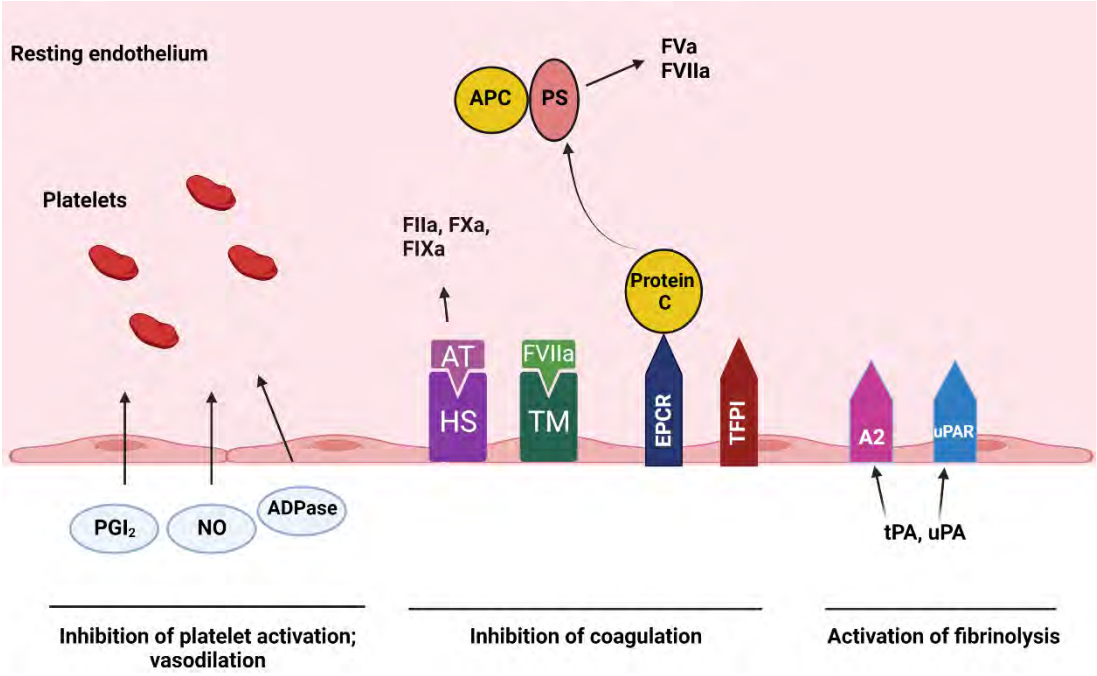


**Figure 1. 6 Overview of the functions of a resting endothelium**

A resting endothelium ensures circulating platelets remain in a quiescent state by the release of platelet inhibitors; prostacyclin ($PGI_2$) and nitric oxide (NO), in addition to the anti-platelet activity of the ADPase CD39. A resting endothelium also inhibits coagulation; the endothelium produces heparan sulphate proteoglycans, which activate anti-thrombin III, which in turn inactivates thrombin (FIIa), factor IXa and factor Xa. Endothelial cell protein C receptor (EPCR) plays a key role in the activity of thrombomodulin, which catalyses the activation of protein C, which inhibits the coagulation cascade by inactivating Factor Va and VIIIa. The endothelium releases tissue factor pathway inhibitor (TFPI), which binds and inactivates factor VIIIa and Xa. Tissue plasminogen activator (tPA) and urokinase plasminogen activator (uPA) are released from the endothelium and interact with their corresponding receptors; annexin A2 and urokinase plasminogen activator receptor (uPAR) enabling plasmin generation on the endothelial cell surface.

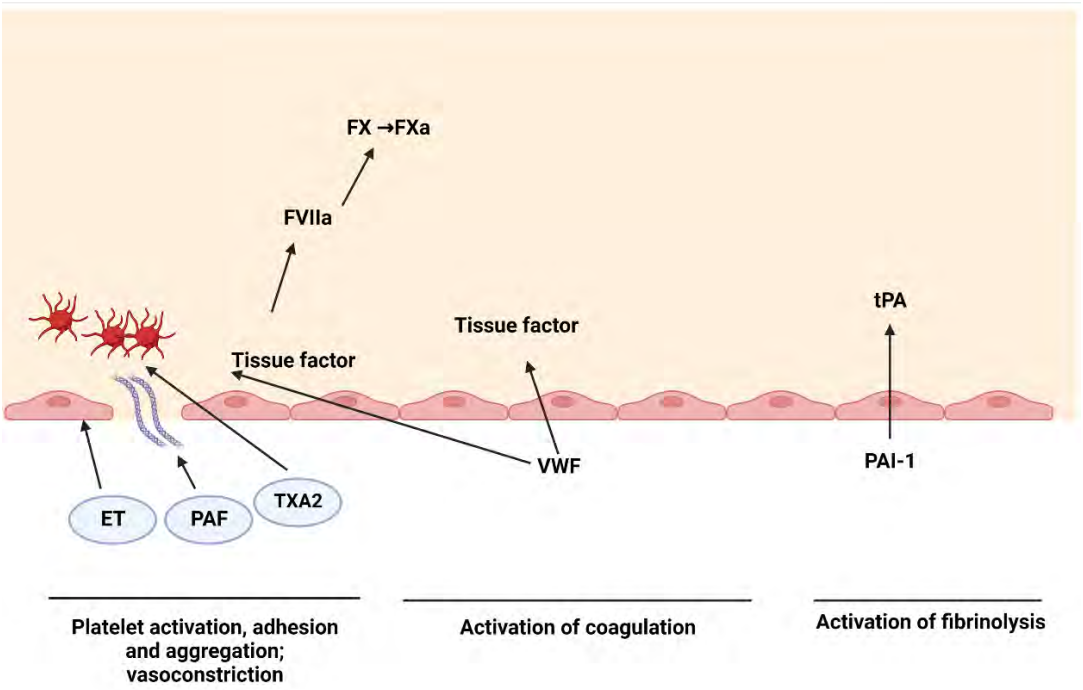


**Figure 1. 7 Overview of the shift in endothelial cell activity in response to vessel wall injury**

Upon vessel wall injury, extracellular matrix (ECM) proteins such as collagen are exposed to the blood stream, in response the endothelium facilitates platelet activation and adhesion, activation of the coagulation cascade and inhibits fibrinolysis to ensure the formation of a stable platelet plug. The endothelium releases platelet activators platelet-activating factor (PAF) and thromboxane $A_2$ (TXA2) which helps to recruit platelets to the site of injury. In addition, secretion of endothelin (ET) from endothelial cells leads to vasoconstriction. Von Willebrand factor (VWF) is also released from endothelial cells allowing it to contribute to platelet-collagen binding. Tissue factor released from the damage endothelium can activate the extrinsic pathway of the coagulation cascade. The endothelium can also facilitate the inhibition of fibrinolysis via the release of plasminogen activator inhibitor-1 (PAI-1) which can inhibit the activity of tissue plasminogen activator (tPA).

### 1.5.2 Nitric oxide

In a normal healthy vessel, platelet inhibitory pathways are important for ensuring that platelets remain in a quiescent, unreactive state and will only become reactive in response to vascular damage. This is particularly important in high pressure vessels where platelets come into close proximity with the vessel wall (Bye, Unsworth and Gibbins, 2016). The two primary platelet inhibitory signalling molecules are nitric oxide (NO) and prostacyclin ($PGI_2$), these are released by healthy intact endothelial cells (Bye *et al*., 2016; Mellion *et al*., 1981). NO is synthesised from L-arginine in a two-step oxidation reaction catalysed by a family of enzymes known as NO synthases (NOS) (Bye *et al*., 2016; Mellion *et al*., 1981). Three isoforms of NOS exist, inducible (iNOS), neuronal (nNOS) and endothelial (eNOS). Endothelial NOS is the main source of vascular NO, eNOS is constitutively expressed by endothelial cells, in addition to this small amounts iNOS have been described in recent studies. NO is thought to inhibit platelet activation by binding soluble guanylyl cyclase, this leads to an increase in intracellular levels of cyclic guanosine monophosphate, which regulates protein kinase G (PKG) activity (Mellion *et al*, 1981; Bye, Unsworth and Gibbins, 2016). The role of endothelial derived NO as a key regulator of platelet activation *in vivo* supports the inclusion of endothelial cells in *in vitro* models that aim to assess platelet activation.

### 1.5.3 Prostacyclin

Prostacyclin ($PGI_2$) is a member of the prostaglandin family, it plays a key role in the cardiovascular system. $PGI_2$ is released from the endothelium and acts as a potent vasodilator, in addition to being a powerful inhibitor of platelet activation (Yau *et al*., 2015). $PGI_2$ works by activating prostacyclin receptors (IP) found on the surface of platelets. IP receptors are G-protein coupled receptors, coupled to the $G_S$ subtype of G-proteins. This leads to changes in cyclic nucleotide levels as IP receptor activation leads to increased adenyl cyclase activity resulting in increased levels of cAMP. The accumulation of cAMP leads to the activation of protein kinase A (PKA). PKA phosphorylates several key proteins leading to the inhibition of several pathways including those responsible for initiating granule secretion, increasing intracellular calcium and actin polymerization.

### 1.5.4 CD39

E-NTPDase (CD39) is a member of the ectonucleoside triphosphate diphosphohydrolase family and is responsible for converting ATP and ADP into AMP (Kanthi *et al*., 2014). CD39 consists of two transmembrane domains, a small cytoplasmic domain and an extracellular hydrophobic domain which contains five apyrase conserved regions that are responsible for the catabolism of nucleotides (Kanthi *et al*., 2014; Maliszewski *et al*., n.d.). CD39 is seen as a key endothelial derived platelet inhibitor as it preferentially hydrolyses ADP, which is released from activated platelets and as previously discussed is an important mediator of platelet aggregation.

## 1.6 Current thrombosis models

### 1.6.1 *In vivo* thrombosis models

Thrombosis is a complex disease with many factors contributing to the development and progression of thrombosis. Murine models provide a valuable tool, enabling researchers to analyse the pathophysiology of thrombosis. Currently there are gene deletion and overexpression models for most of the known genes involved in haemostasis (Westrick *et al*., 2007). This enables researchers to explore the effects of single or multiple gene variations in an effort to elucidate the key factors involved in thrombosis. There a several methods used for inducing and investigating thrombosis in these mouse models, these include laser injury models, Ferric Chloride models, rose Bengal model and mechanical injury models (Westrick *et al*., 2007). Each of these models have contributed to furthering our understanding of thrombosis, however they all have limitations.

Laser injury models use argon-ion laser damage on the desired vessel to induce an occlusive thrombus. Fluorescently labelled platelets are used for the visualisation of the forming thrombus, in addition to this, fluorescently labelled antibodies specific for key thrombosis components such as fibrin and CD41 can be utilised (Falati *et al*., 2002). Despite the advantages fluorescent imaging provides it does lead to a common limitation amongst all current *in vivo* models, vessel choice. The fluorophores used emit in the visible spectrum and would become scattered in large

vessels, as a result small vessels are used such as the mesenteric arterioles and venules (Flaumenhaft *et al*., 2007; Westrick *et al*., 2007). These vessels do not accurately reflect human coronary arteries or the vascular environment of atherothrombosis, thus limiting this model's ability to accurately portray what occurs during arterial thrombosis in humans.

The ferric chloride model utilises ferric chloride to induce vessel damage and thrombus formation. The ferric chloride injury method was first described in 1944 where it was applied to the inferior vena cava of a rabbit, following application with ferric chloride thrombosis was induced (Day *et al*., 2004). This method was later adapted for rat carotid arteries, it was found that when ferric chloride is applied topically to the vessel of interest an occlusive thrombus forms, in addition to this the time to occlusion is concentration dependent (Kurz *et al*., 1990). When ferric chloride injury was used in combination with scanning electron microscopy it was revealed that endothelial damage was present in addition to the presence of an occlusive thrombus containing activated platelets, fibrin and red blood cells (Kurz *et al*., 1990). The evidence of a damaged endothelium in this model was a key finding as endothelial damage is a key driver of thrombosis in humans. One limitation of the ferric chloride model is the lack of consensus on the appropriate concentration of ferric chloride thus creating variability between different researchers using this model. In a study using plasminogen activator inhibitor 1 (Pai1) deficient mice 10% ferric chloride was found to be the most effective concentration in this study (Farrehi *et al*., 1998). In contrast Wang and Xu used a concentration of 2.5% in C57BL5/J mice and found this concentration was more sensitive for studying thrombosis and anti-platelet drugs compared to higher concentrations (Wang and Xu, 2005). Other studies using this model have used concentrations of 20% (Smyth *et al*., 2001) and 15% (Schlachterman *et al*., 2005) this indicates that the concentration of ferric chloride used in the model needs to be optimised for each study, which could create variability in the model and make comparison of different studies difficult.

Although some models choose to use lasers or chemical as a damage stimulus there are also many models that use physical methods of damage to induce occlusion. Ligation models are a common form of mechanical injury stimulus, ligations that

induce stasis are used to study venous thrombosis (Henke *et al*., 2006; Westrick *et al*., 2007). *Tymvios et al* have developed a non-lethal model of platelet thromboembolism allowing for the assessment of thromboembolic responses in real time. Although this is a novel and effective model it is primarily a model of venous thromboembolism rather than arterial thrombosis associated with cardiovascular disease. Another common physical injury model is the mechanical wire injury model, this method uses an angioplasty guide wire which is inserted into the femoral or carotid artery and used to initiate damage to the vessel (Lindner *et al*., 1993; Roque e*t al*., 2000). Reactive oxygen species are one of the key contributors to the development of the atherothrombotic vessel environment. Rose Bengal is a photosensitizing dye, which when excited with 543-nm wavelength light produces reactive oxygen intermediates (Westrick *et al*., 2007). As a result, rose Bengal is being utilised in mouse model studies in attempt to reproduce the atherothrombotic environment observed in human thrombosis (Danenberg *et al*., 2003). Although *in vivo* models have furthered our understanding of the disease and have some aspects that faithfully mimic the disease state in humans they still suffer from several limitations, including the obvious issue of the models being non-human tissue and the ethical issues surrounding the use of animals. *In vitro* thrombosis models have the advantage of being able to use human cells and human whole blood in an effort to accurately replicate arterial thrombosis in humans.

### 1.6.2 *in vitro* thrombosis models

A key breakthrough in the field of platelet research was the development of the light transmission aggregometry (LTA) technique by Gustav Born in the 1960's (Born GVR. 1962; Born GVR and Cross MJ. 1963). LTA is an *in vitro* technique for testing the reactivity of platelets, LTA is based on the principle that it is easier for light to pass through a clear solution than an opaque one (Born GVR. 1962; Born GVR and Cross MJ. 1963). Human whole blood is centrifuged to produce platelet rich plasma (PRP), which is then transferred to a cuvette and mixed with a magnetic stir bar. A photosensor is used to detect the level of light passing through the solution, when aggregates form the level of light passing through the solution increases. Light

transmission is then defined using control solutions and from this a percentage aggregation can be calculated. The technique quickly became the gold standard *in vitro* test for assessing platelet activation and aggregation and is still widely used today (Chan e*t al*., 2018). One of the key strengths of LTA is that the two stages of platelet aggregation, primary activation and secondary signalling amplification, can be visualised in real time. However, the technique is not without limitations, LTA can be expensive and time consuming, in addition the technique required specialised equipment and the researcher should be suitably trained before performing the technique (Chan e*t al*., 2018).

In the 1990's, building on the same principles as LTA but with some modifications, the 96-well plate aggregation assay was developed (Fratantoni JC *et al.,* 1990; Bednar B *et al.,* 1995). Like LTA, 96-well plate aggregation uses PRP, which is added to wells containing agonists, commonly collagen or ADP, before being shaken by a plate shaker. Finally, light absorbance is measured using a plate reader, this can then be converted into percentage aggregation (Fratantoni JC *et al.,* 1990; Bednar B *et al.,* 1995). The key advantage of this technique is that it allows multiple experimental wells to be assayed in one run, making it higher throughput assay compared with LTA and in turn more efficient (Chan e*t al*., 2018). Plate based aggregometry is associated with some limitations, one being the fact that it is an endpoint assay and therefore it is not possible to platelet activation and aggregation in real time using this technique (Chan e*t al*., 2018). Furthermore, although LTA and plate-based aggregation assays have been beneficial tools for furthering our understanding of platelet reactivity they suffer from a major limitation when it comes to modelling thrombosis. This limitation is the lack of additional components present in an atherothrombotic vessel environment, such as endothelial cells. The emergence of 2D and 3D microfluidic models have begun to address this limitation in thrombosis modelling and may lead to the development of a new gold standard model.

Fluidic devices provide a valuable *in vitro* tool to investigate thrombosis, while addressing some of the limitations of *in vivo* animal models by using human blood and replicating the appropriate haemodynamic forces. However, a major emerging

issue with *in vitro* models is variation between models. Recent technological advances have allowed more flexibility in the design of fluidic devices but has impeded standardization and the ability to compare results between studies. A major source of variation between the different models is the dimensions of the flow channel, the size and aspect ratio of the channel is important in determining whether platelet-platelet interactions or platelet-surface interactions dominate within the channel. Therefore, it is quite alarming to discover that the flow channel dimension is only reported in a minority of papers (Coenen *et al*., 2017).

Another limiting factor of many of these models is the absence of factors that are crucial to making an *in vitro* physiologically relevant, such as endothelial cells and human whole blood. Several models (Dardik *et al*., 1998; Tanahashi *et al*., 2001) choose to use platelet-rich plasma as an alternative to whole blood. This can be an issue in limiting the physiological relevance of a model, especially when looking at certain anti-thrombotic compounds. For example, dipyridamole is a phosphodiesterase (PDE) inhibitor, which inhibits PDE5 in platelets, the anti-thrombotic effects observed however, have been attributed to its inhibition of adenosine reuptake by red blood cells (Coenen *et al*., 2017). Therefore, testing the efficacy of this drug in a model without red blood cells could possibly yield results that are not faithful to what would be observed *in vivo*.

Another important thing to consider when developing a physiological relevant thrombosis model is the shear stress levels present within the model. Shear stress levels are not uniform throughout the cardiovascular system and vary amongst vessel types, with typically higher shear rates being observed in arterial vessels (5–40 dynes/cm$^2$) compared to venous (1–5 dynes/cm$^2$) (Dela paz *et al*., 2009). As a result, it is essential that shear stress is considered when developing a thrombus model and the correct shear stress level is used to assess the researchers' specific research question. Furthermore, the shear stress within a vessel can increase with stenosis, this is observed in cardiovascular disease with the development of an atherosclerotic plaque (Sakariassen *et al*., 2015). It has been reported that the shear stress levels under pathological conditions can reach up to 160 dynes/cm$^2$ (Sakariassen *et al*., 2015), any researcher wishing to model thrombosis in this environment should

ensure that the correct shear stress level is appropriate and accurate.

Many basic forms of *in vitro* models still do not incorporate endothelial cells and therefore do not consider the role of the endothelium and endothelial dysfunction in thrombus formation (de Witt *et al*., 2014). Most of these basic *in vitro* models use a single ligand (commonly type I collagen) to promote platelet adhesion and mimic vascular damage (de Witt *et al*., 2014). The failure to acknowledge and analyse the contribution of the endothelium is one of the major limiting factors of current *in vitro* models reducing their relevance to human disease. Therefore, the development of a model which contains endothelial cells in addition to dysfunctional endothelial cells would provide a model which more accurately portrays arterial thrombosis in humans, facilitating a more translational model to test novel anti-thrombotics. It would also provide a novel *in vitro* platform to investigate anti-thrombotics which target the endothelium or endothelial mediated pathways.

## 1.7 Aims and hypothesis

Currently there is not a gold standard *in vitro* or *in vivo* thrombosis model. Although current models have been beneficial in furthering our understanding of thrombosis, they suffer from several limitations. One key limitation of current *in vitro* thrombosis models is the absence of endothelial cells, which play a pivotal role in regulating platelet activity. The overall aim of this project was therefore to develop an *in vitro* model of human arterial thrombosis which incorporates endothelial cells allowing for endothelial cell contribution to thrombus development and anti-thrombotic drug efficacy to be assessed.

The principal aims of the work presented in this thesis were to:

1. Develop and characterize a simple fluidic based model of thrombosis sensitive to regulation by endothelial cells incorporated into the fluidic chambers
2. Establish an endothelialised model sensitive to endothelial dysfunction
3. Determine the contribution of healthy and dysfunctional endothelial cells to the efficacy of standard antiplatelet drugs
4. Characterize the anti-thrombotic capacity of endothelial cells from different vascular beds (coronary artery and umbilical vein) to optimise the model using the most cost-effective but appropriate cell type
5. Investigate potential novel anti-thrombotics using the endothelialised model

### Hypothesis

Endothelial cells play a key role in the regulation of thrombus formation and should therefore be incorporated into *in vitro* thrombosis models.

# 2. Material and methods

## 2.1 Materials

### 2.1.1 Reagent

Unless stated, all general reagents, including those used to make buffers, were chemical grade and purchased from Sigma Aldrich (Poole, United Kingdom). Information on the platelet agonists and inhibitors used in this study can be found in Table 2.1.

**Table 2. 1 Platelet agonists and inhibitors**

| Reagent | Source |
|---|---|
| ADP | Sigma Aldrich (Poole, United Kingdom) |
| Apyrase | Sigma Aldrich (Poole, United Kingdom) |
| Aspirin | Sigma Aldrich (Poole, United Kingdom) |
| Celecoxib | Tocris (Abingdon, United Kingdom) |
| Collagen type 1 | Labmedics Ltd (Abingdon, United Kingdom) |
| Clopidogrel hydrogen sulphate | Tocris (Abingdon, United Kingdom) |
| Indomethacin | Sigma Aldrich (Poole, United Kingdom) |
| POM-1 | Tocris (Abingdon, United Kingdom) |
| Prostaglandin E1 | Sigma Aldrich (Poole, United Kingdom) |
| Sodium Nitroprusside | Sigma Aldrich (Poole, United Kingdom) |

### 2.1.2 Tyrodes-HEPES buffer

Tyrodes-HEPES buffer was prepared using, 134mM of NaCl, 2.9mM of KCl, 0.34mM of $Na_2HPO_4$, 12mM of $NaHCO_3$, 1mM of $MgCl_2$, 20mM of HEPES and 5mM of Glucose in sterile $H_2O$. The pH was adjusted to 7.3 using 1M NaOH.

### 2.1.3 Other reagents

Angiotensin II and angiotensin 1-7 were purchased from Tocris (Abingdon, United Kingdom). Dimethyl sulfoxide was purchased from Thermo Fisher Scientific (Massachusetts, USA). Nomega-nitro-L-arginine (L-NNA) was purchased from Abcam (Cambridge, United Kingdom). Endothelial cell growth medium MV2 and supplement packs were obtained from Promocell (Heidelberg, Germany). Laemmli 4X loading buffer was purchased from Bio-Rad (California, USA).

### 2.1.4 Antibodies

The primary and secondary antibodies used in this study for western blotting and flow cytometry are presented in Table 2.2 and Table 2.3.

**Table 2. 2 The primary antibodies used in this study**

| Target | Species | Application | Dilution | Source |
|---|---|---|---|---|
| β-actin | Mouse | Western blotting | 1:10000 | Abcam (Cambridge, United Kingdom) |
| ACE2 | Rabbit | Western blotting | 1:1000 | Abcam (Cambridge, United Kingdom) |
| AT1R | Rabbit | Western blotting | 1:2000 | Abcam (Cambridge, United Kingdom) |
| AT2R | Rabbit | Western blotting | 1:1000 | Abcam (Cambridge, United Kingdom) |
| CD39 | Rabbit | Western blotting | 1:1000 | Abcam (Cambridge, United Kingdom) |
| CD62P | Mouse | Flow cytometry | 1:25 | BD Biosciences (New Jersey, USA) |
| CD63 | Mouse | Flow cytometry | 1:25 | BD Biosciences (New Jersey, USA) |
| COX-1 | Rabbit | Western blotting | 1:1000 | Cell Signalling Technology (London, United Kingdom) |
| COX-2 | Rabbit | Western blotting | 1:1000 | Cell Signalling Technology (London, United Kingdom) |
| ICAM-1 | Mouse | Western blotting | 1:1000 | Abcam (Cambridge, United Kingdom) |
| MAS1 | Rabbit | Western blotting | 1:2000 | Abcam (Cambridge, United Kingdom) |

**Table 2. 3 The secondary antibodies used in this study**

| Antibody | Conjugate | Dilution | Source |
|---|---|---|---|
| Goat anti-rabbit IgG | Horseradish Peroxidase | 1:5000 | Cell Signalling Technology (London, United Kingdom) |
| Goat anti-mouse IgG | Horseradish Peroxidase | 1:5000 | Cell Signalling Technology (London, United Kingdom) |

## 2.2 Methods

### 2.2.1 Blood sample collection

Blood was collected from consenting healthy donors (males and females, 18-65 years) at Manchester Metropolitan University (MMU) according to a protocol approved by the local ethical committee of MMU (ethos number: 10199). Participants with anaemia or who had taken aspirin within 10 days of the collection were excluded from the study. Venous blood was taken from donors using a 21-gauge needle (BD Vacutainer) and was collected into BD Vacutainer tubes (purchased from Bunzl Healthcare, Manchester, UK) containing 0.105 M (3.2%) buffered sodium citrate anticoagulant, 9:1 *v/v*. The tubes were gently inverted to allow the blood to mix with the anticoagulant and prevent clotting.

### 2.2.2 Human platelet preparation

To obtain platelet rich plasma (PRP), human whole blood collected from donors was centrifuged at 100 x g for 20 minutes and the supernatant removed. To obtain washed platelets, PRP was centrifuged at 1400 x g for 10 minutes in order to isolate a platelet pellet. $PGI_2$ (50ng/ml) was added to the tubes prior to centrifugation to prevent platelet activation. The platelet pellet was then washed and resuspended in 5 ml of Tyrodes-HEPES buffer by centrifugation at 1400 x g for 10 minutes at room temperature. Finally, the platelet pellet was resuspended in 1 ml of Tyrodes buffer, with platelet number being determined using a Sysmex automatic haematology analyser (Sysmex XS- 1000i) before being adjusted to the required density.

## 2.3 Cell culture

Human umbilical vein endothelial cells (HUVECs) were obtained from Caltag-Medsystems Ltd and Human coronary artery endothelial cells (HCAECs) were obtained from PromoCell, Heidelberg, Germany. Both cell types were cultured in endothelial cell growth medium MV2 medium (Promocell) supplemented with human recombinant epidermal growth factor (5ng/ml), basic fibroblast growth factor (10ng/ml), insulin-like growth factor (20ng/ml), endothelial growth factor 165 (0.5ng/ml), ascorbic acid (1µg/ml), hydrocortisone (0.2µg/ml) and 20% heat inactivated Fetal Bovine Serum (FBS) (Gibco, Paisley, UK) referred to as full growth medium (FGM). Cells are adherent and were cultured in T75 flasks (NuncTM, Thermo Scientific), coated with 0.1% gelatin, and incubated at 37$^{o}$C with 5% $CO_2$. The media was replaced every 48 hours. Once cells reached 80-90% confluence they were passaged and used for experiments between passages 3-8. For passaging, cells were washed twice with warm Phosphate Buffer Saline (PBS) (Lonza) and incubated with Trypsin-EDTA (Lonza) for two minutes at 37ºC with 5% $CO_2$. Trypsin was inhibited by adding full growth medium, cells were re-suspended and transferred to falcon tube and centrifuged at 300g for five minutes. The supernatant was discarded and cells were re-suspended in full growth medium before being plated onto T75 flasks at a seeding density of 2 x $10^6$.

## 2.4 *In vitro* thrombosis model setups

### 2.4.1 *In vitro* thrombosis model using exogenous endothelial derived platelet inhibitors

Ibidi µ-slide VI$^{0.4}$ channels were coated with type I collagen fibrils (derived from equine tendons; Labmedics) (100µg/ml) and incubated at room temperature for one hour. Exogenous endothelial derived platelet inhibitors were prepared in advance, including, sodium nitroprusside (10µM), PGE (10µM), Apyrase (4U/ml). Following collection of whole blood, platelets were fluorescently labelled by the addition of 3,3'-Dihexyloxacarbocyanine iodide fluorescent indicator ($DIOC_6$) (1µM), followed by a 15 minute incubation at room temperature. This was then followed by a 10-minute

incubation in endothelial derived platelet inhibitors. Two reservoirs were attached to a stand, one for Tyrodes buffer and one for blood, these were connected to a three way tap connected to siliconized tubing. Tubing was also connected to a withdrawal syringe pump, this allowed blood to be perfused through the collagen coated channel at a physiological relevant shear stress (1.5 dynes/cm$^2$) (Figure 2.3.1). Thrombus formation was imaged using the Celena® S digital imaging system, images were analysed using Fiji ImageJ software to determine platelet number, area coverage and average thrombi size.

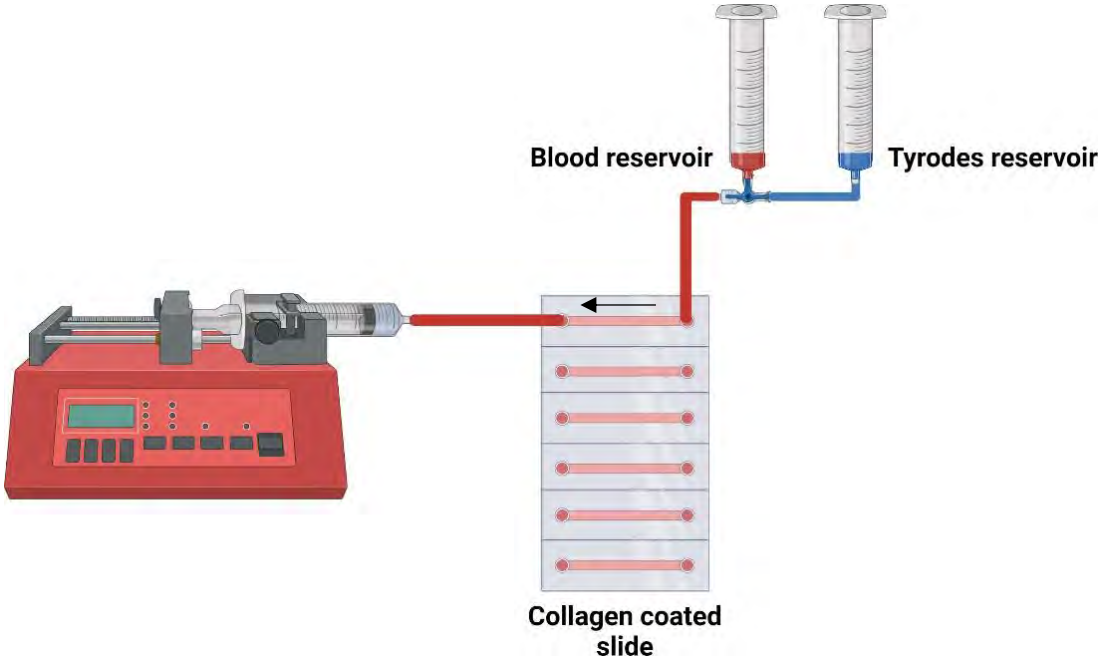


**Figure 2. 1 In vitro thrombosis model basic setup**

Ibidi µ-slide VI$^{0.4}$ channels were coated with type I collagen fibrils (derived from equine tendons; Labmedics) (100µg/ml) and incubated at room temperature for one hour. Once whole blood was collected, platelets were fluorescently labelled by the addition of 3,3'-Dihexyloxacarbocyanine iodide fluorescent indicator ($DIOC_6$) (1µM) followed by a 15-minute incubation at room temperature. Two reservoirs were attached to a stand, one for Tyrodes buffer and one for blood, these were connected to a three way tap connected to siliconized tubing. Tubing was also connected to a withdrawal syringe pump, this allowed blood to be perfused over the collagen coated channel at a physiological relevant shear stress (1.5 dynes/cm$^2$). Arrow indicates the direction of flow.

### 2.4.2 *In vitro* thrombosis model incorporating HUVECs

HUVECs were seeded onto *Ibidi µ-slide VI*$^{0.4}$ slides (plating density 5 x$10^5$/ml) before being incubated for 48 hours at 37ºC with 5% $CO_2$ to allow a confluent monolayer to form. Alternate, HUVEC-free channels were coated with type I collagen fibrils (derived from equine tendons; Labmedics) (100µg/ml) one hour prior to blood perfusion. Following collection of whole blood, platelets were fluorescently labelled by the addition of $DIOC_6$ (1µM) followed by 15-minute incubation at room temperature. The syringe pump system was set up as described in 2.3.1, siliconized connective tubing was used to link endothlialised channels upstream of collagen coated channels, this allowed blood to be perfused over endothelial cells before passing over collagen at a physiological relevant shear stress (1.5 dynes/$cm^2$) (Figure 2.2). Prior to blood perfusion Tyrodes buffer was perfused through the system and the endothelial cell compartment was monitored and imaged to ensure the endothelial layer remained intact. This process was repeated following blood perfusion to assess if any thrombi had formed on the endothelial cells and if the cells remained intact. As described in 2.3.1, Thrombus formation in the collagen compartment was imaged using the Celena® S digital imaging system, images were analysed using Fiji ImageJ software to determine platelet number, area coverage and average thrombi size. Results were reported as raw pixel data or a percentage of the control where appropriate. For experiments reporting percentage of control, a no cell control was used and experimental conditions were calculated as a percentage of this control. This setup was also utilised for activated endothelium model runs with HUVECs seeded on slides, and then cultured for 48 hours +/- 24 hours of TNF-alpha treatment.

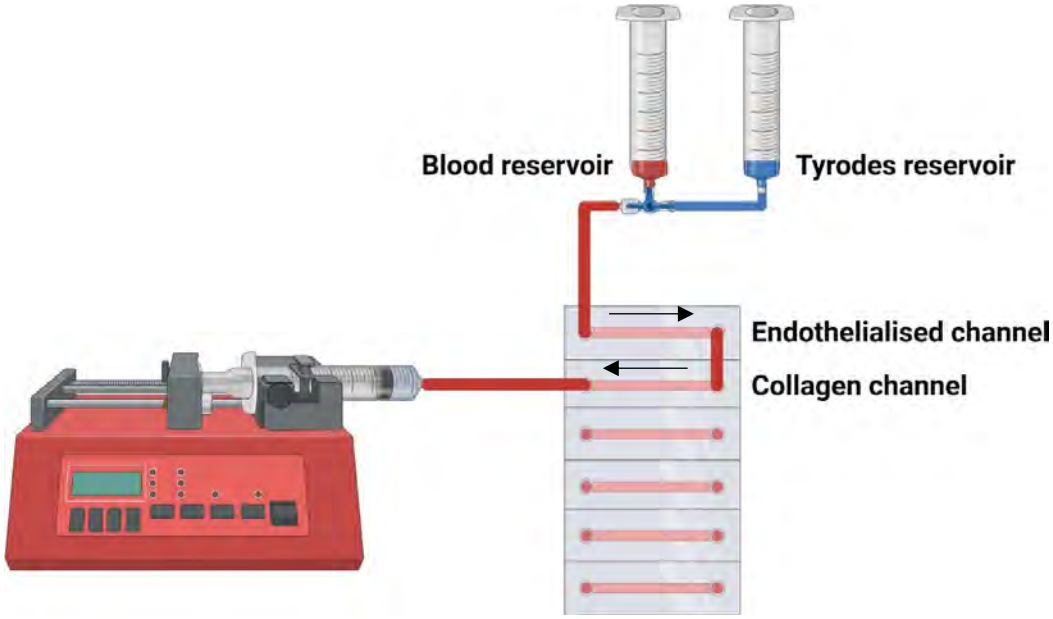


**Figure 2. 2 Incorporation of endothelial cells into the model**

Reservoirs containing blood and Tyrodes were connected to an Ibidi µ-slide ($VI^{0.4}$) via a 3-way tap and siliconized tubing. Two chambers are connected via tubing and blood is drawn through the two chamber at a defined shear rate using a syringe pump. The first chamber is seeded with a confluent layer of human umbilical vein endothelial cells (HUVECs), the second chamber is downstream of this chamber and is coated with type I collagen fibrils (derived from equine tendons; Labmedics) (100µg/ml), exposing blood to endothelial cells immediately prior to encountering exposed collagen. Three experiments can be performed per slide. Arrows indicate the direction of flow.

### 2.4.3 Higher throughput *in vitro* thrombosis model

Two Ibidi $VI^{0.4}$ µ-slides were connected to each other via siliconized tubing, HUVECs were seeded onto the first µ-slide (plating density 5 $x10^5$/ml) before being incubated for 48 hours at 37ºC with 5% $CO_2$ to allow a confluent monolayer to form. The channels of the second µ-slide were coated with type I collagen fibrils (derived from equine tendons; Labmedics) (100µg/ml) one hour prior to blood perfusion. Once whole blood was collected, platelets were fluorescently labelled by the addition of $DIOC_6$ (1µM) followed by 15-minute incubation at room temperature. The first µ-slide was connected to six pairs of reservoirs containing either Tyrodes buffer or human whole blood, via siliconized tubing. Corresponding channels of the two µ-slides were lined up and connected via siliconized tubing. The second µ-slide was connected to a six syringe withdrawal pump, which enables blood to be perfused through all 6 channels per slide, over endothelial cells before passing over collagen at the same physiological relevant shear stress (1.5 dynes/$cm^2$) (Figure 2.3). Prior to blood perfusion Tyrodes buffer was perfused through the system and the endothelial cell compartment was monitored and imaged to ensure the endothelial layer remained intact. This process was repeated following blood perfusion to assess if any thrombi had formed on the endothelial cells and if the cells remained intact. Thrombus formation was imaged using the Celena® S digital imaging system, images were analysed using Fiji ImageJ software to determine platelet number, area coverage and average thrombi size. Results were reported as raw pixel data or a percentage of the control where appropriate. For experiments reporting percentage of control, a no cell control was used, and experimental conditions were calculated as a percentage of this control. This setup allowed six conditions to be run at the same time.

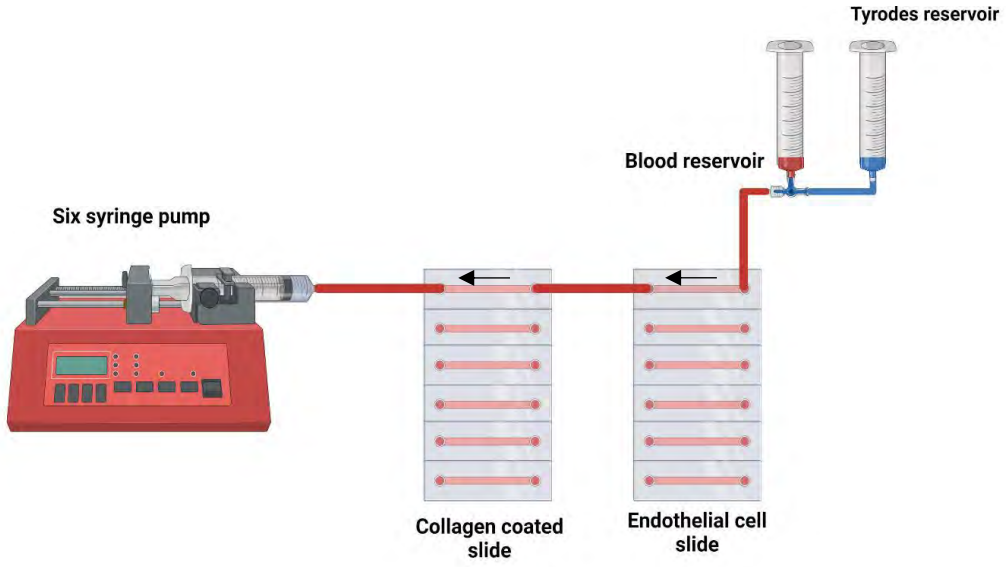


**Figure 2. 3 Higher throughput in vitro thrombosis**

Six pairs of reservoirs containing blood or tyrodes buffer were connected to an Ibidi µ-slide ($VI^{0.4}$), this functioned as the endothelial cell compartment of the higher throughput model. This slide was then connected to a second Ibidi µ-slide ($VI^{0.4}$), using siliconized tubing, coated in collagen. The second slide was then connected to a six-syringe pump and blood is drawn through the two slides at a defined shear rate, exposing blood to endothelial cells immediately prior to encountering collagen. This model setup allows six channels to be run simultaneously. Arrows indicate the direction of flow.

### 2.4.4 *In vitro* model of arterial thrombosis

The arterial thrombosis model utilised the setup described in 2.3.4 with HCAECs seeded onto *Ibidi µ-slide VI*$^{0.1}$ (plating density 5 x$10^5$/ml) before being incubated for 48 hours at 37ºC with 5% CO2 to allow a confluent monolayer to form. This setup allowed blood to be perfused over arterial endothelial cells before passing over collagen (100 µg/ml) at a physiological relevant shear stress (5 dynes/$cm^2$). Prior to blood perfusion Tyrodes buffer was perfused through the system and the endothelial cell compartment was monitored and imaged to ensure the endothelial layer remained intact. This process was repeated following blood perfusion to assess if any thrombi had formed on the endothelial cells and if the cells remained intact. Thrombus formation was imaged using the Celena® S digital imaging system, images were analysed using Fiji ImageJ software to determine platelet number, area coverage and average thrombi size. Results were reported as raw pixel data or a percentage of the control where appropriate. For experiments reporting percentage of control, a no cell control was used, and experimental conditions were calculated as a percentage of this control.

## 2.5 Plate based aggregometry

In a flat bottomed, full area, 96-well plate platelet agonists were prepared; collagen (100 µg/mL–0.001 µg/mL; 10X of final desired concentration) or ADP (1000 µM–0.01 µM; 10X of final desired concentration). In separate wells of the 96-well plate ANG 1-7 was prepared (100 µM–0.01 µM; 10X of final desired concentration). Next ANG 1-7 was transferred to a flat bottomed, half-area, 96-well plate containing PRP (prepared as described in 2.2.2), the plate was then left to incubate for 10 minutes at room temperature. Agonists were then added to the plate prior to the plate being placed on an Bioshake iQ orbital shaker at 1200 rpm, at 37°C for 5 minutes. Finally, light absorbance was measured at 450 nm using a plate reader. Finally absorbance was converted to percentage light transmittance (% LT) using the following equation (Bye *et al*., 2018):

$$\% \, LT = 10^{-Abs} \times 100$$

## 2.6 Light transmission aggregometry

Platelet rich plasma (445 μl) was incubated with ANG 1-7 or vehicle control (Tyrodes) (5 μM) at a final concentration of 0.1-10 μM for 5 minutes in siliconized glass cuvettes prior to the addition of agonist (50 μl). The agonists used were ADP (1 μM) and collagen (2 μg/ml). PRP was stimulated for 5 minutes at 37 °C with continuous stirring (1200 rpm) and aggregation measured using a ChronoLog 700 Aggregometer (Labmedics, Oxford) and Aggrolink 8 software. Aggregation was measured at percentage light transmission through the sample, calibrated against platelet poor plasma, taken as 100% light transmission, and non-stimulated PRP taken as 0% light transmission.

## 2.7 Flow cytometry

In a flat-bottomed 96-well plate, 5μL of PRP was incubated with 5μL ANG 1-7 (10X final desired concentrations: 0.1–10μM) or vehicle control (Tyrodes buffer), 0.5μL of antibodies for specific markers of platelet activation: CD62P, PAC-1 and CD63 (Table 2.1) for 5 minutes before the addition of 5μL 100 μM ADP (10X concentration) with a total reaction volume of 50μL made up with Tyrodes. The plate was incubated for 20 minutes in the dark before fixation with 150μL 0.2% formyl saline. Flow cytometric analysis was performed using a MACSQuant flow cytometer (MACsQuant analyzer 16) (Miltenyi Biotec, Bergisch Gladbach, Germany). Percentage positive was analysed using FlowJo.

## 2.8 Western blotting

Western blot equipment was supplied by BioRad. HUVECs, HCAECs or washed platelets were lysed with RIPA lysis buffer (Sigma) containing a protease inhibitor cocktail (Sigma Aldrich, Poole, UK) consisting of aprotinin, bestatin, E-64, leupeptin and pepstatin A to inhibit the activity of serine, cysteine and aspartic proteases, in addition to aminopeptidases. A phosphatase inhibitor cocktail (Sigma Aldrich, Poole, UK) consisting of sodium orthovanadate, sodium molybdate and sodium tartrate was also added to RIPA lysis buffer to inhibit the activity of phosphatases. If necessary,

protein concentrations of cell lysates were then determined by BCA assay (Life Technologies). 4X Laemmli buffer was added to samples in a 1:3 ratio, 5% β-mercaptoethanol was added to each sample prior to boiling at 95°C for 5 minutes to denature proteins. Cell lysates were loaded into wells (15µg per well) of a 15 well precast 4-15% Bis- Tris BioRad gel before being submerged in 1X Tris/Glycine/SDS buffer (25mM Tris, 192mM glycine, 0.1% (w/v) SDS, pH 8.3) prior to separation via SDS PAGE electrophoresis for 45 minutes to 1 hour at 130V. Proteins were then transferred onto nitrocellulose membrane (pore size 45 µm) (Amersham Bioscience) using the wet transfer method, a gel and membrane "sandwich" was constructed and then submerged in transfer buffer (20% methanol, 25mM Tris 190mM Glycine) for 90 minutes at 90V. Once transfer was complete membranes were blocked in 5% bovine serum albumin (BSA) in Tris buffered saline (20mM Tris, 140mM NaCl) with 0.1% (v/v) Tween®-20 (TBST) for 1 hour at room temperature. Primary antibodies against proteins of interest were diluted in 5% BSA in TBST and incubated with the membrane overnight at 4°C. Non- bound primary antibodies were removed with 3 TBST washes at 10-minute intervals. Membranes were incubated with HRP-conjugated secondary antibodies diluted in TBS containing 5% BSA/0.05% Tween for 1 hour at room temperature. Finally membranes were washed with TBS/0.05% Tween before being developed using ECL (Merck,Darmstadt, Germany) on an odyssey Fc imaging system (Li-cor). Band intensity was analysed using ImageJ. β-actin was used as a loading control for all blots, in addition proteins of interest were normalised to β-actin prior to comparing band intensity between different experimental conditions.

## 2.9 Gene expression analysis

### 2.9.1 RNA extraction and purification

Total RNA was extracted from endothelial cells using the Norgen total RNA purification kit, according to manufacturer's instructions: Cells were washed with PBS prior to lysis with RL buffer, the lysate was then added to microcentrifuge tube with 200µl of 100% ethanol. Next the lysate was centrifuged at ≥ 3,500 x g (~6,000 RPM) for 1 minute to allow the RNA to bind to a spin column. The bound RNA was then

washed before being eluted from the spin column into a collection tube. The purified RNA sample was then stored at -80$^{o}$C.

### 2.9.2 Quantitative real-time polymerase chain reaction

Isolated RNA (250 ng) was reverse transcribed to complementary DNA (cDNA) in a 20µl reaction volume using the QuantiNova reverse transcription kit (Qiagen) according to the manufacturer's instructions: Genomic DNA was removed to purify the RNA sample via incubation of samples in QuantiNova gDNA removal mix at 45$^{o}$C for 2 minutes. A reverse transcription master mix was added to each sample prior to reverse transcription. Samples were incubated at 25$^{o}$Cfor 3 minutes to allow primer annealing followed by 45$^{o}$C for 10 minutes, finally samples were incubated at 85$^{o}$C for 5 minutes to inactivate the reverse transcription enzyme and stop the reaction. Primers were designed using NCBI primer-blast and purchased from Merck (Darmstadt, Germany). PCR reactions were conducted using the CFX Connect RT PCR thermocycler (Biorad) in 96-well plates. For each reaction cDNA (125 ng/ml) ng/ml), primer mix (100 nM) and iQ SYBR® Green Supermix (Bio-Rad) were combined. Reaction conditions were as follows: One step of 95$^{o}$C for 5 minutes, then 40 cycles of 95$^{o}$C for 20 seconds, 62$^{o}$C for 20 seconds and 72$^{o}$C for 25 seconds. Ct values for genes of interest were normalised to the housekeeper gene RPLP0, before being analysed using the ΔΔCt method (Livak and Schmittgen, 2001). A list of primers is detailed in Table 2.4.

**Table 2.4 Primers used in this study**

| **Gene** | **Sequences** | |
|---|---|---|
| ENTPD1 | Forward | 5'ACACATCCATGTGCCCATCACA |
| | Reverse | 5'GGTGCCTTCCTCTGGATGCACT |
| NOS3 | Forward | 5'TCGGCCGGAACAGCACAAGA |
| | Reverse | 5'AAAGGCGCAGAAGTGGGGGT |
| PTGS1 | Forward | 5'ACGCACAGGAGCCTGCACTC |
| | Reverse | 5'GGTCAAGGCCGAAGCGGACA |
| PTGS2 | Forward | 5'CTGGGCCATGGGGTGGACTT |

| | | |
|---|---|---|
| | Reverse | 5’CCTGCCCCACAGCAAACCGT |
| RPLP0 | Forward | 5’GCAGCAGATCCGCATGTCCC |
| | Reverse | 5’TCCCCCGGATATGAGGCAGCA |

## 2.10 Statistical analysis

The number of biological repeats performed for each set of experiments were based on previously published data, all blood experiments were performed using blood from a minimum of three separate donors (Sasikumar P, et al. 2018; Unsworth A, et al. 2020). Data were analysed and, when appropriate, normalised to the vehicle control. Statistical analysis was carried out using GraphPad Prism software (GraphPad, San Diego, CA, USA), first a Shapiro-Wilk test was conducted to confirm normal distribution of data. Statistical significance was assessed by unpaired two-tailed Student’s t-test or one-way ANOVA. Post-hoc analysis was conducted on all ANOVA tests using either Bonferroni or Tukey analysis. For data sets without normal distribution an unpaired, non-parametric Mann-Whitney test was used to confirm significance. The level of significance of p-values was as follows: *$p \leq 0.05$, **$p \leq 0.01$, ***$p \leq 0.001$. All data were expressed as mean ± standard error of the mean (SEM).

# 3. Endothelial cells regulate thrombus formation when incorporated into an *in vitro* thrombosis model

## 3.1 Introduction

Currently there is no gold standard thrombosis model. Both *in vitro* and *in vivo* thrombosis models are beneficial tools for furthering our understanding of atherothrombosis (Coenen *et al*., 2017; Day *et al*., 2004). However, they are not without their limitations, with *in vivo* models often failing to accurately replicate the vascular environment observed in atherothrombosis. Firstly, the vessel of choice used in animal models, such as the mesenteric artery, are not the vessels typically associated with atherothrombosis in humans. Secondly, the animals used can be described as healthy and not suffering from atherothrombosis with a vessel wall injury being used to mimic a plaque rupture (Coenen *et al*., 2017). As described previously, the vessel environment is much more complex in atherothrombosis, with endothelial dysfunction playing a key role in the development of an occlusive thrombus (Davignon and Ganz, 2004; Gimbrone, 2017). In addition, there is a lot of variability between current *in vivo* methods, especially in terms of the damage stimuli used (Westrick *et al*., 2007). Multiple methods can be used to cause vessel injury and mimic plaque rupture including laser, chemical and physical damage methods (Westrick *et al*., 2007). This variation is further compounded by the fact there is a lack of standardisation, even within each damage type. For example, the concentration of ferric chloride used in studies that opt for this as a damage method varies greatly between studies, with some using a concentration of 2.5% (Wang and Xu, 2005) and others as high as 20% (Smyth *et al*., 2001). This variation between *in vivo* models and lack of standardisation is a major limitation of current *in vivo* thrombosis models.

Emerging humanised *In vitro* thrombosis models have addressed some of the limitations of *in vivo* animal models by using human whole blood and replicating the appropriate haemodynamic forces. However, variation between different models has been a growing issue, with recent technological advances allowing more innovative model design but at the cost of standardisation. This lack of

standardisation could present a major limitation as it makes comparing results difficult and potentially inaccurate. Another major limitation associated with current *in vitro* thrombosis models is that many fail to consider the role of the endothelium in the formation and regulation of a thrombus. Therefore, the development of a model which contains endothelial cells is essential for accurate modelling of atherothrombosis.

Thrombus formation in arteries is classically thought of as a platelet-driven process, with circulating platelets becoming activated in response to vessel wall injury and the exposure of ECM proteins (Gale, 2011; Jackson *et al*., 2009). The activated platelets begin to adhere to the site of injury and initiate the process of secondary signalling amplification, which is essential for recruiting circulating platelets to the site of the growing thrombus (Estevez and Du, 2017). In addition to platelet activation, vessel wall injury also initiates the coagulation cascade leading to the production of thrombin which is a potent platelet activator and is also key for the conversion of fibrinogen to fibrin which forms a mesh over the aggregated platelets and stabilises the thrombus (Hoffman M., 2003).

However, this view of thrombus formation is simplistic and does not consider the contributions of the endothelium. The endothelium is often thought of as a passive barrier between blood and the surrounding tissues, whereas in fact it is dynamic and shifts in response to the demands of the vessel environment. In a healthy undamaged blood vessel the endothelium inhibits both platelet activation and initiation of the coagulation cascade, in addition to activating fibrinolysis (Yau *et al*., 2015). The resting endothelium helps keep platelets in their quiescent state by releasing potent platelet inhibitors such as NO and prostacyclin. Additionally, endothelial CD39 preferentially hydrolyses ADP, a potent platelet activator and an important mediator of platelet aggregation (Hamilos *et al*., 2018).

The resting endothelium also inhibits the coagulation cascade through several anticoagulant mechanisms (Figure 1.6.1), such as releasing TFPI which can bind and inactivate the pro-coagulants factor VIIa and Xa (Hackeng *et al*., 2006; Palta *et al*., 2014). The endothelium also regulates coagulation via the production of heparan sulphate proteoglycans which activate antithrombin III, an anticoagulant responsible

for inactivating thrombin and factor Xa (van Hinsbergh, 2001). Endothelial cells also express thrombomodulin which can activate protein C, in turn inactivating factor Va and factor VIIIa, two key co-factors in the coagulation cascade (Ishii *et al*., 1986). The endothelium also plays a key role in regulating fibrinolysis, a process that prevents excessive clot growth. The key enzyme in this process is plasmin which is responsible for the breakdown of fibrin. Plasmin is activated by tissue plasminogen activator (tPA) which cleaves plasminogen at the Arg561–Val562 peptide bond to yield plasmin. tPA itself is synthesised and released into the vessel environment by the endothelial cells directly (Emeis, 1995; Rijken and Lijnen, 2009).

Upon vessel wall injury the endothelium no longer inhibits platelet adhesion or activation of the coagulation cascade, but instead shifts in response and drives activation of platelets and the coagulation cascade. ECM proteins such as collagen are exposed following vessel wall injury and initiate the process of platelet adhesion and platelet activation (Yau *et al*., 2015). In addition, the endothelium begins to release TXA2 which activates circulating platelets, close to the site of the vessel wall injury and begins the process of driving platelet signalling amplification (Yau *et al*., 2015). Endothelial cells also release von Willebrand factor (VWF) which is essential for facilitating platelet adhesion to the exposed collagen follow vessel wall injury (Stockschlaeder *et al*., 2014). VWF is released from the Weibel-Palade bodies of endothelial cells in the form of ultra-large multimers which form high strength bonds with platelets. This is essential in high shear vessels such as arteries where a collagen platelet bond alone is too weak to ensure the formation of a stable clot. VWF also plays an important role in the coagulation cascade by stabilising circulating factor VIII, this is achieved through non-covalent interactions which result in the formation of a tightly bound complex (Stockschlaeder *et al*., 2014).

The dynamic nature of the endothelium and the ability of endothelial cells to regulate platelet activity supports the incorporation of endothelial cells into a model that aims to accurately model thrombosis. Furthermore, the inclusion of endothelial cells, and potentially the incorporation of dysfunctional cells could have several advantages, including the assessment of antiplatelet drug efficacy in different vessel environments. Dual anti-platelet therapy (DAPT) is the standard of care for the

secondary prevention of coronary artery disease and involves the administration of two antiplatelet drugs, aspirin and a $P2Y_{12}$ inhibitor (Degrauwe *et al*., 2017). Aspirin blocks the cyclooxygenase (COX) enzyme in platelets and so inhibits the production of TXA2, a potent platelet activator and key mediator in the amplification of platelet aggregation. As discussed previously, when platelets are activated they release various secondary mediators that drive secondary amplification and encourage platelet aggregation. One of these potent mediators is ADP which activates platelets via the $P2Y_{12}$ receptor. By targeting TXA2 production and $P2Y_{12}$ receptor activation, DAPT prevents the secondary signalling amplification phase of platelet aggregation and therefore reduces the risk of thrombotic events (Wilson *et al*., 2017). The anti-thrombotic effects of DAPT were previously thought to be solely due to its effects on platelets. Emerging evidence has however suggested that mediators released from the endothelium may impact the effectiveness of DAPT and may explain some of the variability in response observed in some patients to this therapy. It has been suggested that blockade of the platelet $P2Y_{12}$ receptor enhances the anti-platelet activity of NO, with some evidence suggesting that $P2Y_{12}$ blockade may increase NO potency by 100,000 fold (Kirkby *et al*., 2013). In addition to $P2Y_{12}$ blockade potentiating NO activity, it has also been shown that $P2Y_{12}$ blockade may also enhance the anti-platelet activity of prostacyclin (Chan *et al*., 2016). It has previously been hypothesised that poor response to DAPT may be due to an individual's platelet response to the effects of aspirin or $P2Y_{12}$ inhibitors, but the emerging evidence suggests that the vessel environment should be considered when assessing the efficacy of DAPT (Chan *et al*., 2016). As studies have demonstrated that $P2Y_{12}$ blockade synergizes strongly with mediators released from the endothelium, the condition of a patient's endothelium may dictate the effectiveness of DAPT for that individual. For example, people with cardiovascular disease often experience endothelial dysfunction which leads to a reduction in the bioavailability of NO, which may explain poor DAPT efficacy in some patients with a history of cardiovascular disease. An endothelialised thrombosis model would allow for an accurate assessment of DAPT efficacy and enable the contribution of endothelial health on DAPT efficacy to be determined.

The aim of this chapter was to develop a simple *in vitro* model of thrombosis, which incorporated endothelial cells, sufficient in function and number to negatively regulate thrombus formation. The model was optimised and the contribution of endothelial-derived inhibitors assessed, as is observed *in vivo*. Next, this study aimed to induce endothelial activation and dysfunction, and assess the effect on thrombus formation. In addition, the model was utilised to assess DAPT drug efficacy in the presence of healthy and dysfunctional endothelial cells.

In this chapter, the initial version of the endothelialised thrombosis model was optimised and assessed. The impact of the presence of healthy endothelial cells was analysed and compared to that of dysfunctional endothelial cells. The effect of endothelial cells, both healthy and activated, on thrombus formation was analysed. Application of the model was also demonstrated in this chapter, with the model being used to assess DAPT efficacy in the presence of healthy and activated endothelial cells.

### 3.1.1 Aims and hypothesis

The principal aims of the work presented in this chapter were to:

1. Develop and characterize a simple fluidic based model of thrombosis, sensitive to regulation by endothelial cells incorporated into the fluidic chambers
2. Assess the effects of endothelial cell derived mediators on thrombus formation in the model
3. Establish an endothelialised model sensitive to endothelial dysfunction
4. Determine the contribution of healthy and dysfunctional endothelial cells to the efficacy of standard antiplatelet drugs

**Hypothesis**

Endothelial cells play a key role in regulating platelet activity, as a result endothelial dysfunction negatively effects antiplatelet drug efficacy.

## 3.2 Summary of *in vitro* model setups used in this chapter

Initial experiments were performed using an *in vitro* thrombosis model with exogenous derived platelet inhibitors as described in 2.4.1. Two reservoirs were attached to a stand, one for Tyrodes buffer and one for blood, these were connected to a three-way tap connected to siliconized tubing. Tubing was also connected to a withdrawal syringe pump, this allowed blood to be perfused through the collagen coated channel at a physiological relevant shear stress (1.5 dynes/cm$^2$) (Figure 2.1).

The first experiments incorporating endothelial cells into the *in vitro* thrombosis model utilised the setup described in 2.4.2. HUVECs were seeded onto *Ibidi µ-slide VI$^{0.4}$* slides (plating density 5 x10$^5$/ml) before being incubated for 48 hours at 37ºC with 5% $CO_2$ to allow a confluent monolayer to form. Alternate, HUVEC-free channels were coated with type I collagen fibrils (derived from equine tendons; Labmedics) (100µg/ml) one hour prior to blood perfusion. Siliconized connective tubing linked endothelialised channels upstream of collagen coated channels, this allowed blood to be perfused over endothelial cells before passing over collagen at a physiological relevant shear stress (1.5 dynes/cm$^2$) (Figure 2.2).

Later in the chapter a higher throughput model was developed which utilised a six-syringe pump setup as described in 2.4.3. Two Ibidi VI$^{0.4}$ µ-slides were connected to each other via siliconized tubing, HUVECs were seeded onto the first µ-slide (plating density 5 x10$^5$/ml) before being incubated for 48 hours at 37ºC with 5% $CO_2$ to allow a confluent monolayer to form. The channels of the second µ-slide were coated with type I collagen fibrils (derived from equine tendons; Labmedics) (100µg/ml) one hour prior to blood perfusion. The first µ-slide was connected to six pairs of reservoirs containing either Tyrodes buffer or human whole blood, via siliconized tubing. Corresponding channels of the two µ-slides were lined up and connected via siliconized tubing. The second µ-slide was connected to a six-syringe withdrawal pump, which enables blood to be perfused through all 6 channels per slide, over endothelial cells before passing over collagen at the same physiological relevant shear stress (1.5 dynes/cm$^2$) (Figure 2.3).

## 3.3 Results

### 3.3.1 Endothelial derived factors regulate thrombus formation

To demonstrate the role of endothelial cells in the regulation of platelet function and validate the importance of incorporating endothelial cells into a thrombosis model, the effect of exogenously applied endothelial-derived platelet inhibitors was investigated on thrombus formation under venous (Figure 3.1) and arterial (Figure 3.2) flow conditions. Using the standard *in vitro* thrombosis model described in section 2.3.1, thrombus formation on immobilised collagen (100μg/ml) was determined in the presence of 0.1% dimethyl sulfoxide (control), apyrase (4U/ml), $PGE_2$ (10μM) and NO donor sodium nitroprusside (SNP; 100μM). At a low wall shear stress of 1.5 dyne/$cm^2$, the presence of apyrase 30 min prior to and during perfusion (Figure 3.1.A, top right panel) resulted in a significant reduction in average thrombus size (Figure 3.1.B) (72.1%, $p<0.01$), in addition to a significant reduction in area coverage (Figure 3.1.C) (65.2%, $p<0.01$. Exogenous addition of $PGE_i$, which was used as a more cost-effective alternative to prostacyclin, and possesses a longer half-life, caused a significant reduction in average thrombi size (Figure 3.1.B) (54.8%, $p<0.05$), in addition to a significant reduction in area coverage (Figure 3.1.C) (40.1%, $p<0.05$). The incubation of sodium nitroprusside (SNP) in blood prior to perfusion over collagen at 1.5 dyne/$cm^2$ resulted in a significant reduction in in average thrombi size (58.6%, $p<0.05$), in addition to a significant reduction area coverage (Figure 3.1.C) (86.3%, $p<0.01$). Experiments performed at an arterial shear rate (5 dyne/$cm^2$), were performed in Ibidi VI $^{0.1}$ microslides, which allow higher shear rates to be achieved, with minimal blood required. Results demonstrated much larger thrombi compared to those under venous flow rates. The platelet-rich thrombi also lined up with the direction of flow along the collagen fibres. Under the higher shear conditions, apyrase failed to reduced thrombus adhesion (Figure 3.2.A, top right panel) indicated by area coverage or thrombus size. $PGE_1$ however, reduced thrombus size by 66% ($p<0.01$) (Figure 3.2.B) and area coverage by 10% ($p<0.05$) (Figure 3.2.C), while NO generated from SNP reduced thrombus size by 70% ($p<0.01$) (Figure 3.2.B) but did not reduce area coverage (Figure 3.2.C).

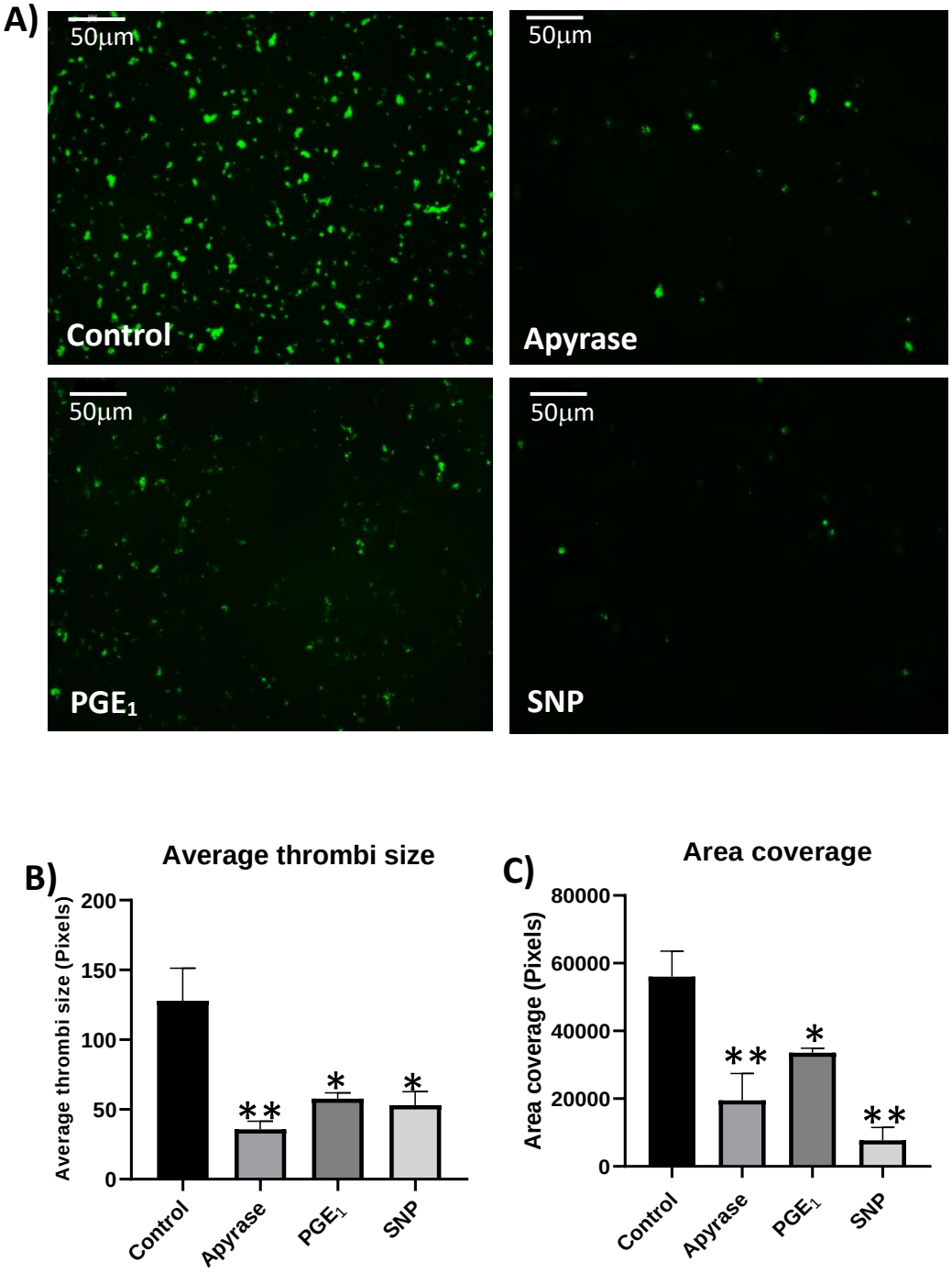


**Figure 3. 1 Endothelial derived factors regulate thrombus formation under venous shear stress**

Human whole blood incubated with $DIOC_6$ was perfused over collagen coated µ-slides in the presence of the NO donor, sodium nitroprusside (SNP-; 100µM), prostaglandin $E_2$ ($PGE_2$; 10µM), apyrase (4U/ml), or vehicle control. Platelet adhesion and thrombus formation were analysed using Celena® S digital imaging system (A). Average thrombi size (B) and area coverage (C) was calculated using Image J. Data represents mean ± SEM, n =3 (each n represents an individual donor, with 5 images taken per condition for analysis); *p<0.05; **p<0.01.

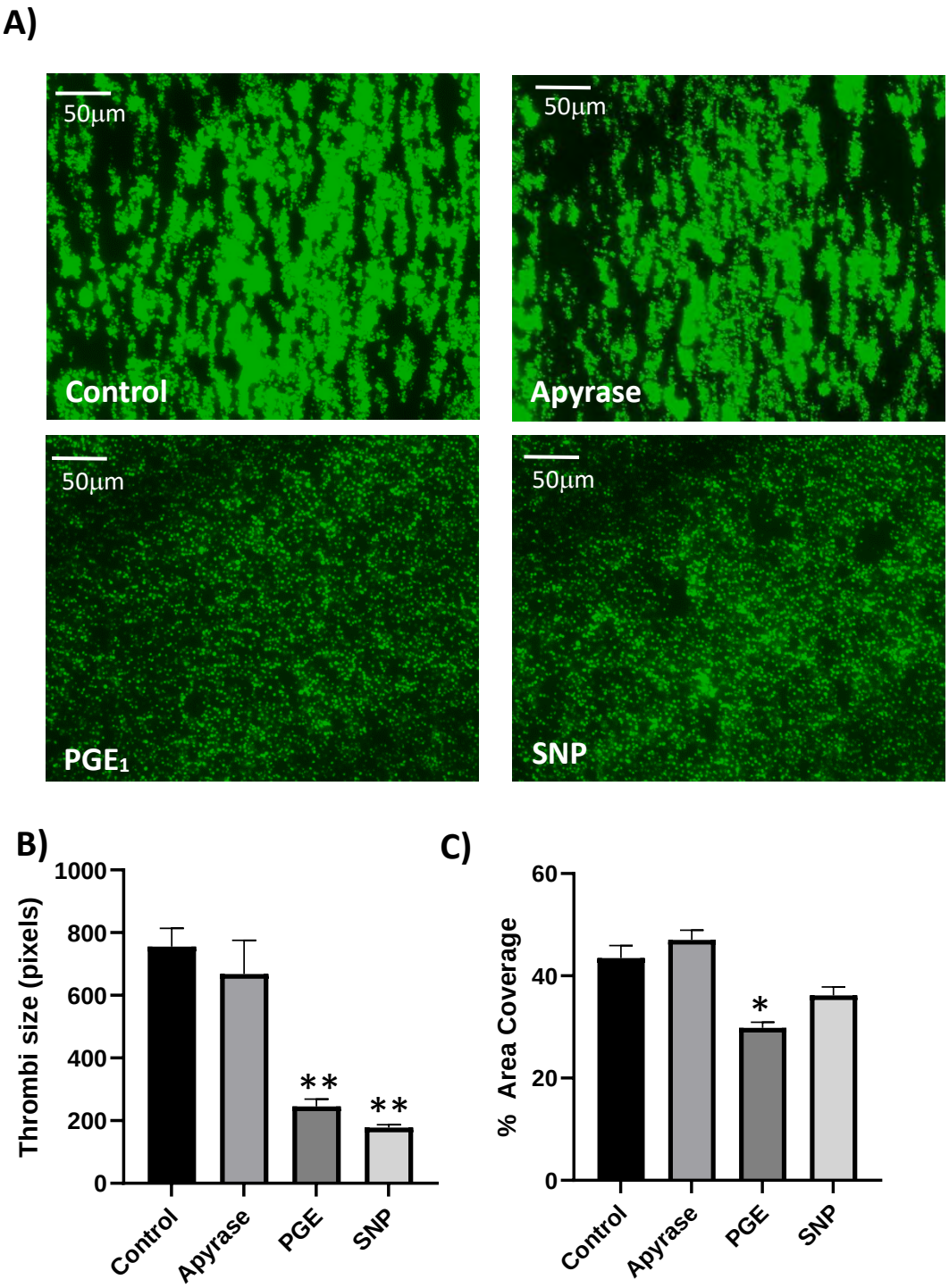


**Figure 3. 2 Endothelial derived factors regulate thrombus formation under arterial shear stress**

Human whole blood incubated with $DIOC_6$ was perfused over collagen coated µ-slides in the presence of the nitric oxide donor, sodium nitroprusside (SNP-; 100µM), prostaglandin E2 ($PGE_2$; 10µM), apyrase (4U/ml), or vehicle control at 15 dyne/$cm^2$. Platelet adhesion and thrombus formation was analysed using Celena® S digital imaging system (A). Average thrombi size (B) and area coverage (C) was calculated using Image J. Data represents mean ± SEM, n =5 (each n represents an individual donor, with 5 images taken per condition for analysis); *p<0.05; **p<0.01.

### 3.3.2 Incorporation of endothelial cells into the model

Experiments using the basic model, successfully demonstrated that endothelial derived soluble mediators could regulate thrombus formation at venous and arterial wall shear stress. It also gave an indication of the contributions of each of the inhibitors under the different shear conditions. The next step in the optimisation of the model was the incorporation of endothelial cells. The closed nature of microfluidic chambers makes it difficult to access the channel to evoke damage which would expose the subendothelial matrix. The simplest approach to include endothelial cells in the model was therefore to seed endothelial cells in an a chamber immediately upstream to a chamber with immobilised collagen.

Using Ibidi VI $^{0.4}$ microslides, chambers were paired, the upstream chamber in each pair being seeded with HUVECs and the downstream being coated with collagen (100μg/ml). HUVECS were seeded 48h prior to the experiment, to allow a confluent monolayer to form (Figure 3.4.A), and collagen coating was performed 1h prior to the experiments. The paired chambers were connected with a small section of silicone tubing. This setup allowed blood to be perfused over the endothelial cells prior to perfusion over collagen, at a physiologically relevant shear rate (Figure 2.3.2) HUVECs were chosen at this initial stage as they represent the most commonly used type of human endothelial cell and they are the most cost effective. A no cell control was used for these experiments, with the upstream chamber containing no cells and the downstream coated with collagen (100μg/ml).

In the initial stages of development, a low shear stress was used due to the size of the microfluidic chambers adopted. Ibidi VI$^{0.4}$ microslides were used in the model initially, to facilitate maximal endothelial cell content, to enhance the probability of there a being sufficient number of endothelial cells to regulate thrombus growth. However, the relatively large diameter of the chambers restricted experiments to 1.5 dyne/cm$^2$, due to the flow rate and therefore amount of blood that would be required to achieve higher shear rates.

Results demonstrated that the incorporation of endothelial cells resulted in a significant reduction in average thrombi size (31.0%, $p<0.05$, Fig 3.3.B), in addition to

a significant reduction thrombi area coverage (34.9%, $p<0.001$, Fig 3.3.C). Analysis of the HUVEC coated chambers following the experiments confirmed that an intact monolayer remained following completion of each experiment and that there was no platelet adhesion or thrombus formation on the HUVECs themselves (Figure 3.4).

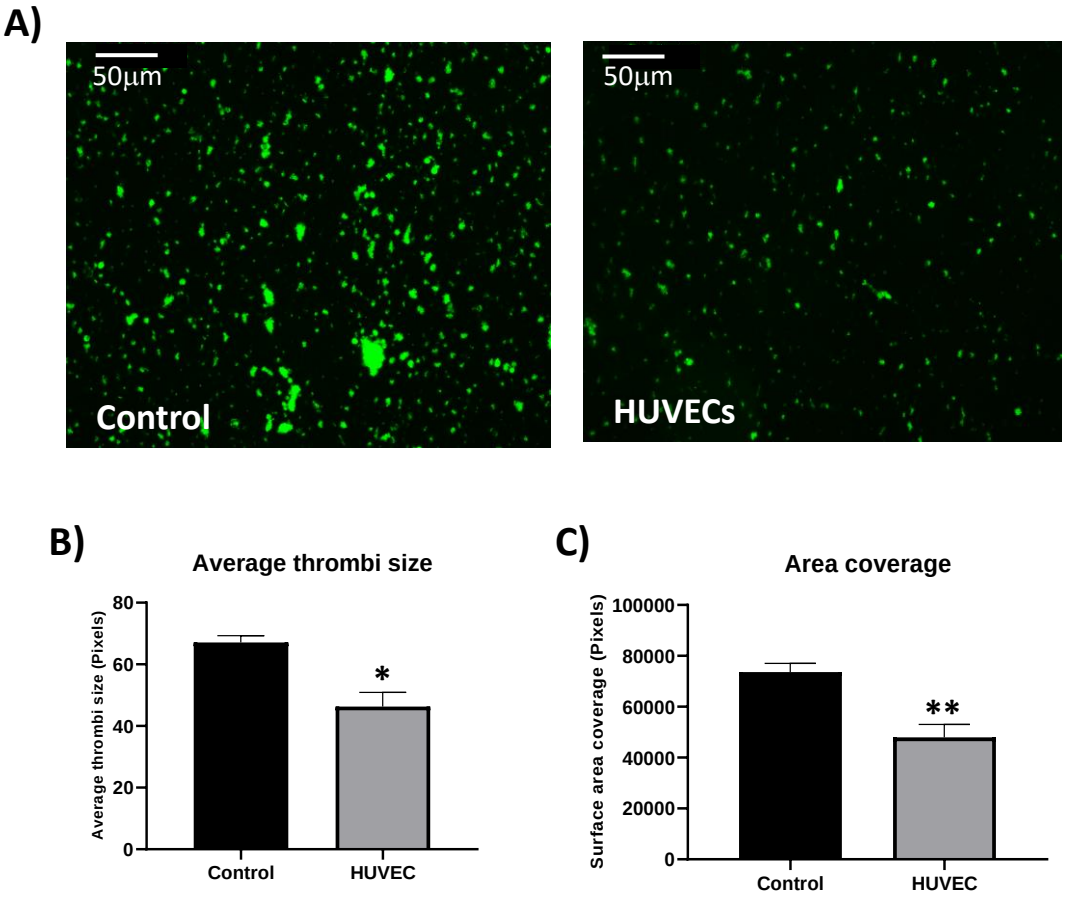


**Figure 3. 3 Incorporation of endothelial cells reduces thrombus formation**

Whole blood labelled with $DIOC_6$ was perfused through HUVEC coated chambers prior to collagen coated chambers and platelet adhesion and thrombus size analysed (A). The presence of HUVECs significantly reduced thrombi size (B) and area coverage (C). Data represents mean ± SEM; n=5 (each n represents an individual donor, with 5 images taken per condition for analysis) *$p<0.05$, **$p<0.01$

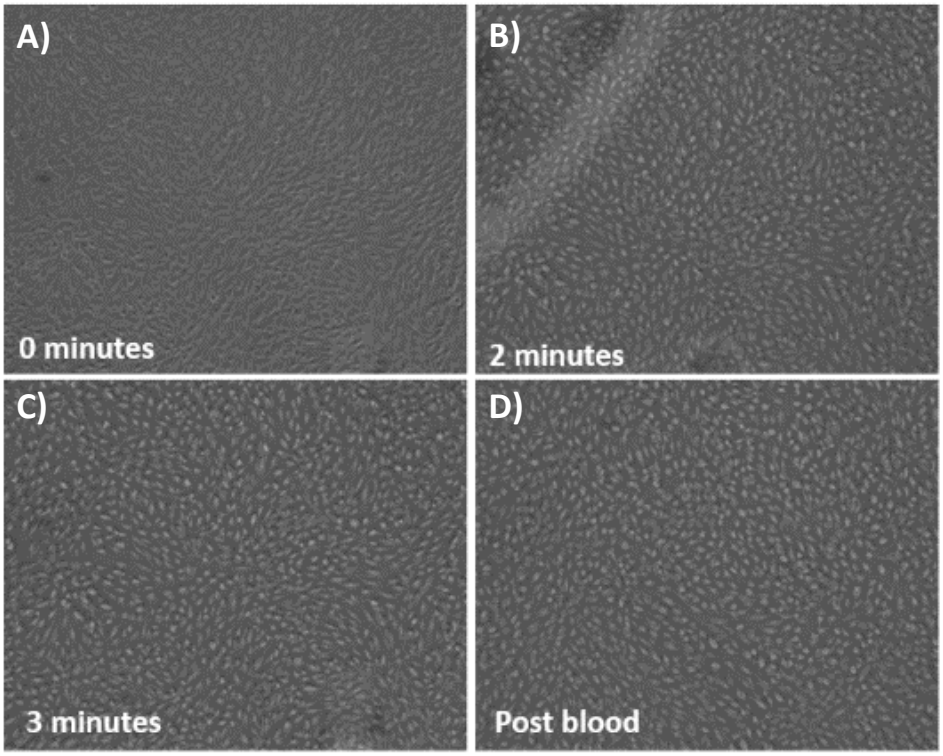


**Figure 3. 4 A confluent monolayer of endothelial cells which remain intact following blood perfusion at shear stress**

Endothelial cells were cultured on µ-ibidi slides for 48 hours prior to blood perfusion (A). We were able to demonstrate endothelial cells remained intact following several minutes of Tyrodes-HEPES perfusion (B,C). In addition, the confluent monolayer was still consistent following blood perfusion (D).

### 3.3.3 Elucidating the mechanism responsible for HUVEC-mediated reduction in thrombus formation observed in the model

Assessment of exogenously added endothelial derived platelet inhibitors (Figure 3.1) demonstrated that under low shear stress conditions, CD39, prostacyclin and NO could negatively regulate platelet activation and thrombus formation. However, these experiments were performed using standard experimental doses of apyrase, $PGE_1$ and SNP. To establish which of these mediators was responsible for reduced thrombus formation mediated by HUVECs, experiments were performed in the presence of pharmacological inhibitors. L-NNA is a NO synthase inhibitor that potently inhibits endothelial NO synthase (eNOS) and was therefore chosen to assess the contributions of eNOS in the endothelialised model. HUVECs were incubated with L-NNA (100µM) or DMSO (0.1%) for 30 minutes, then washed with Tyrodes buffer prior to perfusion with human whole blood. Thrombus formation on collagen was then assessed (Figure 3.5.A). Incubation with L-NNA significantly increased average thrombi size (28.3%, $p<0.001$) (Figure 3.5.B), in addition to significantly increasing area coverage (46.4%, $p<0.05$) (Figure 3.5.C).

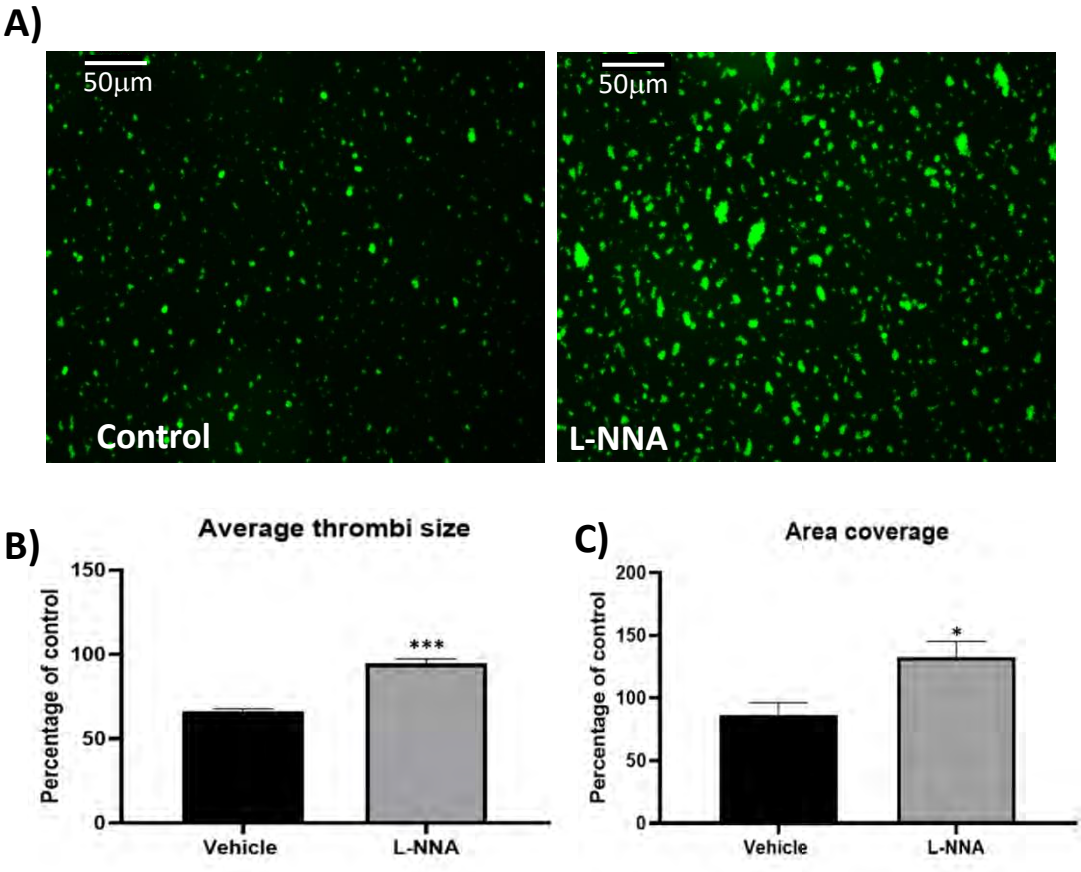


**Figure 3. 5 Inhibition of eNOS leads to an increase in thrombus size**

Whole blood labelled with $DIOC_6$ was perfused through HUVEC coated chambers following 30-minute treatment with L-NNA (100μM) or vehicle control, prior to perfusion over immoblised collagen, platelet adhesion and thrombus size were then analysed (A). Incubation with L-NNA significantly increased average thrombi size (B), in addition to significantly increasing area coverage (C). Data represents mean ± SEM; n=3 (each n represents an individual donor, with 5 images taken per condition for analysis). *p<0.05, ***p<0.001.

### 3.3.4 Inhibition of COX enzymes had no significant effect on thrombus formation

Endothelial-derived $PGI_2$ acts as a potent vasodilator and inhibitor of platelet activation *in vivo*. The cyclooxygenase enzymes, COX-1 and COX-2 are responsible for the production of $PGI_2$ in endothelial cells. The non-selective COX inhibitor indomethacin was used to determine if $PGI_2$ was responsible for the reduction in thrombus formation observed in the endothelialised model. HUVECs were incubated with indomethacin (10µM) or DMSO (0.1%) for 30 minutes, then washed thoroughly with Tyrodes buffer prior to perfusion with human whole blood. Thrombus formation on collagen was then assessed (Figure 3.6.A). Incubation with indomethacin had no significant effect on average thrombi size (21.4%, p=0.065) (Figure 3.6.B) or area coverage (15.1%, p=0.391) (Figure 3.6.C), compared to the unstimulated control.

The COX-1 enzyme is responsible for the production of the potent platelet activator Thromboxane A2 in platelets. As indomethacin is a non-selective inhibitor any indomethacin not cleared by the Tyrodes has the potential to inhibit the COX-1 enzyme in platelets. As COX-2 is reported to be the main producer of $PGI_2$ in endothelial cells, Celecoxib, a selective COX-2 inhibitor, was used in a second set of experiments. This would prevent any effects on platelet COX activity and further determine if endothelial derived $PGI_2$ was exerting any effect in the endothelialised model. HUVECs were incubated in celecoxib (10µM) or DMSO (0.1%) for 30 minutes, then washed thoroughly with Tyrodes buffer prior to perfusion with human whole blood. Thrombus formation on collagen was then assessed (Figure 3.7.A). Incubation with celecoxib had no significant effect on average thrombi size (14.4%, p=0.298) (Figure 3.7.B) or area coverage (2.1%, p=0.933) (Figure 3.7.C), compared to the unstimulated control.

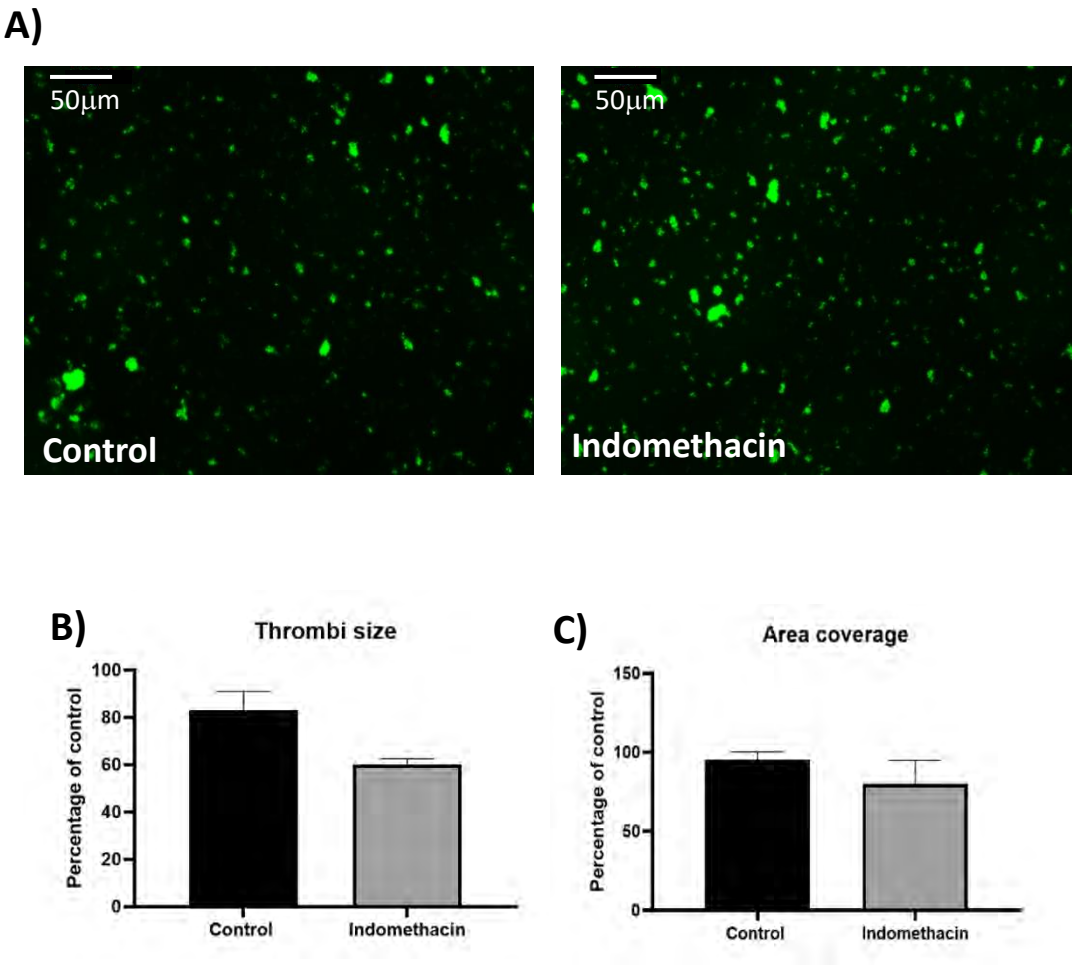


**Figure 3. 6 Inhibition of COX enzymes had no significant effect on thrombus formation**

Whole blood labelled with $DIOC_6$ was perfused through HUVEC coated chambers following 30-minute treatment with indomethacin (10μM) or vehicle control, prior to perfusion over immoblised collagen, platelet adhesion and thrombus size were then analysed (A). Incubation with indomethacin had no significant effect on average thrombi size (B) or area coverage (C). Data represents mean ± SEM; n=3 (each n represents an individual donor, with 5 images taken per condition for analysis).

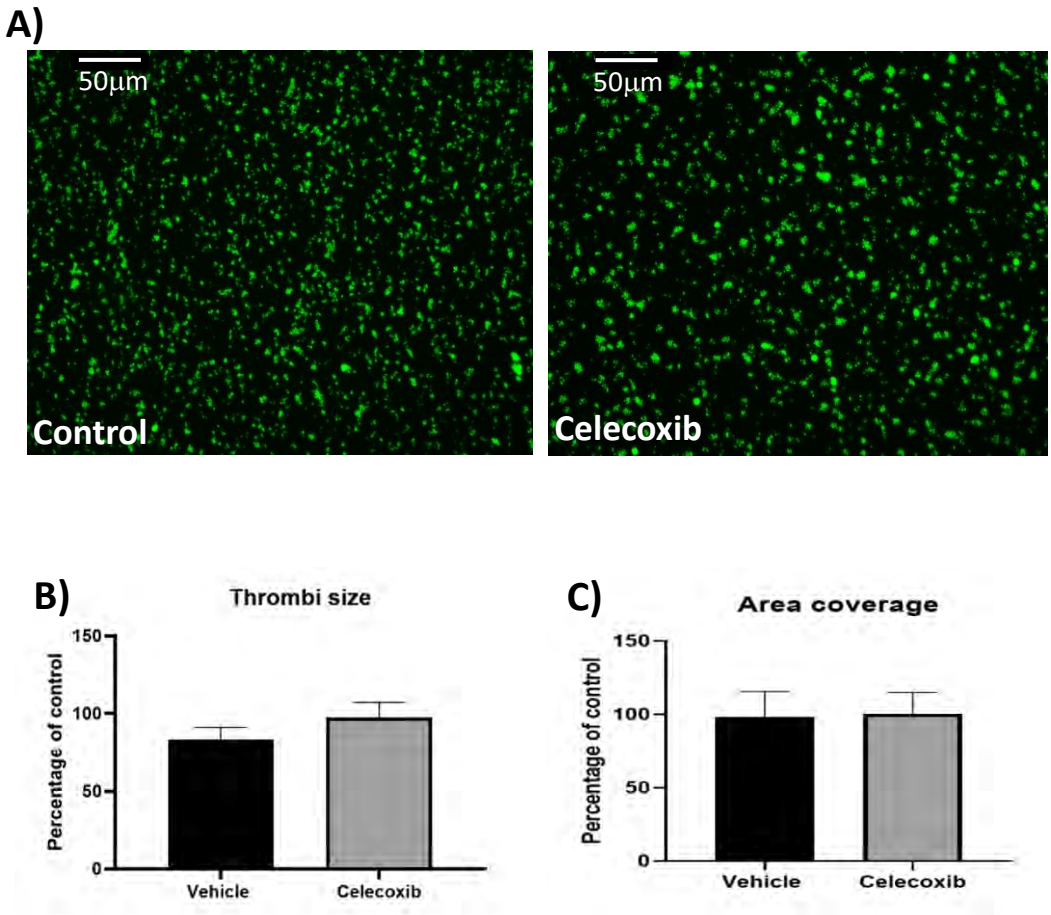


**Figure 3. 7 Selective inhibition of COX-2 has no effect on thrombus formation**

Whole blood labelled with $DIOC_6$ was perfused through HUVEC coated chambers following 30-minute treatment with celecoxib (10µM) or vehicle control, prior to perfusion over immoblised collagen, platelet adhesion and thrombus size were then analysed (A). Incubation with indomethacin had no significant effect on average thrombi size (B) or area coverage (C). Data represents mean ± SEM; n=3 (each n represents an individual donor, with 5 images taken per condition for analysis).

### 3.3.5 Inhibition of CD39 significantly increases thrombi size

Next, the effects of endothelial derived CD39 in the model was assessed to determine if it contributes to the reduction in thrombus formation observed when endothelial cells were present. CD39 is an ectonucleotidase responsible for the hydrolysis of the potent platelet activator ADP, converting it to AMP (Kanthi *et al*., 2014). POM-1 is an ecto-NTPDase inhibitor which has demonstrated selectivity for CD39 (Alvarez-Sanchez *et al*., 2019), HUVECs were incubated with POM-1 (100µM) or DMSO (0.1%) for 30 minutes, then washed thoroughly with Tyrodes buffer prior to perfusion with human whole blood. Thrombus formation on collagen was then assessed (Figure 3.8.A). Incubation with POM-1 significantly increased average thrombi size (Figure 3.8.B) (13.7%, $p<0.05$), in addition to an increase in area coverage (Figure 3.8.C) (20.6%, $p<0.01$).

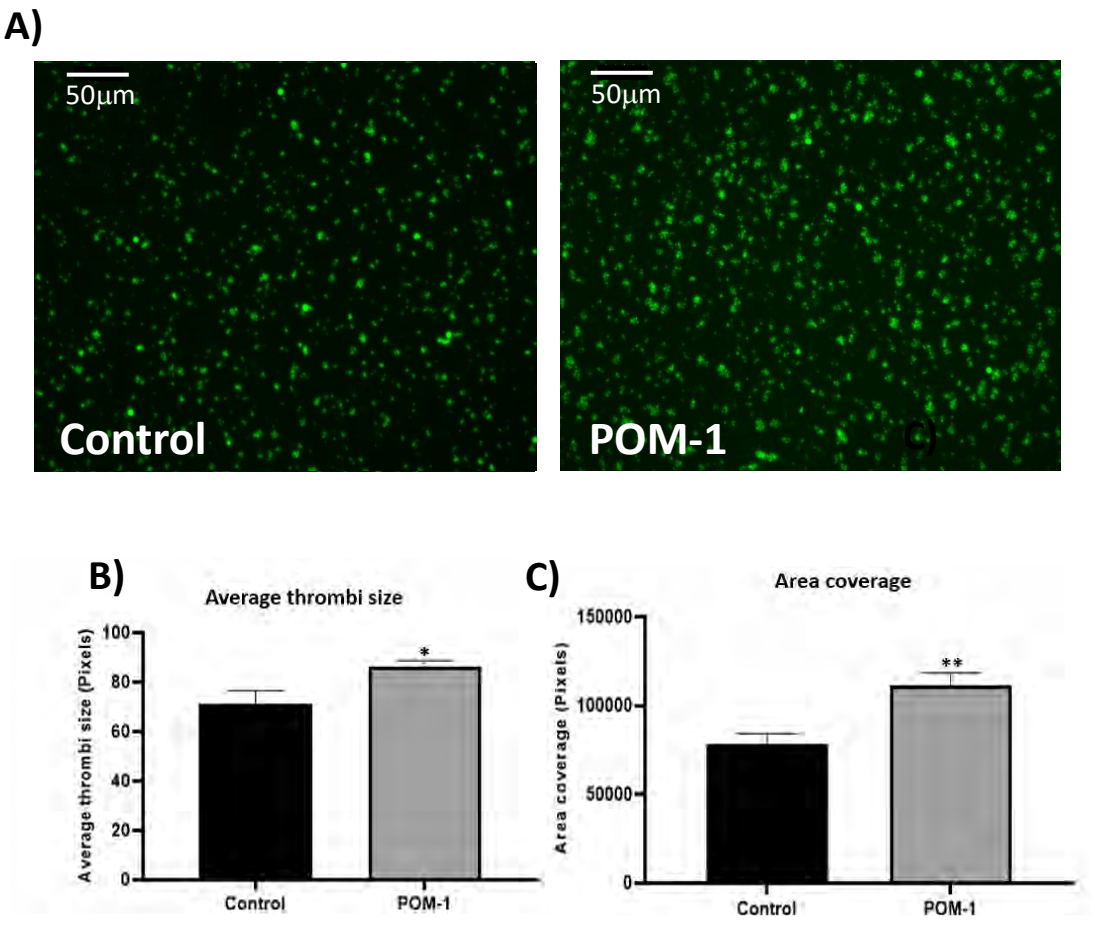


**Figure 3. 8 Inhibition of CD39 significantly increases thrombi size**

Whole blood labelled with $DIOC_6$ was perfused through HUVEC coated chambers following 30-minute treatment with POM-1 (100µM) or vehicle control, prior to perfusion over immoblised collagen, platelet adhesion and thrombus size were then analysed (A). Incubation with POM-1 significantly increased average thrombi size (B) ($p<0.05$) and area coverage ($p<0.01$) (C). Data represents mean ± SEM; n=3 (each n represents an individual donor, with 5 images taken per condition for analysis).

### 3.3.6 TNF-alpha stimulation increases cell adhesion molecule expression

Following the successful incorporation of healthy endothelial cells into the model, and confirmation that model was sensitive enough to detect the anti-thrombotic effects of endothelial cells, the next goal was to assess whether endothelial cell activation had an impact on thrombus formation and if the model could detect it. The vessel environment in cardiovascular disease is pro-inflammatory and is associated with the release of pro-inflammatory cytokines such as TNF-alpha (Lusis A, 2000). As a result, it was decided that TNF-alpha stimulation should be used to mimic the endothelial activation and endothelial dysfunction observed in cardiovascular disease. First, it was essential to ensure that TNF-alpha elicited a response comparable to that already reported (Teasdale *et al*., 2017; Xia *et al*., 1998). Several studies have reported changes in endothelial cell morphology following TNF-alpha stimulation, with cells becoming more elongated (Stroka *et al*., 2012). Brightfield imaging demonstrated that following 24 hours incubation with TNF-alpha (10ng/µl), the HUVECS changed from a classical cobblestone morphology to the more elongated phenotype (Figure 3.9.A). Another well characterised effect of TNF-alpha stimulation of endothelial cells is the increase in expression of the inflammatory cell adhesion molecules ICAM-1 and VCAM-1. Western blotting (Figure 3.9.C) revealed that following 24 hours incubation with TNF-alpha (10ng/ul) VCAM-1 (Figure 3.9.C) and ICAM-1 (Figure 3.9.D) levels were significantly increased ($p<0.01$).

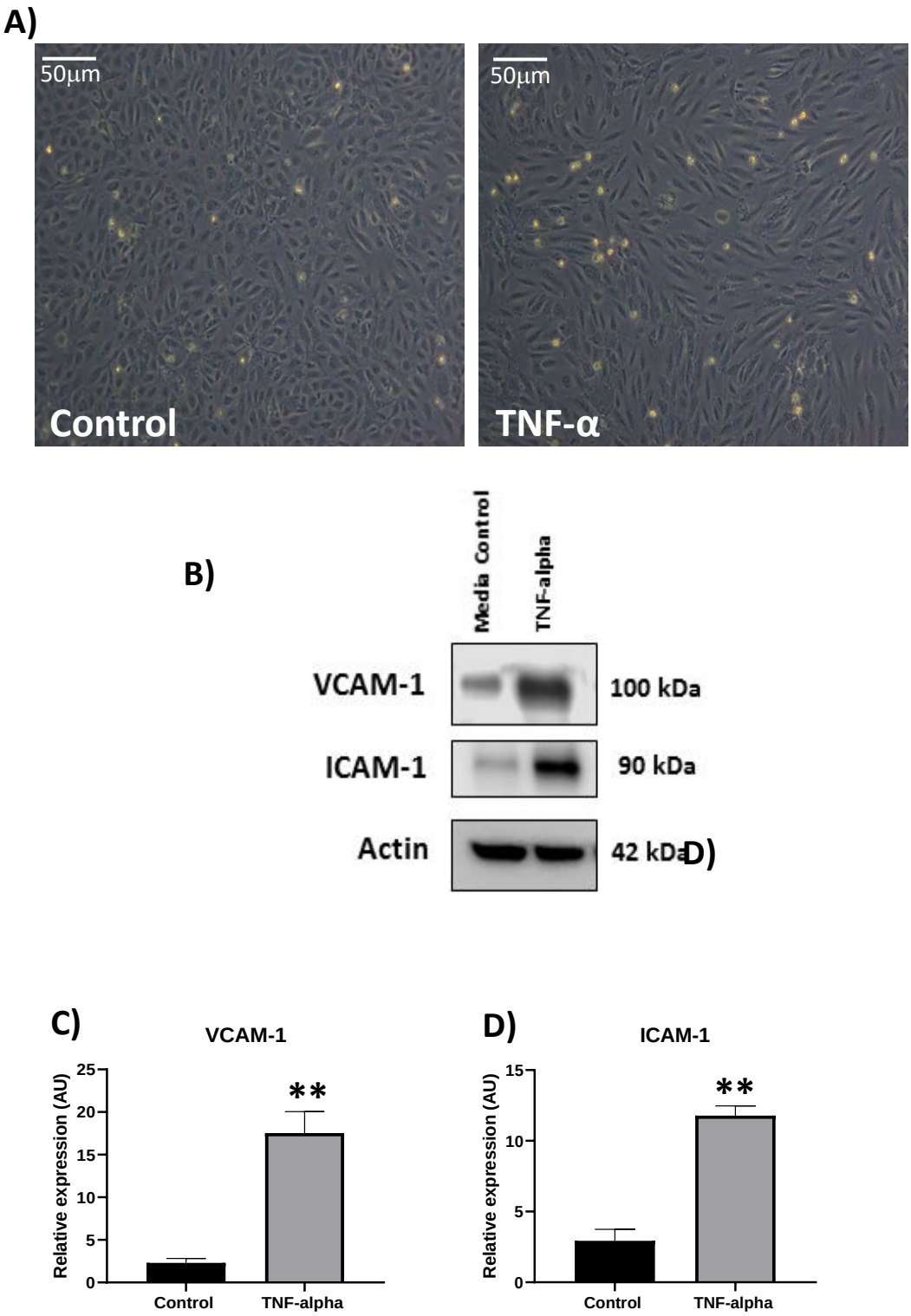


**Figure 3. 9 HUVEC activation following TNF-alpha treatment**

Following stimulation with TNF-alpha (10ng/ml) for 24h, HUVECs were imaged using brightfield microscopy (A) prior to being lysed for Western blotting (B). Western blots demonstrated increased VCAM-1 ($p<0.01$) (C) and ICAM-1 ($p<0.01$) (D). Data represents mean ± SEM relative expression following normalisation to β-actin; n=3 ***p<0.01*

### 3.3.7 TNF-alpha abolished anti-thrombotic effects of HUVECs

The next step in the optimisation of the model was the incorporation of TNF-alpha activated endothelial cells, in order to replicate the pro-inflammatory vessel environment observed in atherothrombosis. This was achieved by culturing human umbilical vein endothelial cells (HUVECs) in chambers, upstream to ones lined with collagen and stimulated with TNF-alpha (10ng/ul) for 24 hours (Figure 2.3.2). A no cell control was used in addition to a channel lined with unstimulated HUVECs. Thrombus formation on the collagen following perfusion of human whole blood was then assessed (Figure 3.10.A). As previously demonstrated, the presence of healthy endothelial cells significantly reduced thrombi area coverage (Figure 3.10.B) (41.1%, $p<0.05$) in addition to a significant reduction in average thrombi size (Figure 3.10.C) (39.4%, $p<0.05$). The incorporation of activated endothelial cells resulted in a significant increase in area coverage (Figure 3.10.B) (45.4%, $p<0.05$) in addition to a significant increase in average thrombi size (Figure 3.10.C) (31.0%, $p<0.05$), when compared with unstimulated HUVECs.

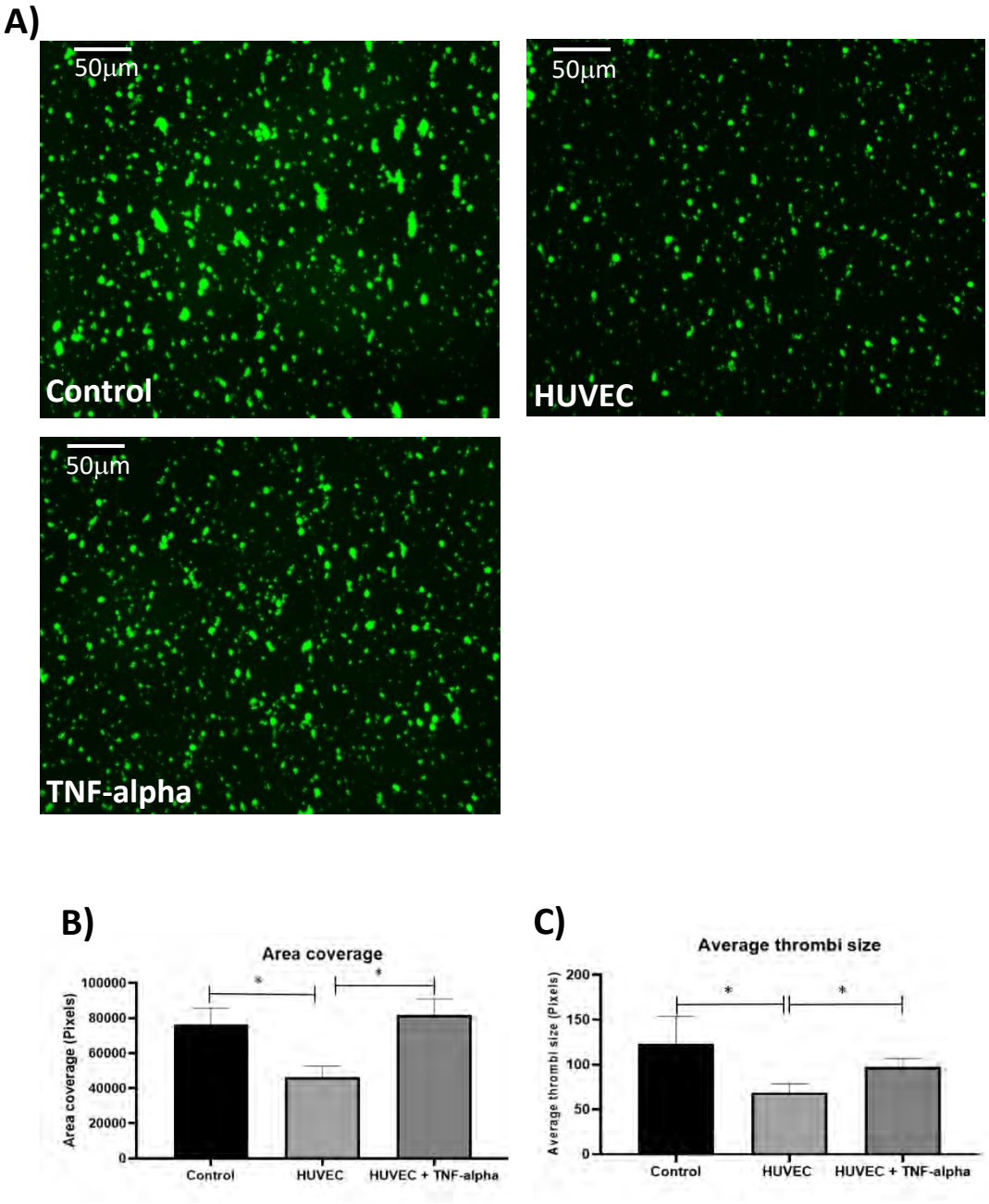


**Figure 3. 10 Activation of endothelial cells abolishes anti-thrombotic protection**

Whole blood labelled with $DIOC_6$ was perfused through HUVEC coated chambers following 24h treatment with TNF-alpha or vehicle control, prior to perfusion over immoblised collagen and platelet adhesion and thrombus size analysed (A). Endothelial activation significantly increased area coverage (B) and average thrombi size (C) activation significantly increased area. Data represents mean ± SEM; n=3 (each n represents an individual donor, with 5 images taken per condition for analysis). *p<0.05.

### 3.3.8 TNF-alpha significantly reduces eNOS levels

As previously shown, inhibiting eNOS with HUVECs present in the model lead to an increase in thrombus formation, indicating that eNOS may be having an effect in the endothelialised model. Therefore, it was important to determine if TNF-alpha stimulation was having any effect on eNOS levels, as a loss of eNOS may be responsible for the increase in thrombus formation observed when TNF-alpha stimulated endothelial cells were present in the model. eNOS undergoes phosphorylation at a number of sites including serine 1177 (S1177), which leads to eNOS activation. Western blotting (Figure 3.11.A) revealed that TNF-stimulation significantly reduced eNOS phosphorylation (Figure 3.11.B) ($p<0.05$), further blotting revealed a significant reduction in total eNOS (Figure 3.11.C) ($p<0.01$) following TNF-alpha stimulation. Real time PCR was used to assess the effect of TNF-alpha stimulation on eNOS gene expression. TNF-alpha stimulation significantly reduced eNOS gene expression (Figure 3.11.D) ($p<0.01$).

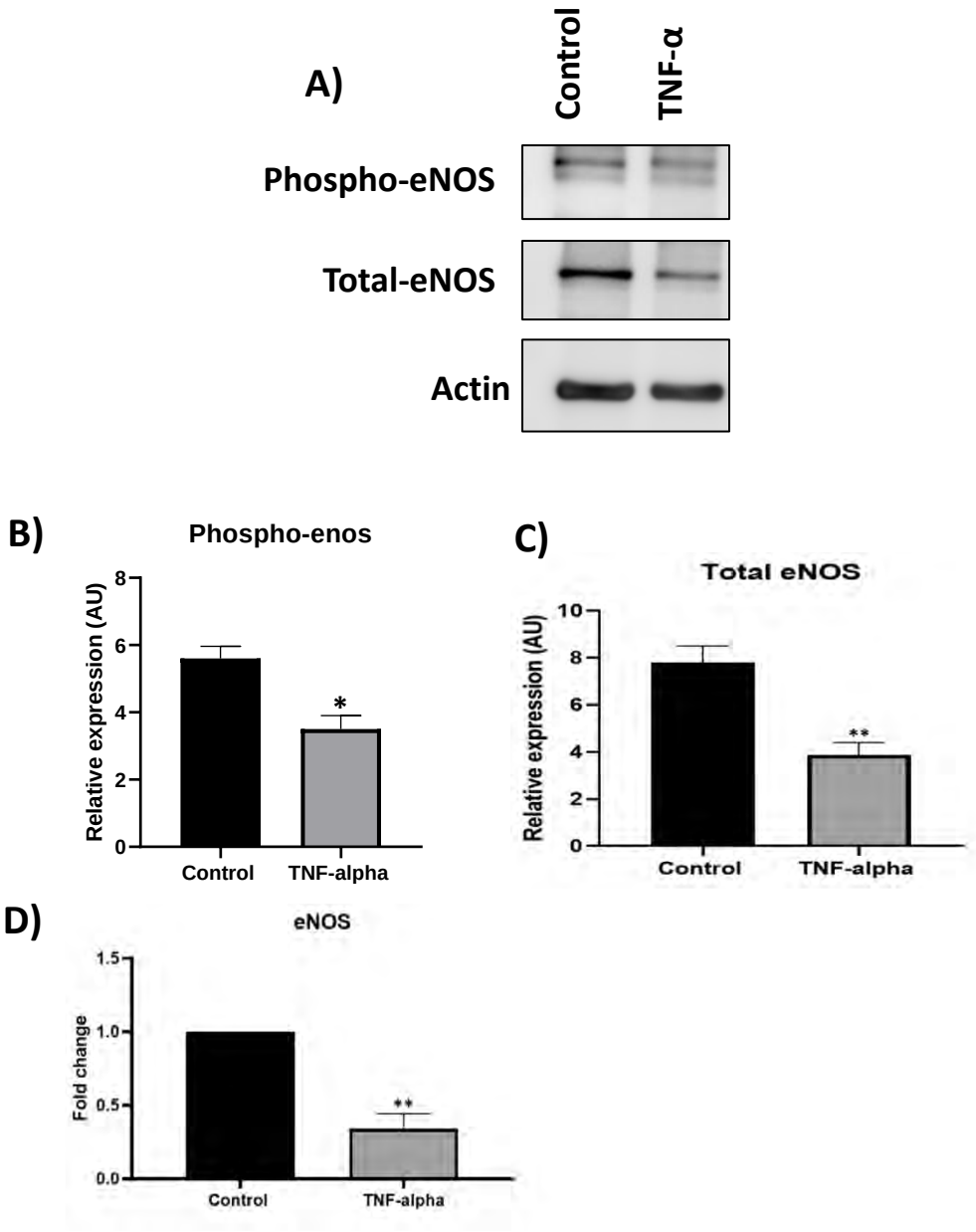


**Figure 3. 11 TNF-alpha significantly reduces eNOS levels**

HUVECs were stimulated with TNF-alpha (10ng/µl) for 24h prior to being lysed for western blotting and real time PCR. Western blots analysed changes in phosphor-eNOS and total eNOS (A), a significant decrease in phosphor-eNOS (B) and total eNOS (C) protein levels following TNF-alpha stimulation was observed. A significant decrease in eNOS gene expression was demonstrated following TNF-α stimulation (D). (A) is a representative blot, Data represents mean ± SEM relative expression following normalisation to β-actin; n=3, ***p<0.01.*

### 3.3.9 TNF-alpha has no effect on COX-1 levels but significantly increases expression of COX-2

The incorporation of TNF-alpha activated endothelial cells into the model resulted in changes in thrombus formation. Therefore, it was important to determine if TNF-alpha was having any effects on endothelial derived platelet mediators and elucidate the mechanism responsible for the increase in thrombus formation following TNF-alpha stimulation. Real time PCR was used to assess any changes in COX-1 and COX-2 gene expression, following 24-hour TNF-alpha (10ng/µl) stimulation, in addition to western blotting to assess any changes in protein levels (Figure 3.12.A). There was no significant difference in COX-1 gene expression in the TNF-alpha stimulated HUVECS compared to unstimulated HUVECS (Figure 3.12.D). In addition, western blotting revealed no significant changes in COX-1 protein levels following TNF-alpha stimulation (Figure 3.12.B). In contrast, a significant increase in both COX-2 gene expression ($p<0.01$; Figure 3.12.E) and protein levels ($p<0.05$; Figure 3.12.C) were observed following TNF-alpha stimulation.

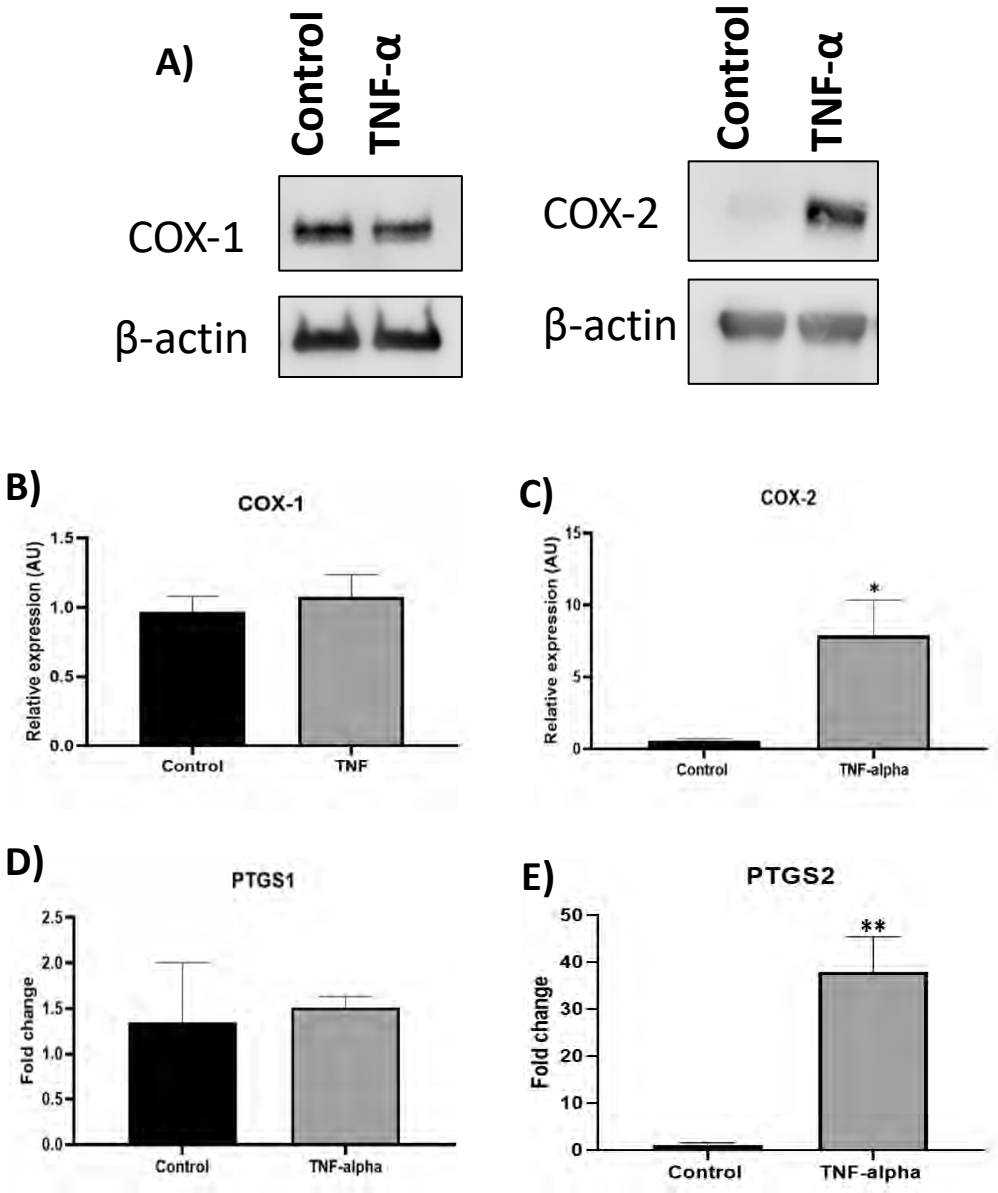


**Figure 3. 12 TNF-alpha has no effect on COX-1 levels but significantly increases expression of COX-2**

HUVECs were stimulated with TNF-alpha (10ng/ml) for 24h prior to being lysed for Western blotting (A) and real time PCR. Western blots demonstrated no significant changes in COX-1 (B) and a significant increase in COX-2 (C) following TNF-α stimulation. No significant changes in COX-1 gene expression were observed (D). A significant increase in COX-2 gene expression was demonstrated following TNF- α stimulation (E). Data represents mean ± SEM relative expression following normalisation to β-actin; n=3 **p<0.05, **p<0.01*

### 3.2.10 TNF-alpha reduces CD39 levels

It was previously shown (page 73) that a reduction in CD39 can lead to an increase in thrombus formation, therefore it was important to assess if TNF-alpha stimulation had any effect on CD39 expression. Real time PCR was used to assess any changes in gene expression following 24-hour TNF-alpha (10ng/µl) stimulation, in addition to western blotting (Figure 3.13.A) to assess any changes in protein levels. No significant changes in CD39 protein levels were observed following TNF-alpha stimulation (Figure 3.13.B). Real time PCR revealed a significant reduction in CD39 gene expression ($p<0.001$; Figure 3.13.C) following TNF- alpha stimulation.

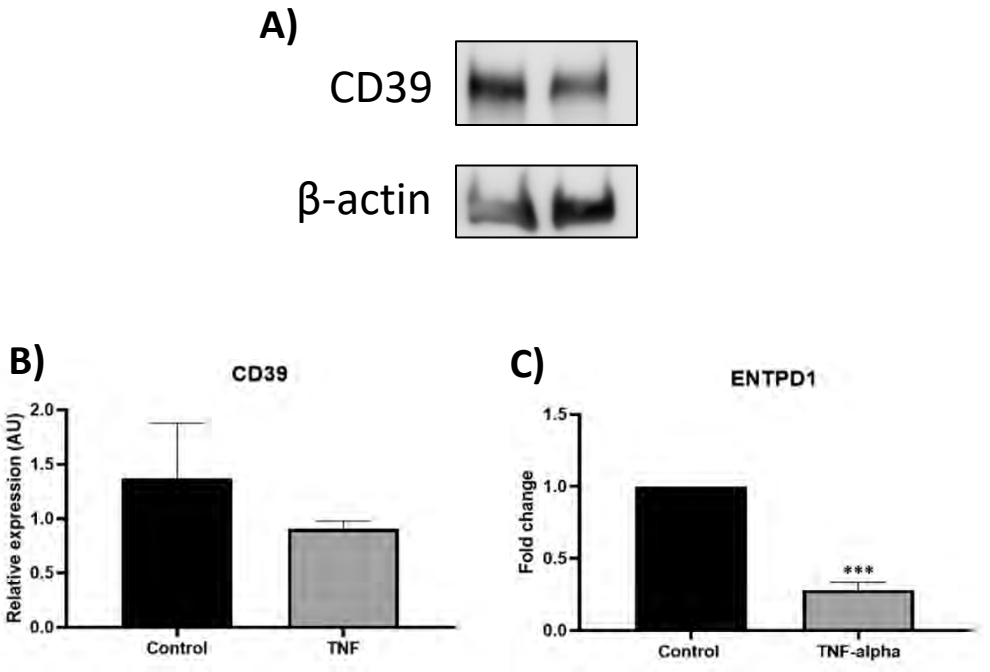


**Figure 3. 13 TNF-alpha reduces CD39 levels**

HUVECs were stimulated with TNF-alpha (10ng/ml) for 24h prior to being lysed for western blotting (A) and real time PCR. Western blots demonstrated no significant changes in CD39 protein levels following TNF-alpha stimulation (A). A significant decrease in ENTPD1 gene expression was demonstrated following TNF- α stimulation (B). Data represents mean ± SEM relative expression following normalisation to β-actin; n=3*, ***p<0.001*

### 3.2.11 Increasing the throughput of the model

Considering the potential applications of the model it was determined that ideally researchers may wish to compare multiple conditions at the same time, therefore increasing the throughput of the model was essential for optimisation of the model and for encouraging uptake by other researchers. To achieve this, the syringe pump was updated from a single pump to a six-syringe version, the new incarnation of the model would use two Ibidi micro-slides instead of a single slide. One slide would have channels lined with endothelial cells and the second slide with channels coated with collagen. The two slides were set up adjacent to each other and joined with connective tubing, this allowed blood to be perfused over the endothelial cell channels prior to perfusion over the collagen channels. It was important to investigate if there was any variation or significant difference between the different channels. To assess this, a model run was performed on a single six channel collagen coated slide with blood from one donor, this was repeated three times. Thrombus formation on the individual collagen channels following perfusion of human whole blood was then assessed (Figure 3.14.A). There was no significant difference in average thrombi size (Figure 3.14.B) between the channels in addition to no significant difference in platelet area coverage (Figure 3.14.C).

A)

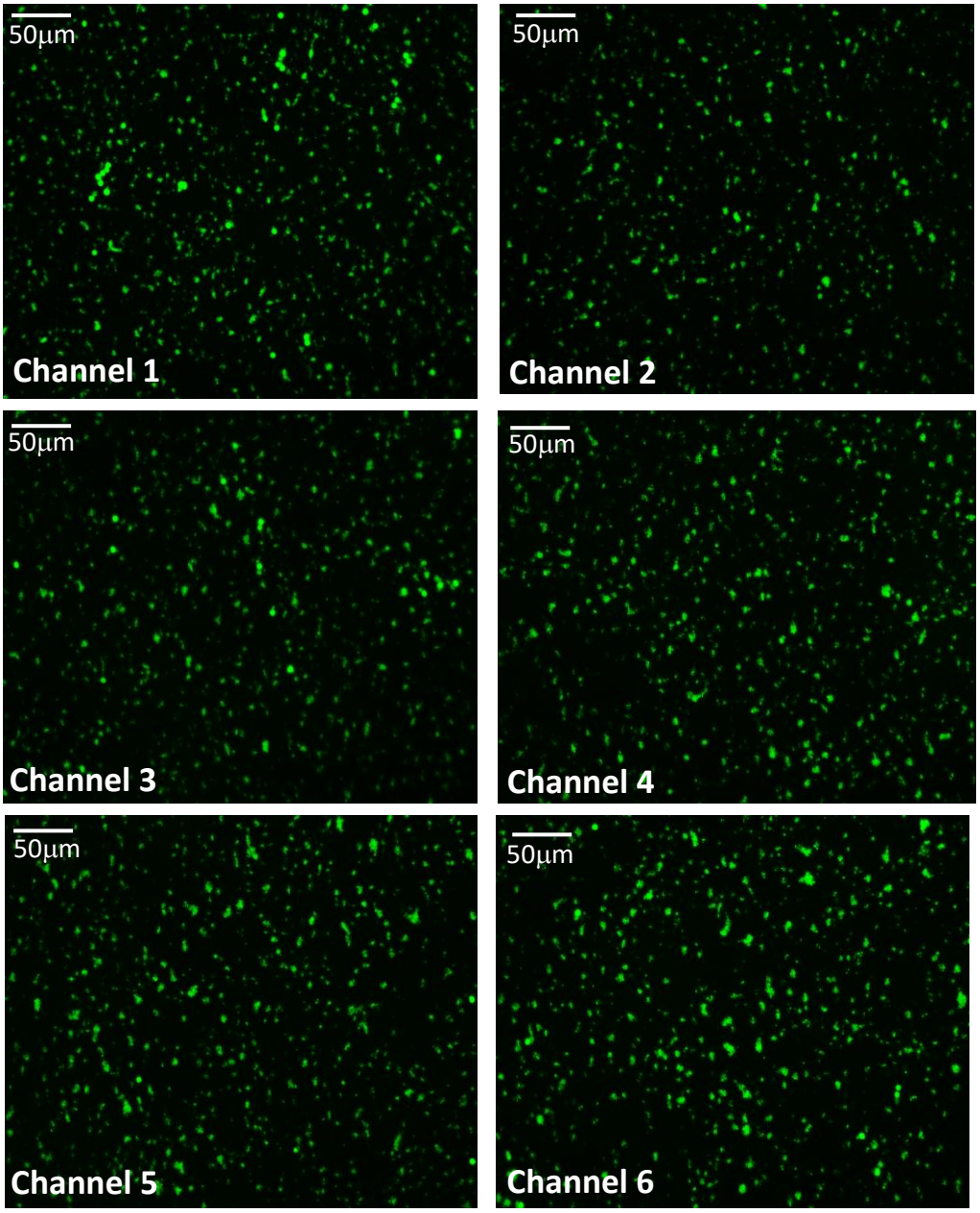
50µm
Channel 1
50µm
Channel 2
50µm
Channel 3
50µm
Channel 4
50µm
Channel 5
50µm
Channel 6

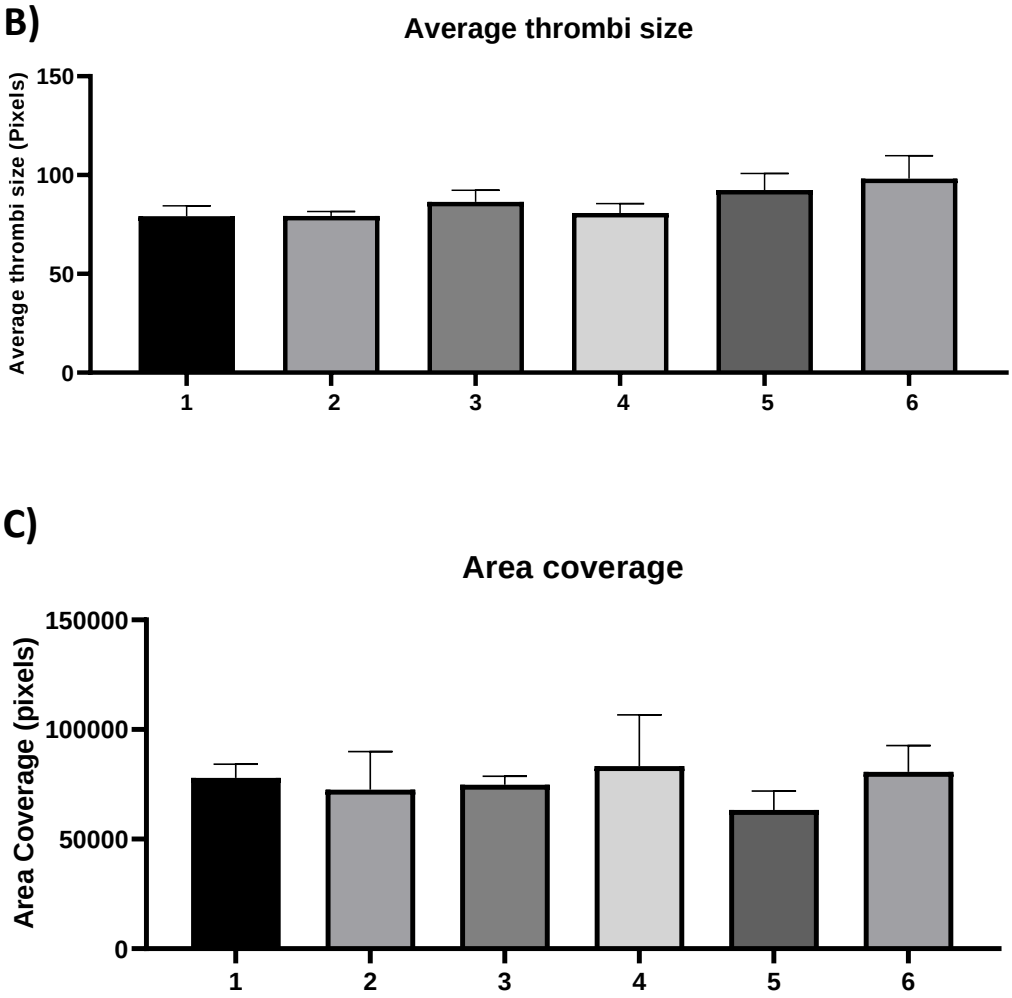


**Figure 3. 14 TNF-alpha reduces CD39 levels**

Whole blood labelled with $DIOC_6$ was perfused over collagen coated µ-slides. Platelet adhesion and thrombus formation was analysed using Celena® S digital imaging system (A). Average thrombi size (B) and area coverage (C) was calculated using Image J. Data represents mean ± SEM, n =3 (all n numbers are from a single donor).

### 3.2.12 Anti-platelet drugs significantly reduce average thrombi size in an endothelialised thrombosis model

Increasing the throughput of the model allowed us to demonstrate potential applications of the model, one such application could be the analysis of anti- platelet drug efficacy. Emerging evidence has suggested that the efficacy of some anti-platelet drugs is potentiated by NO release from endothelial cells (Chan *et al*., 2016; Kirkby *et al*., 2013) and therefore an endothelialised model is essential for accurately assessing the effects of anti-platelet compounds *in vivo*. Dual anti- platelet therapy (DAPT) is the standard of care for the secondary prevention of atherothrombotic events and is the combination of aspirin and a $P2Y_{12}$ receptor antagonist (Degrauwe *et al*., 2017). To demonstrate the application of the model, experiments with DAPT drugs, aspirin and clopidogrel, were conducted to evaluate if the reduction in platelet aggregation observed *in vivo* could be replicated in the endothelialised model. Aspirin (30µM) and clopidogrel (10µM), separately and in combination, were incubated in human whole blood for 30 minutes, while HUVECs were also incubated with the two compounds for 30 minutes. For the untreated control, DMSO (0.1%) was incubated in human whole blood and HUVECs for 30 minutes. Human whole blood was then perfused over the HUVECs prior to perfusion over the collagen channel. Thrombus formation on collagen was then assessed (Figure 3.15.A). Average thrombus size was significantly reduced (Figure 3.15.B) following treatment with aspirin ($p<0.05$), clopidogrel ($p<0.01$) and both in combination ($p<0.01$). No significant differences in platelet area coverage (Figure 3.15.C) was observed with any of the drug treatments.

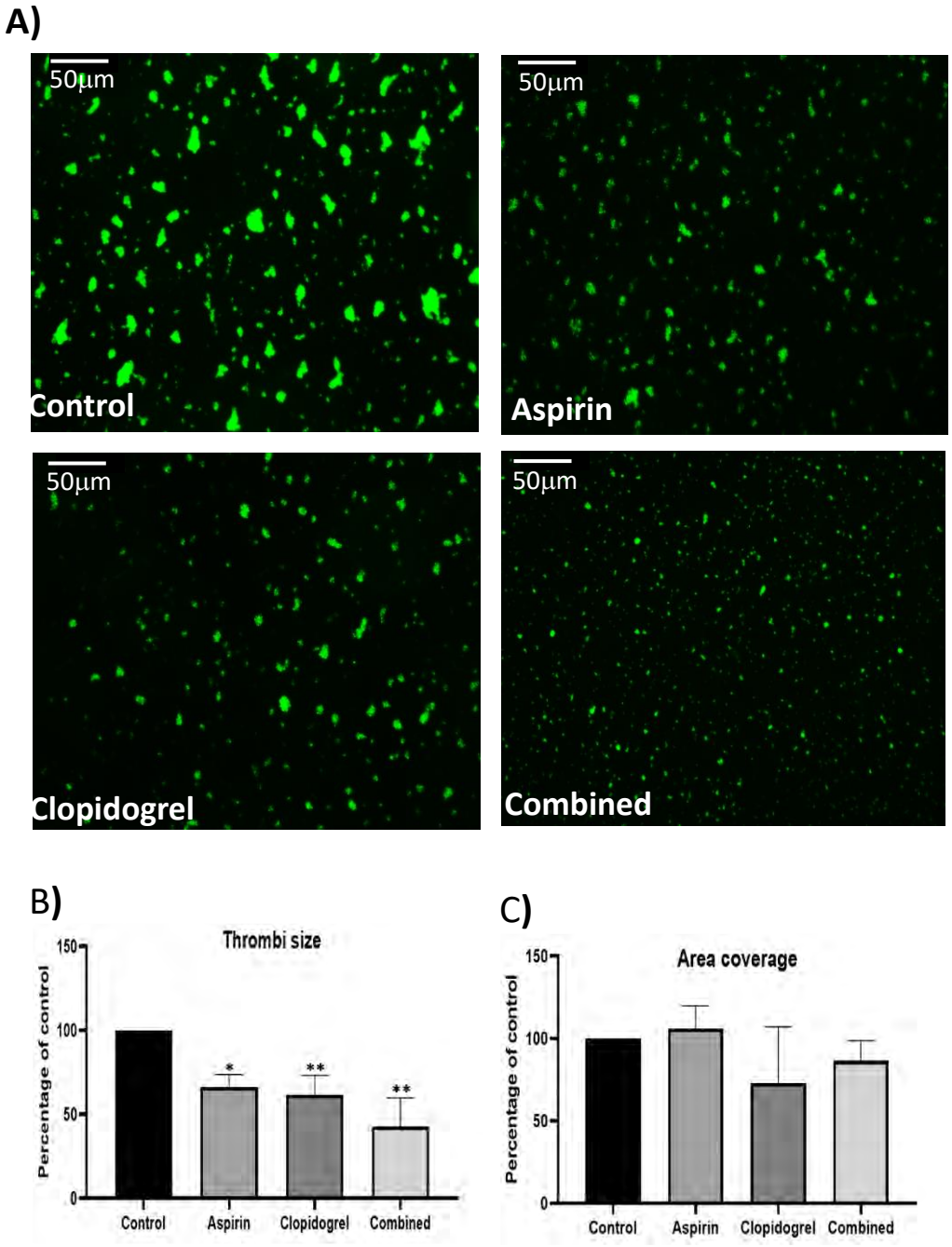


**Figure 3. 15 Anti-platelet drugs significantly reduce average thrombi size in an endothelialised thrombosis model**

Whole blood labelled with $DIOC_6$ was incubated with either vehicle control, aspirin, clopidogrel or aspirin and clopidogrel prior to perfusion through HUVEC coated chambers, HUVECs were treated with either vehicle control, aspirin (30μM), clopidogrel (10μM) or aspirin and clopidogrel for 30 minutes before blood perfusion. Platelet adhesion and thrombus formation was analysed using Celena® S digital imaging system (A). Average thrombi size (B) significantly decreased with all treatments. There was no significant difference in area coverage following any of the treatments (C). Data represents mean ± SEM; n=3 (each n represents an individual donor, with 5 images taken per condition for analysis. *p<0.05, **p<0.01

### 3.2.13 TNF-alpha abolishes the effects of anti-platelet drugs

Many patients with cardiovascular disease are given DAPT as secondary prevention of thrombotic events, however many of these patients will have endothelial activation and dysfunction leading to a loss of NO production. As previously discussed, emerging evidence has suggested that NO release from the endothelium may potentiate the effects of DAPT. Therefore, some patients, especially those with endothelial dysfunction, may experience a poor response to DAPT. This link between endothelial cell function and DAPT efficacy may account for the variation in response observed in patients with cardiovascular disease. The model with HUVECs stimulated with TNF-alpha was used to assess the effect of endothelial dysfunction on DAPT efficacy. Aspirin (30µM) and clopidogrel (10µM), separately and in combination, were incubated in human whole blood for 30-minutes, TNF-alpha stimulated HUVECs were also incubated in the two compounds for 30-minutes. For the untreated control, DMSO (0.1%) was incubated in human whole blood and HUVECs for 30 minutes. Human whole blood was then perfused over the HUVECs prior to perfusion over the collagen channel (Figure 3.16.A). There was no significant difference in average thrombi size (Figure 3.16.B) or platelet area coverage (Figure 3.16.C) following treatment with aspirin or clopidogrel, both separately and in combination.

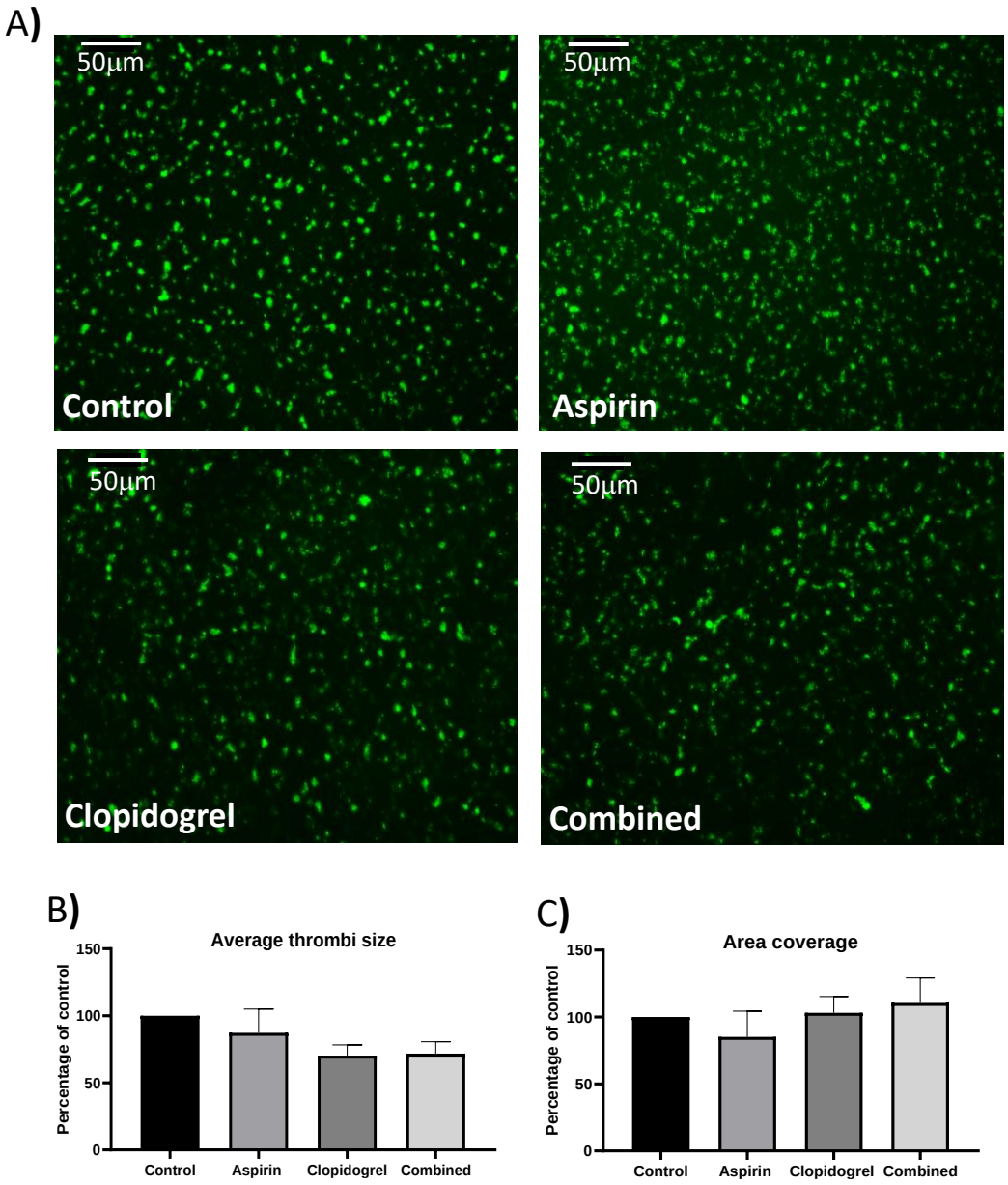


**Figure 3. 16 TNF-alpha abolishes the effects of anti-platelet drugs**

Whole blood labelled with $DIOC_6$ was incubated with either vehicle control, aspirin, clopidogrel, aspirin and clopidogrel prior to perfused through TNF-alpha stimulated HUVEC coated chambers. Prior to perfusion HUVECs were treated with either vehicle control, aspirin (30µM), clopidogrel (10µM) or aspirin and clopidogrel for 30-minutes. Platelet adhesion and thrombus formation was analysed using Celena® S digital imaging system (A). There was no significant difference in average thrombi size (B) or area coverage (C). Data represents mean ± SE; n=3 (each n represents an individual donor, with 5 images taken per condition for analysis).

## 3.4 Discussion

The aim of this chapter was to establish an endothelialised *in vitro* thrombosis model which would allow for the assessment of endothelial cell regulation of thrombus formation. Many of the current *in vitro* thrombus models use human whole blood and appropriate shear stress but are limited by the absence of factors that are crucial for replicating a physiologically relevant *in vitro* model (Coenen *et al*., 2017). For example, there is often an absence of endothelial cells in the models and so therefore they cannot account for the role of the endothelium and endothelial dysfunction in thrombus formation.

As previously described, several mediators released from the endothelium can inhibit platelet activation and therefore regulate thrombus formation, these include NO, prostacyclin and CD39 (Yau *et al*., 2015). All three mediators used in the experiment significantly reduced average thrombi size and area coverage, thus helping support the incorporation of endothelial cells into the model. The incorporation of HUVECs into the model significantly reduced average thrombi size and area coverage, further emphasising the role of the endothelium in regulating platelet activity and highlighting the importance of incorporating them into an *in vitro* thrombosis model. A visible difference in thrombus formation between venous flow and arterial flow was observed (Figure 3.1 and Figure 3.2). Under venous flow large platelet aggregates formed, however in the presence of endothelial platelet inhibitors these aggregates reduced in size and number, suggested the inhibitors were affecting platelet adhesion and aggregation. Similarly, large platelet aggregates formed under arterial flow, however in the presence of NO and $PGE_2$ these aggregates reduced in size and an increase in single platelet adhesion was observed. These results suggest that under arterial flow rates these mediators may be unable to inhibit platelet adhesion but can still block the secondary signalling amplification and thus block the formation of large platelet aggregates.

L-NNA is a well-established inhibitor of NO synthase (Clark *et al*., 2003; Mayer *et al*., 1993) and was therefore chosen to elucidate the role of NO in the endothelialsed model. Incubation of endothelial cells in L-NNA resulted in a significant increase in

thrombus size and area coverage suggesting that NO release from the endothelial cells present in the model may be responsible for reducing thrombus formation.

The COX enzymes play pivotal roles in thrombosis and haemostasis, with the COX pathway being responsible for the production of the potent platelet activator $TXA_2$, in addition to the platelet inhibitor prostacyclin (Félétou *et al*., 2011). Next, it was important to determine what effect blockade of the endothelial COX activity would have on thrombus formation in the model, in order to determine if COX activity was contributing to the reduction in thrombus size observed when endothelial cells were present in the model. To achieve this, the non-selective COX inhibitor indomethacin was used, treatment with indomethacin had no significant effect on thrombus formation. As previously mentioned, the COX-1 enzyme can promote thrombus via the production of $TXA_2$. COX-1 expression in platelets and is responsible for platelet $TXA_2$production and so inhibition of platelet COX-1 has the potential to mask any effects of endothelial cell COX blockade (Luo *et al*., 2016). Although appropriate steps were taken to ensure that the indomethacin had been thoroughly flushed from the system prior to blood perfusion, it was important to rule out the potential for residual indomethacin to be causing platelet inhibition. As a result, it was decided to repeat the experiment using a selective COX-2 inhibitor. Historically, the COX-2 enzyme was incorrectly thought of as being solely involved in in the pathophysiology of inflammation and pain (Day and Graham, 2004). As a result, selective COX-2 inhibitors, known as coxibs, were developed in an attempt to treat pain and inflammation while avoiding the gastric adverse events associated with gut COX-1 inhibition that were observed with non-selective COX inhibitors (Day and Graham, 2004). However, it soon emerged that these new compounds increased the risk of cardiovascular adverse events, such as stroke and myocardial infarction (Day and Graham, 2004). Although COX-2 is often thought of as the inducible form of the enzyme, evidence from clinical studies has suggested that COX-2 is constitutively expressed in some tissues, including the vascular endothelium (Funk and FitzGerald, 2007), where it helps to maintain haemostasis via the release of prostacyclin. Incubation with celecoxib had no significant effect on thrombus formation, suggesting that COX enzyme activity may not be responsible for the endothelial cell

thrombus regulation observed in the model.

The final endothelial mediator assessed was CD39, which plays a key role in regulating platelet activity by catalysing the conversion of ADP, a potent platelet activator, to AMP (Kanthi *et al*., 2014). The CD39 inhibitor, POM-1 was used to assess if CD39 was contributing to the reduction in thrombus formation observed when endothelial cells were incorporated into the model. POM-1 stimulation resulted in a significant increase in average thrombi size and area coverage. A study investigating endothelial dysfunction in patients with pulmonary arterial hypertension (PAH) found that CD39 expression was significantly reduced in the endothelial cells of diseased small arteries (Helenius *et al*., 2015). This decrease in CD39 expression and activity was also observed in cultured endothelial cells from PAH patients (Helenius *et al*., 2015). This evidence suggests that loss of CD39 expression is an additional component of endothelial dysfunction and may explain the observed increase in thrombus formation when CD39 was inhibited in the model. However, brightfield imaging revealed that POM-1 was causing some morphology changes and preventing the cells from reaching full confluency. This suggested that POM-1 was potentially having a cytotoxic effect on the endothelial cells, as a result the increase in thrombus formation may be attributed to a loss in endothelial cells rather than solely to endothelial CD39 inhibition. An interesting point to note is despite the loss of some endothelial cells, the difference in average thrombus between the control and POM-1 was not as large as that observed between healthy endothelial cells and no cell controls in previous experiments. This suggests that even a small number of endothelial cells incorporated into the model can still have an impact on platelet regulation and thrombus formation, thus highlighting the sensitivity of the model to the contribution of endothelial cells.

The release of pro-inflammatory cytokines from foam cells plays a key role in the early development of an atherosclerotic plaque and contributes to the change in vessel environment observed in cardiovascular disease (Fatkhullina *et al*., 2016). This process leads to endothelial activation and dysfunction and so in order to accurately model atherothrombosis, the presence of activated and dysfunctional endothelial cells in an *in vitro* model is essential. Previous studies have shown that endothelial

cells undergo morphological alterations in response to TNF-alpha exposure (Stroka *et al*., 2012). Most notably, TNF-alpha has been shown to lead to a wide distribution of cell area and aspect ratio in HUVECs. Therefore, the morphological changes observed, with HUVECs transitioning from the classical "cobblestone" morphology to a wider elongated form helped to confirm that TNF-alpha was working correctly at the chosen concentration and time point. It has been suggested that this change in cell shape is caused by F-actin rearrangement, suggesting a link between endothelial cell morphology and cytoskeletal dynamics during an inflammatory response (Stroka *et al*., 2012). As these alterations in cell morphology occur in response to cytokine stimulus it is likely that the process plays a role in regulating the efficiency of leukocyte adhesion (Lee *et al*., 2018). It has been well established that TNF-alpha activates endothelial cells, this leads to the upregulation of cell adhesion molecules, including VCAM-1 and ICAM-1 (Teasdale *et al*., 2017; Xia *et al*., 1998). It was successfully demonstrated, using western blotting, that stimulation of HUVECs with TNF-alpha (10ng/µl) for 24 hours lead to a significant increase in in cell adhesion molecules VCAM-1 and ICAM-1. These data suggested that TNF-alpha can be used to induce an activated endothelial cell phenotype in HUVECs and could therefore be utilised to mimic endothelial activation in the thrombosis model.

The incorporation of activated endothelial cells into the model led to significant increases in average thrombi size and area coverage compared with healthy unstimulated endothelial cells. These data indicate that the incorporation of activated endothelial cells potentially created a pro-thrombotic environment within the model and also highlighted that the model is sensitive to changes in the endothelial cell compartment. In addition to endothelial activation, endothelial dysfunction is also observed in and is a key component of the pathogenesis of thrombosis. Endothelial dysfunction is used to describe a reduction in the production and bioavailability of NO, which impedes endothelial cell inhibition of platelet activation and leads to the generation of a pro-thrombotic vessel environment (Gimbrone, 2017). It was demonstrated that TNF-alpha stimulation caused an increase in thrombus formation and abolished the anti-platelet effects previously observed with healthy endothelial cells. As a result, it was important to investigate if endothelial dysfunction within the model was responsible for this. Western blotting was used to elucidate if TNF-alpha

stimulation was having any effect on eNOS levels. It was demonstrated that TNF-alpha stimulation significantly decreased phospho-eNOS levels and further analysis revealed this was likely due to a decrease in total eNOS levels (Figure 3.10). This was confirmed using real-time PCR which showed a significant decrease in eNOS gene abundance following TNF-alpha stimulation (Figure 3.11). This decrease in eNOS abundance indicates that endothelial cell dysfunction was being replicated in the model using TNF-alpha stimulation. Being able to induce endothelial activation and dysfunction is important for producing a physiological relevant model of human atherothrombosis. It was decided that NO bioavailability should also be assessed to further confirm if TNF-alpha stimulation was induced endothelial dysfunction in the model. This was attempted using a Griess assay, unfortunately it was determined that the assay was not sensitive enough to accurately measure differences in NO bioavailability in HUVECs. This may have been due to the HUVECS only producing low concentration of NO.

As previously discussed, prostacyclin and CD39 are additional endothelial-derived mediators that can inhibit platelet activation. Therefore, it was important to determine if TNF-alpha stimulation was having any effect on the expression of these mediators and if this may also be responsible for the observed increase in thrombus formation. COX-1 is found in vascular endothelial cells and is responsible for the production of a range of prostaglandins, most notably TXA2 (DeWitt *et al*., 1983; Tang and Vanhoutte, 2008). In the cardiovascular system, platelet COX-1 is the main contributor to TXA2 production, however it can also be generated by endothelial COX-1 (Félétou *et al*., 2011). As TNF-alpha stimulation increased thrombus formation it was important to determine if it was having any effect on COX-1 expression and protein levels as an increase in COX- 1 expression and $TXA_2$ production could be contributing to the increase in thrombus formation. Western blotting and real-time PCR revealed that there were no significant changes in COX-1 protein levels or gene expression following TNF-alpha stimulation. This data suggests the increase in thrombus formation following TNF- alpha stimulation may not be due to any alterations in COX-1 activity. Endothelial COX-2 has been shown to be the dominant source of prostacyclin in the cardiovascular system (Ricciotti *et al*., 2013; Ricciotti and

FitzGerald, 2011). As prostacyclin is a potent inhibitor of platelet activation, changes in endothelial COX-2 expression could have an effect on thrombus formation. Western blotting and real- time PCR demonstrated a significant increase in COX-2 protein levels and gene expression following TNF-alpha stimulation. COX-2 is often described as the inducible COX enzyme and historical evidence has shown the expression of COX-2 increases in response to inflammatory stimulus such as cytokine release (Imseis, 1997; Lin *et al*., 2004). This increase in COX-2 expression further confirms that TNF-alpha is working correctly in the model and producing inflammatory responses in the endothelial cells which correlates with that observed in *in vivo* models.

Next, the effects of TNF-alpha stimulation on CD39 expression was investigated. There is a range of evidence in the literature that suggest a decrease, or complete deficiency in CD39 may play a role in cardiovascular disease, with a decrease in CD39 expression being observed in vascular thrombosis, stroke, atherosclerosis and myocardial ischemia-reperfusion injury (Eltzschig *et al*., 2009, p. 39; Hyman *et al*., 2009; Pinsky *et al*., 2002). Studies have shown that mouse micro-vesicles deficient in CD39 induce a pro-thrombotic and pro-inflammatory response from endothelial cells *in vitro* (Banz *et al*., 2008). Real-time PCR analysis of HUVEC CD39 expression following TNF-alpha stimulation revealed a significant decrease in CD39 gene expression following TNF-alpha stimulation. As previously discussed, suppression of CD39 has been observed in patients with PAH, with studies showing increased thrombosis in patients with severe PAH (Helenius *et al*., 2015). The increase in thrombus formation in the model following TNF-alpha stimulation may be attributed to a decrease in both CD39 and eNOS. As both a reduction in the bioavailability of NO and the suppression of CD39 is observed in cardiovascular disease *in vivo*, these findings suggest that the thrombosis model was accurately replicating key aspects of cardiovascular disease.

Increasing the throughput of the model was the next aim of model optimisation, this would allow researchers to model multiple conditions at the same time. To achieve this a six-syringe pump model was used, this would enable blood to be perfused over six channels simultaneously and allow for the assessment of six experimental

conditions at the same time. The use of six individual syringes in this model setup introduced the potential for variation between the channels, therefore it was important to assess if there were any significant differences between the six channels. To achieve this a single donor was used, to eliminate any donor variability from the analysis, and three model runs were performed. There were no significant differences in average thrombi size or area coverage between the six channels, this indicated that there was no significant variation between the individual channels. These findings confirmed that any significant differences observed in experimental runs would be due to the experimental conditions and not channel variability.

Modelling the efficacy of anti-platelet compounds is one potential application of the model. DAPT is currently used in the prevention of further ischemic events after experiencing acute coronary syndrome. The therapy used a combination of aspirin with a $P2Y_{12}$ inhibitor to inhibit platelet activity and reduce the risk of future ischemic events (Degrauwe *et al*., 2017). Due to the extensive use of DAPT in patients with cardiovascular disease, aspirin and the $P2Y_{12}$ inhibitor clopidogrel were chosen to prove this application of the model. It was successfully demonstrated that treatment with aspirin and clopidogrel, both separately and in combination significantly reduced average thrombus but had no effect on area coverage. The first stage in the development of a thrombus involves the binding of platelets to collagen, which then become activated and undergo shape change and granule secretion. As discussed previously, initial platelet-collagen binding is facilitated by a number of receptors found on the surface of platelets, most notably GPVI (Burkhart *et al*., 2012). As aspirin and clopidogrel do not directly act on GPVI binding and signalling, they do not interfere with the initial adhesion of platelets to collagen. This may explain why no significant difference in area coverage was observed when the DAPT compounds were present in the model. Aspirin exerts anti- platelet effects by inhibiting the COX-1 enzyme in platelets. This enzyme is essential for the production of TXA2 in platelets and when platelets become activated they release TXA2, which can then further activate circulating platelets close to the site of injury, recruiting them to the growing thrombus (Smyth, 2010). Inhibition of COX-1 by aspirin prevents the production of TXA2 and inhibits the formation of large platelet aggregates (Ajjan *et al*., 2009).

Clopidogrel is a $P2Y_{12}$ receptor inhibitor, $P2Y_{12}$ is the receptor for the potent platelet activator ADP. A key component of platelet activation is granule secretion, which includes the release of ADP found in platelet dense granules. This causes a positive feedback loop, through which activated platelets release ADP, which can bind to $P2Y_{12}$ receptors on neighbouring platelets, causing them to also become activated and to release more ADP. This results in the secondary amplification of platelet signalling (Estevez and Du, 2017; Sangkuhl *et al*., 2011). Both of $TXA_2$ and ADP release are important in the secondary signalling amplification observed in the formation of a stable thrombus and therefore inhibition of both using DAPT would lead to a decrease in thrombus. As mentioned previously, the use of aspirin and clopidogrel in the model demonstrated a significant reduction in average thrombus size. These findings highlight the ability of the model to be used as a tool for assessing anti-platelet drug efficacy.

The combination of aspirin and clopidogrel has been a successful treatment for many patients, with studies showing that DAPT reduces the number of patients that experience adverse cardiovascular outcomes by 20% when compared with aspirin alone (Al-Zakwani *et al*., 2020). Despite this effectiveness of DAPT, around 10% of patients will go on to experience atherothrombotic events even while receiving the therapy (Angiolillo D., 2009). Dual poor responsiveness (DPR) that has been identified in several patients, this is where poor responsiveness to both DAPT drugs is reported in the same patient and can lead to recurrent ischemic events (Gori *et al*., 2008). The ADRIE study identified a number of independent predictors of DPR, including body weight, CRP levels and diabetes (Fontana *et al*., 2010).

Diabetes, like atherosclerosis, is associated with the occurrence of endothelial dysfunction and this loss of NO availability could be responsible for the poor response observed in some diabetic patients (Hadi and Suwaidi, 2007). Research from Tim Warner's lab has demonstrated that NO has a synergistic relationship with $P2Y_{12}$ blockade (Chan *et al*., 2016). It has been suggesting that DAPT might actually potentiate the inhibitory actions of NO and this may actually be a key aspect in determining the effectiveness of DAPT (Chan *et al*., 2016; Kirkby *et al*., 2013). Therefore, it can be hypothesized that endothelial dysfunction may be responsible

for the DPR observed in some people, including those with diabetes. To test this theory, the thrombosis model with TNF-alpha stimulated HUVECs was used, as it had previously been shown that eNOS expression was reduced in this form of the model and theorised that it would provide an accurate assessment of the effect of endothelial dysfunction on DAPT efficacy. Treatment with aspirin and clopidogrel both separately and in combination, in the presence of dysfunctional endothelial cells, had no significant effect on area coverage or average thrombus size. These findings help support the role of NO in facilitating DAPT efficacy, in addition to suggesting that endothelial dysfunction could be responsible for the DPR observed in some patient populations, including those with diabetes. A potential future experiment that could be performed to help support the role of endothelial cells in DAPT efficacy would be to compare the effects of DAPT on thrombus formation when there are no cells in the model versus when endothelial cells are present.

In conclusion, endothelial cells were successfully incorporated into the thrombosis model and demonstrate their ability to regulate thrombus formation. Utilisation of a range of techniques revealed that eNOS and CD39 activity may be responsible the reduction in thrombus formation observed when endothelial cells were present in the model. The use of TNF-alpha stimulation, enabled the development of a version of the model that successfully incorporated activated and dysfunctional endothelial cells, thus accurately replicating this aspect of the vessel environment observed in atherothrombosis. Finally, the applicability of the model was assessed by assessing anti-platelet drug efficacy in the presence of healthy and dysfunctional endothelial cells.

# 4. *In vitro* thrombosis model optimisation for arterial flow and different endothelial cell types

## 4.1 Introduction

As discussed in the chapter 3, one major limitation of current *in vitro* thrombosis models is the lack of endothelial cells in the model, meaning endothelial cell regulation of platelet activity is not considered or replicated with many of these models. There are some emerging models that incorporate endothelial cells, however some of these models may introduce a new limitation; variation in terms of the type of endothelial cell being used in the model (Coenen *et al*., 2017). Several different types of endothelial cells, from different vessel beds, have been used in emerging thrombosis models, included HUVECs, lymphatic endothelial cells, human brain microvascular endothelial cells and human aortic endothelial cells (Sylman *et al*., 2015; Navarro-Nunez *et al*., 2015; Tanahashi *et al*., 2001; Tomita *et al*., 2001; Coenen *et al*., 2017).

Another issue that arises from this variation in cell choice is the relevance of that cell type to the disease state being modelled. Some studies use venous cells when modelling arterial thrombosis, despite a distinctive endothelial cell heterogeneity being observed *in vivo* (Coenen *et al*., 2017). It is important to consider whether endothelial cells from the appropriate vascular bed are needed to answer specific research question. For example, how important is it that arterial cells are used when modelling arterial thrombosis, is it essential to use brain microvascular endothelial cells when modelling stroke? Therefore, analysis is needed to assess if there is any difference in endothelial cell regulation of thrombus formation between endothelial cells from different vessel beds.

The diverse nature of the endothelium was identified as early as the 1960's, with researchers recognising that a vast array of endothelial cells existed that differed from each other in terms of both structure and function (Florey., 1966). Structural differences between endothelial cells from different vessel beds was first identified utilising electron microscopy (Aird., 2015). These studies revealed that the endothelium of veins and arteries are made up of a continuous monolayer of

endothelial cells (Aird., 2015). In contrast, the endothelium of certain capillaries can be fenestrated with large gaps between cells. This difference in structure accounts for the difference in function of these vessels. For example, a fenestrated endothelium is often found in vessels involved in secretions, such as in the gastrointestinal system. In addition to vessels involved in filtration, such endothelial cells of the kidney (Aird., 2015). The structural differences in endothelial cells in response to vessel function also suggests that biochemical differences between endothelial cells of different vessel beds may also exist. A heterogeneous expression of multiple endothelial mediators from different vessel beds has been identified, including VWF (Page *et al*., 1992; Yamamoto *et al*., 1998), tissue-type plasminogen activator, fibronectin, prostacyclin and angiotensin- converting enzyme (Aird., 2015; Dela-Paz *et al*., 2009).

The differences observed in venous and arterial thrombosis can provide further insights into the distinct difference between venous and arterial endothelial cells. Firstly, there is the difference in vessel environment observed in each disease state, as the shear stress observed in venous vessels is much lower than that observed in arterial vessels (Aird., 2007). Furthermore, endothelial cells native to the valve pockets of veins are exposed to reduced flow velocity during the valve cycle (Lurie *et al*., 2003), in addition to the hypoxic nature of the blood found in these regions (Hamer *et al*., 1981; Aird., 2007). Studies have shown a differential activation of genes in endothelial cells in response to hypoxia, with a distinction being made between microvascular endothelial cells and those originating from arterial and venous cells (Nilsson, 2004). For example, hypoxia-inducible factor 2 alpha (HIF-2alpha) was shown to be significantly induced in microvascular and capillary endothelial cells, while in contrast, HIF-alpha was only weakly induced in venous and arterial endothelial cells (Nilsson, 2004). The features that make the valve pockets of veins prone to thrombosis and clot development may also be key to influencing the function of the endothelial cells of that region (Aird., 2007).

Just like certain aspects of valve pockets make those regions prone to thrombosis, arterial vessels have key anatomical features that make these vessels susceptible to the development of thrombosis (VanderLaan et a., 2003). The branch points of

arteries are particularly susceptible to thrombosis and the development of atherosclerotic plaques (White *et al*., 2016). A key feature of these branch points is the change in flow environment, shifting from protective laminar flow to a disturbed flow phenotype. (White *et al*., 2016; Aird., 2007). This change in flow can lead to increased expression of a number of pro-inflammatory transcription factors in the surrounding endothelial cells, in addition to inducing apoptosis, a key feature observed in plaque rupture (Thondapu *et al*., 2021; Tricot *et al*., 2000). The vessel environment observed in atherothrombosis is often pro-inflammatory, leading to endothelial activation and endothelial dysfunction. The endothelial cells that form a layer over the growing atheromatous plaque are also quite distinct with increased expression of adhesion cell molecules (Cybulsky and Gimbrone., 1991), tissue factor and tissue factor pathway inhibitor (Crawley *et al*., 2000), in addition to the reduced expression of thrombomodulin (Laszik *et al*., 2001). It is important to consider these key aspects and important distinctions from endothelial cells found elsewhere, when creating a physiological relevant model of human arterial thrombosis.

Despite the substantial evidence showing distinct differences between endothelial cells from different vessel beds, HUVECs have been the predominant endothelial cell used in *in vitro* endothelial cell research (Lau *et al*., 2021), with results from many of these studies being extrapolated to inform on the function of other endothelial cell types, including arterial and microvascular. As a result, further research is needed to identify if this one-size fits all approach to endothelial cell research is valid or, if there is indeed a need for researcher to use tissue-specific endothelial cells in order to accurately answer their specific research question.

In this chapter, the differences in the expression of key endothelial derived platelet regulators in arterial and venous endothelial cells were examined. In addition, HCAECs were incorporated into the *in vitro* thrombosis model allowing us to analyse differences in endothelial regulation of thrombus formation between venous and arterial endothelial cells.

### 4.1.1 Aims and hypothesis

The principal aims of the work presented in this chapter were to:

1. Compare the expression of endothelial derived mediators between HUVECs and HCAECs
2. Optimise the model for an arterial flow rate
3. Incorporate HCAECs into the optimised version of the model
4. Compare HUVEC and HCAEC regulation of thrombus formation using the optimised *in vitro* thrombosis model

**Hypothesis**

There is a clear difference in the regulation of thrombus formation between endothelial cells of different vessel beds due to a difference in the expression of key platelet mediators.

## 4.2 Summary of *in vitro* model setups used in this chapter

The higher throughput model was utilised for model experiments in this chapter and was setup as described in 2.4.3. Two Ibidi $VI^{0.4}$ or $VI^{0.1}$ µ-slides were connected to each other via siliconized tubing, HUVECs were seeded onto the first µ-slide (plating density 5 $x10^5$/ml) before being incubated for 48 hours at 37ºC with 5% $CO_2$ to allow a confluent monolayer to form. The channels of the second µ-slide were coated with type I collagen fibrils (derived from equine tendons; Labmedics) (100µg/ml) one hour prior to blood perfusion. The first µ-slide was connected to six pairs of reservoirs containing either Tyrodes buffer or human whole blood, via siliconized tubing. Corresponding channels of the two µ-slides were lined up and connected via siliconized tubing. The second µ-slide was connected to a six-syringe withdrawal pump, which enables blood to be perfused through all six channels per slide, over endothelial cells before passing over collagen at the same physiological relevant shear stress.

## 4.3 Results

### 4.3.1 Comparison of HUVEC and HCAEC regulation of thrombus formation under venous flow

The aim of this chapter was to assess any differences between venous and arterial endothelial cells in the regulation of thrombus formation. The initial endothelialised version of the thrombosis model (Figure 3.4) was chosen to begin the comparison. This version of the model was chosen for this analysis as it had previously been optimised to ensure repeatability and accuracy. HUVECs or HCAECs were cultured in channels upstream to ones lined with collagen and blood from five independent donors was perfused through the system at 1.5 dyne/cm$^2$, thrombus formation was then analysed on the collagen (Figure 4.1.A). A no cell control was used for these experiments, with the upstream chamber containing no cells and the downstream coated with collagen (100μg/ml). Results from the experiments demonstrated a significant reduction in thrombi area coverage when HUVECs (45.2%, $p<0.05$) or HCAECs (66.7%, $p<0.05$) (Figure 4.1.B) were incorporated into the model. In addition, a significant reduction in thrombi area coverage was observed with HCAECs compared with HUVECs (67.8.5%, $p<0.01$) (Figure 4.1.B). Both cell types significantly reduced average thrombus size (HUVEC 49.1%, $p<0.05$; HCAEC 48.1%, $p<0.05$), with no significant differences between the cell types (Figure 4.1.C). No significant difference in average thrombi number was observed when either cell type was compared to the control, however a significant reduction was observed in HCAECs compared with HUVECs (44.5%, $p<0.05$) (Figure 4.1.D).

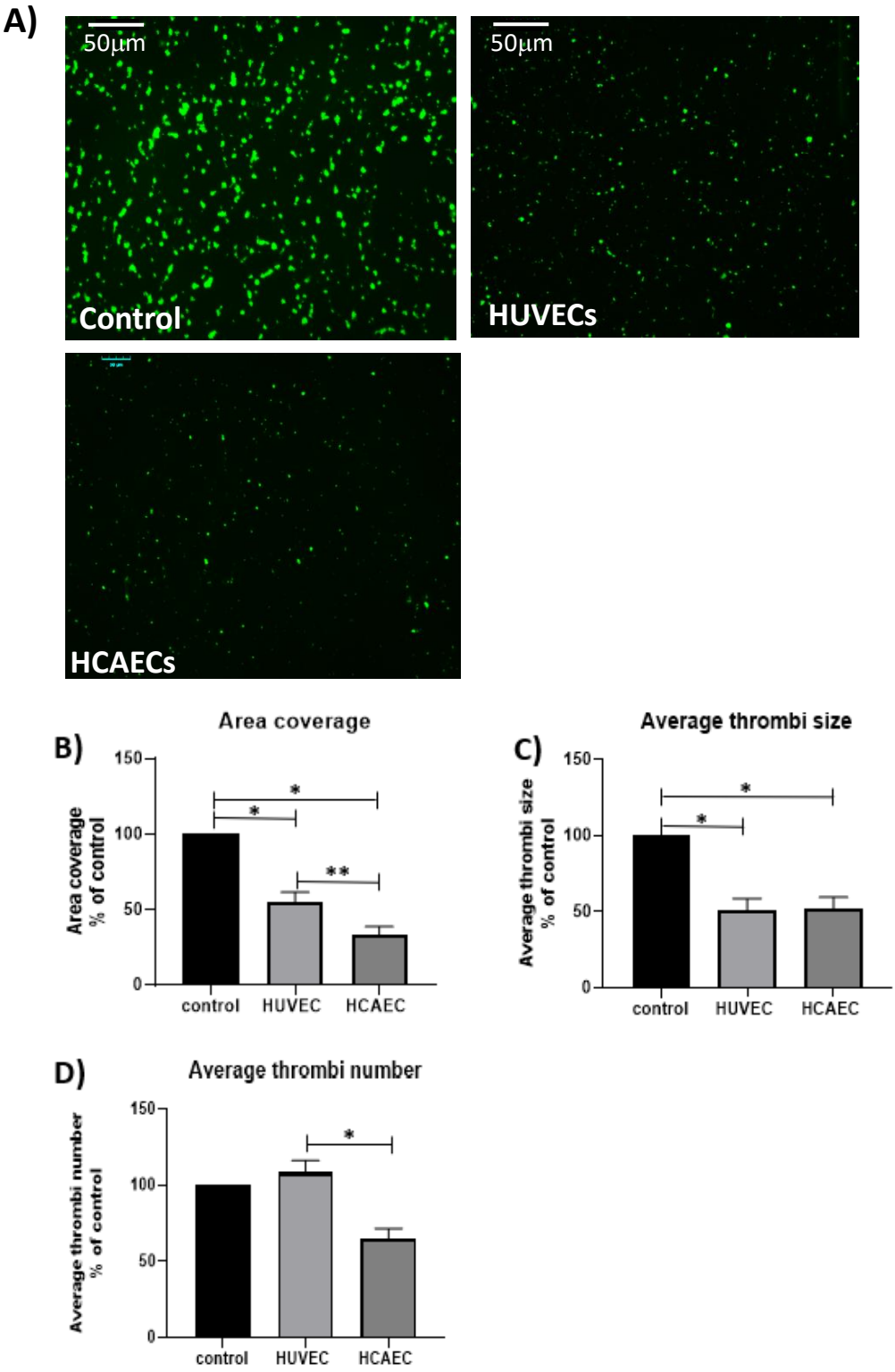


**Figure 4.1 Comparison of HUVEC and HCAEC regulation of thrombus formation under venous flow**

Whole blood labelled with $DIOC_6$ was perfused through no cell control, HUVEC or HCAEC lined chambers prior to collagen coated chambers and platelet adhesion and thrombus size analysed (A). The presence of HUVECs and HCAECs significantly reduced area coverage (B), and average thrombi size (C). There was a significant difference in average thrombi number observed between HUVECs and HCAECs (D), with fewer thrombi forming when HCAECs were incorporated into the model. Data represents mean ± SEM; n=3 *p<0.05, **p<0.01 (each n represents an individual donor, with 5 images taken per condition for analysis).

### 4.3.2 TNF-alpha stimulation increases adhesion molecule expression in HUVECs and HCAECs in a similar manner

It was previously shown that TNF-alpha stimulation increased cell adhesion molecule levels in HUVECs. It was important to confirm if TNF-alpha stimulation elicited the same response in HCAECs and if endothelial activation could be achieved. In addition, it was important to determine if there were any differences in adhesion cell molecule levels between HUVECs and HCAECs. Western blotting (Figure 4.2.A) revealed that following 24 hours incubation with TNF-alpha (10ng/ul), VCAM-1 (Figure 4.2.B) and ICAM-1 (Figure 4.2.C) levels were significantly increased in both HUVECs ($p<0.05$) and HCAECs ($p<0.05$). No significant difference between HUVEC and HCAEC adhesion molecule levels were observed, both pre and post TNF-alpha stimulation.

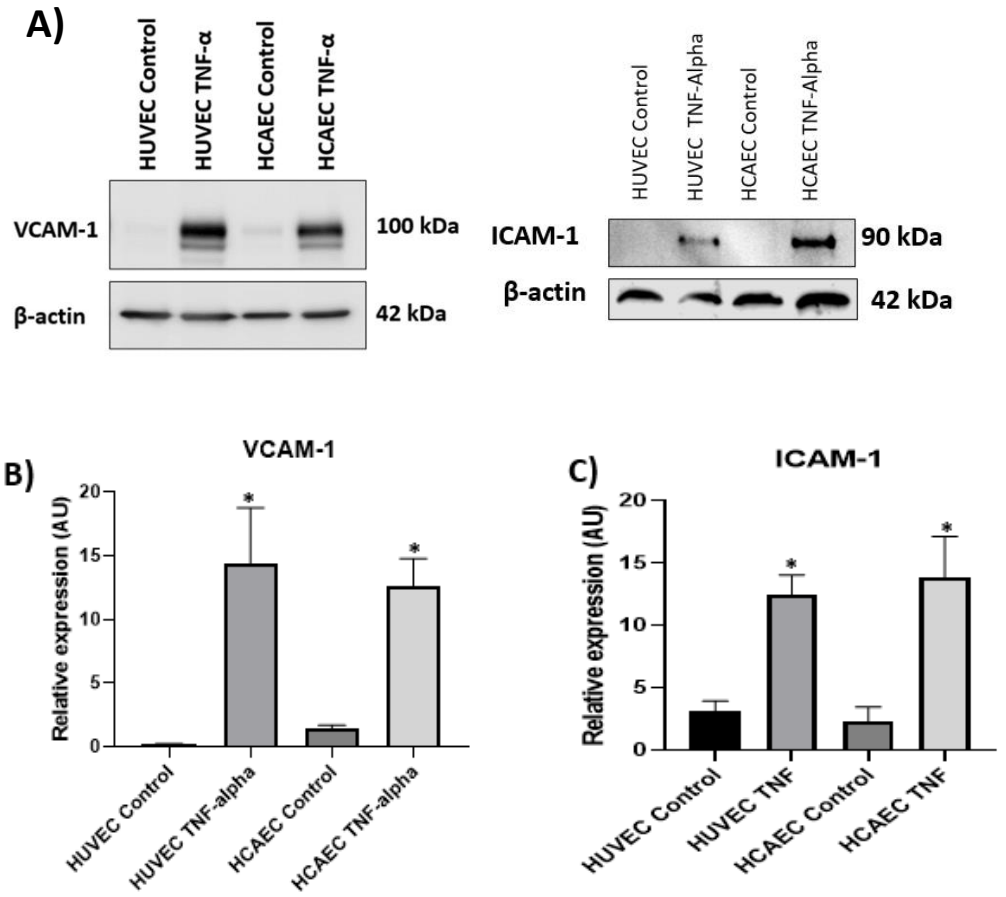


**Figure 4.2 TNF-alpha stimulation increases adhesion cell molecule expression in HUVECs and HCAECs in a similar manner**

Following stimulation with TNF-alpha (10ng/ml) for 24h, cells were lysed for Western blotting (A). Western blots demonstrated a significant increase in VCAM-1 (B) and ICAM-1 (C) in both cell types following TNF-alpha stimulation. Data represents mean ± SEM relative expression following normalisation to β-actin; n=3 ***p<0.05*

### 4.3.3 Higher levels of COX-2 gene expression observed in HCAECs compared with HUVECs

As previously discussed, the COX enzymes play a key role in regulating thrombus formation via the release of prostacyclin and TXA2. As the incorporation of HCAECs into the model reduced thrombus formation it was important to determine if the COX enzymes were contributing to this process and assess if there was any difference in COX enzyme levels between HUVECs and HCAECs. In addition, it was important to determine what effect TNF-alpha stimulation has on arterial endothelial cell COX levels. Western blotting (Figure 4.3.A) revealed no significant difference in COX-1 levels between HUVECs and HCAECs (Figure 4.3.B). In addition, TNF-alpha stimulation had no significant effect on COX-1 levels in HCAECs (Figure 4.3.B). Western blotting demonstrated a significant increase in COX-2 levels following TNF-alpha stimulation in HUVECs and HCAECs ($p<0.05$) (Figure 4.3.C). No significant difference in COX-2 protein levels were observed between HUVECs and HCAECs, however real-time PCR revealed a significant difference in COX-2 gene expression (PTGS2) between HUVECs and HCAECs (Figure 4.3.D).

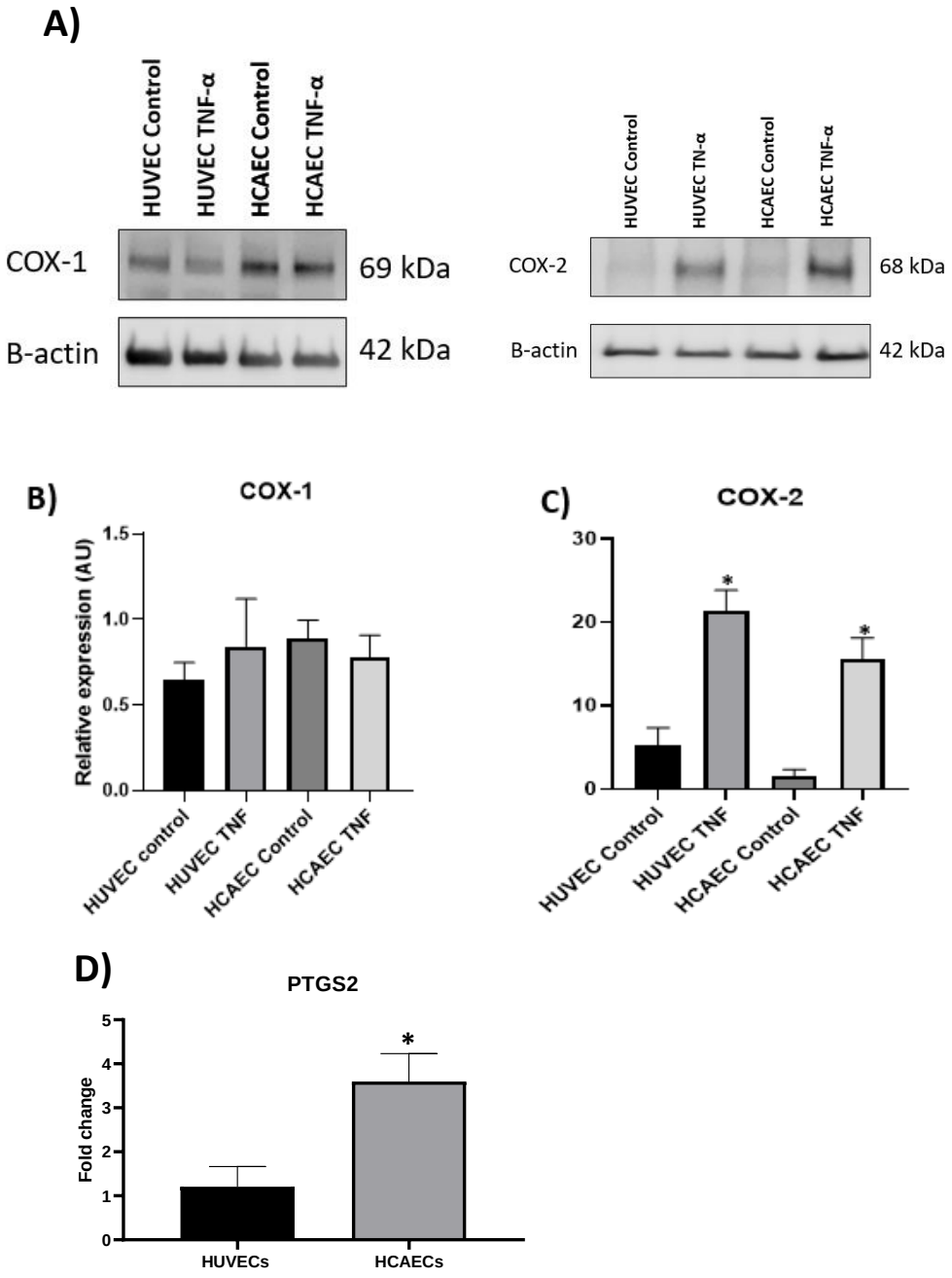


***Figure 4.3 Higher levels of COX-2 gene expression observed in HCAECs compared with HUVECs***

HUVECs and HCAECs were stimulated with TNF-alpha (10ng/ml) for 24h prior to being lysed for Western blotting (A) and real-time PCR. Western blot revealed no significant differences in COX-1 (B) and COX-2 (C) protein levels between HCAECs and HUVECs. Real-time PCR demonstrated higher gene expression of COX-2 in HCAECs compared with HUVECs (D). TNF-alpha stimulation had no significant effect on COX-1 (B) expression in either cell type and significantly increased COX-2 (C) expression in both HUVECs and HCAECs. Data represents mean ± SEM relative expression following normalisation to β-actin; n=3 **p<0.05, **p<0.01*

### 4.3.4 Differences in CD39 expression and TNF response

It was previously shown that a decrease in CD39 can lead to an increase in thrombus formation, indicating that endothelial derived CD39 may play a key role in regulating thrombus formation in the model. Therefore, it was important to assess any differences in CD39 levels between HUVECs and HCAECs, in addition to analysing the effects of TNF-alpha stimulation on CD39 levels in HCAECs. Western blotting (Figure 4.4.A) revealed no significant difference in CD39 levels between HUVECs and HCAECs (Figure 4.4.B). In addition, TNF-alpha stimulation had no significant effect on CD39 levels in HCAECs (Figure 4.4.B). Real-time PCR revealed a significant difference in CD39 gene expression between HUVECs and HCAECs (Figure 4.4.C).

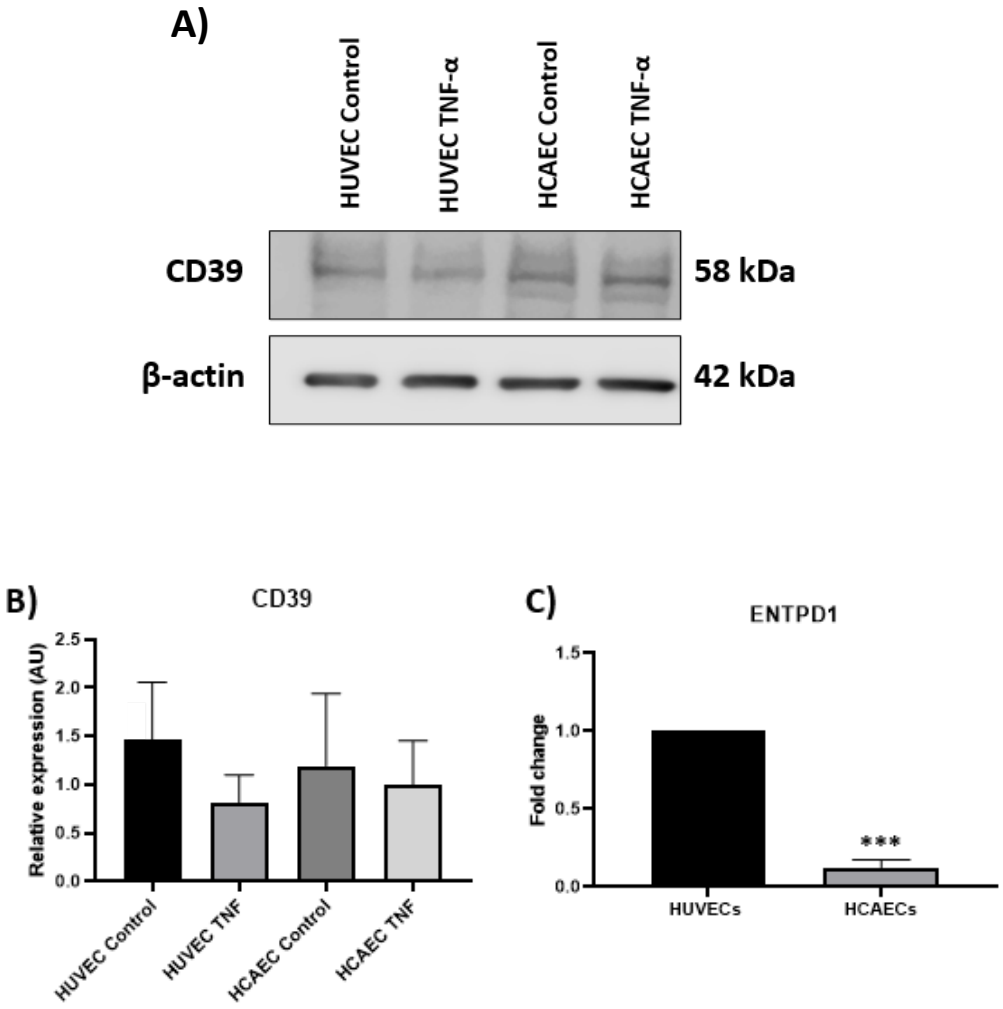


**Figure 4.4 Differences in CD39 expression and TNF response**

HUVECs and HCAECs were stimulated with TNF-alpha (10ng/ml) for 24h prior to being lysed for western blotting (A). Western blot revealed no significant difference in CD39 protein expression between HUVECs and HCAECs (B). Real-time PCR demonstrated significantly reduced ENTPD1 expression in HCAECs compared to HUVECs (C). TNF-alpha stimulation had no significant effect on CD39 expression in either cell type (C). Data represents mean ± SEM relative expression following normalisation to β-actin; n=3*, ***p<0.05*

### 4.3.5 Increased eNOS gene expression was observed in HCAECs with TNF-alpha stimulation reducing eNOS protein levels in both cell types

It was previously demonstrated that endothelial-derived NO is a potential contributor to endothelial regulation of thrombus formation, with inhibition of HUVEC eNOS leading to a significant increase in thrombus formation. In addition, TNF-stimulation can replicate endothelial dysfunction by significantly reducing eNOS expression in HUVECs. Therefore, it was now important to determine if there were any differences in eNOS expression between HUVECs and HCAECs and to assess if TNF-stimulation could achieve endothelial dysfunction in HCAECs. Western blotting (Figure 4.5.A) demonstrated no significant difference in phosphor (Figure 4.5.B) and total eNOS (Figure 4.5.C) levels between HUVECs and HCAECs, however real-time PCR revealed a significant difference in eNOS gene expression between HUVECs and HCAECs (Figure 4.5.D). A reduction in total eNOS protein levels was observed following TNF-alpha stimulation in HCAECs (Figure 4.5.C).

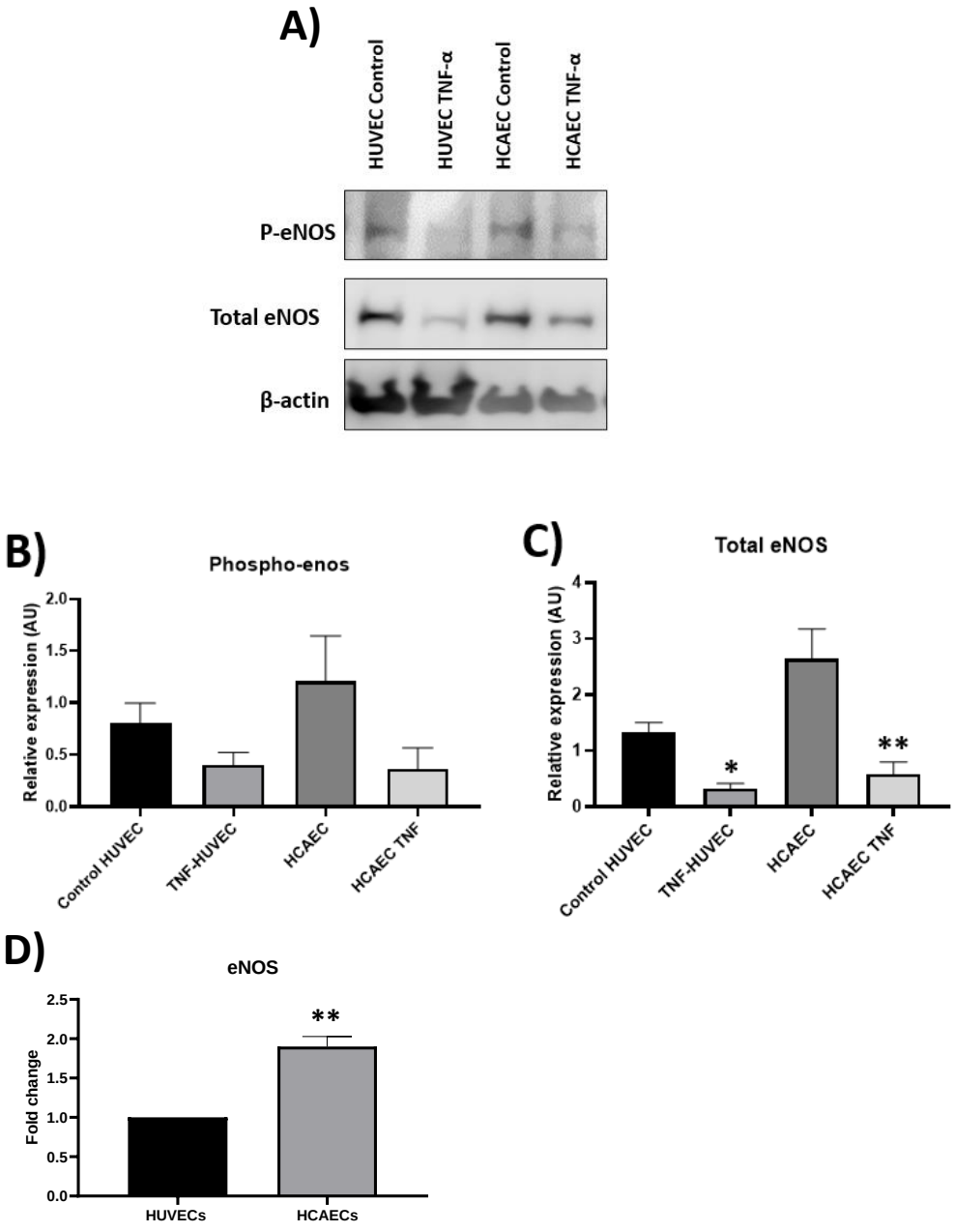


**Figure 4.5 Increase eNOS gene expression was observed in HCAECs with TNF-alpha stimulation reducing eNOS protein levels in both cell types**

HUVECs and HCAECs were stimulated with TNF-alpha (10ng/µl) for 24h prior to being lysed for western blotting and real time PCR. Western blots analysed changes in phosphor-eNOS and total eNOS (A) and a significant decrease in total eNOS protein levels following TNF-alpha stimulation (B). Real-time PCR demonstrated a fold increase in eNOS gene expression in HCAECs compared with HUVECs (D). Data represents mean ± SEM relative expression following normalisation to β-actin; n=3*, **p<0.01*

### 4.3.6 Optimising for arterial flow

As some differences in the levels of endothelial-derived platelet inhibitors were previously observed, including eNOS and CD39, between HUVECs and HCAECs it was decided that the next stage of model optimisation should be the incorporation of HCAECs into the model. The incorporation of arterial endothelial cells into the model would allow us to create a more faithful representation of arterial thrombosis. In addition to incorporating HCAECs into the model, it was essential that the flow rate was increased to an arterial shear rate, to help further replicate the *in vivo* vessel environment. To achieve the previous flow rate of 1.5 dyne/cm$^2$, on the Ibidi VI$^{0.4}$ slides, a pump flow rate of 0.2ml per minute (ml/min) was used. However, in order to achieve the 15 dyne/cm$^2$ needed to replicate arterial flow the flow rate would need to be increased to 2.2ml/min. This increase in flow rate presented an issue in terms of the volume of blood used. In the previous venous model, 1.5ml of blood was used per condition and this would mean a total channel time of ~7 minutes, allowing adequate platelet aggregation and thrombus formation. With the new flow rate of 2.2ml/min a volume of 1.5ml would give less than a minute of channel time. Therefore, it was important to test if this would be adequate for thrombus formation or if a greater volume would be needed. To do this the basic non-endothelialised version of the model was used and three different volumes of blood were assessed, from a single donor, at a flow rate of 2.2ml/min (achieving 5 dyne/cm$^2$). A run at 0.2ml/min (Figure 4.6 A) was performed with the same donor to demonstrate the thrombus formation observed with the previous model flow rate. The three volumes of 2ml (Figure 4.6 B), 5ml (Figure 4.6 C) and 8ml (Figure 4.6 D) demonstrated varying results in terms of thrombus formation.

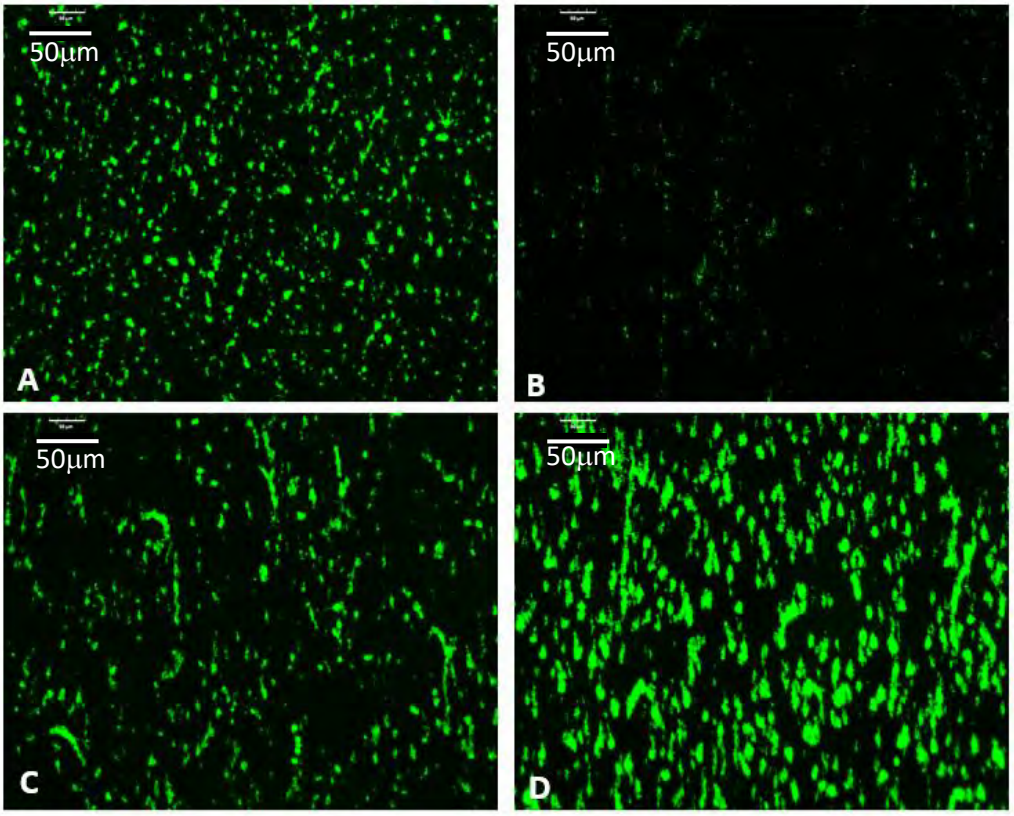


**Figure 4.6 Optimising for an arterial flow rate**

Human whole blood labelled with $DIOC_6$ was perfused over immobilised collagen at venous (A) and arterial flow rates (B, C and D). Different volumes of blood were used to assess thrombus formation at this increased shear rate, included 2ml (B), 5ml (C) and 8ml (D). The Celena® S digital imaging system was used to image thrombus formation on collagen.

### 4.3.7 Optimising 0.1 slides

Although using blood volumes of 5ml and 8ml in the model demonstrated adequate thrombus formation it raised the question of the feasibility and efficiency of using these volumes. In the venous flow model, a volume of 1.5ml of blood would be used per experimental condition, this meant that two vacutainers of blood (~10ml) could be used to analyse six different experimental conditions. However, using a new volume of 5ml per condition would mean that a minimum of six vacutainers (~30ml) would be needed to analyse six different experimental conditions. This may cause issues as not every donor is comfortable with donating this volume of blood and therefore using this volume could cause a restriction to the donor pool. In addition, using this volume of blood per condition could affect the scalability of the model as unattainable volumes of blood would be needed to produce a higher throughput model. The solution to this problem was to change the channel slide, Ibidi have several versions of their channel slides, including the 0.1µm. This size channel slide has a much small channel dimension meaning a lower pump flow rate can achieve the desired shear stress while also using much less blood. To achieve an arterial shear stress of 15 dyne/cm$^2$, a pump flow rate of 47µl/min was needed meaning a blood volume of 329µl was required to achieve ~7 minutes of channel time. This would make the model much more efficient, in addition to making the model scalable. A model run was performed using this setup and demonstrated adequate thrombus formation and area coverage on collagen (Figure 4.7).

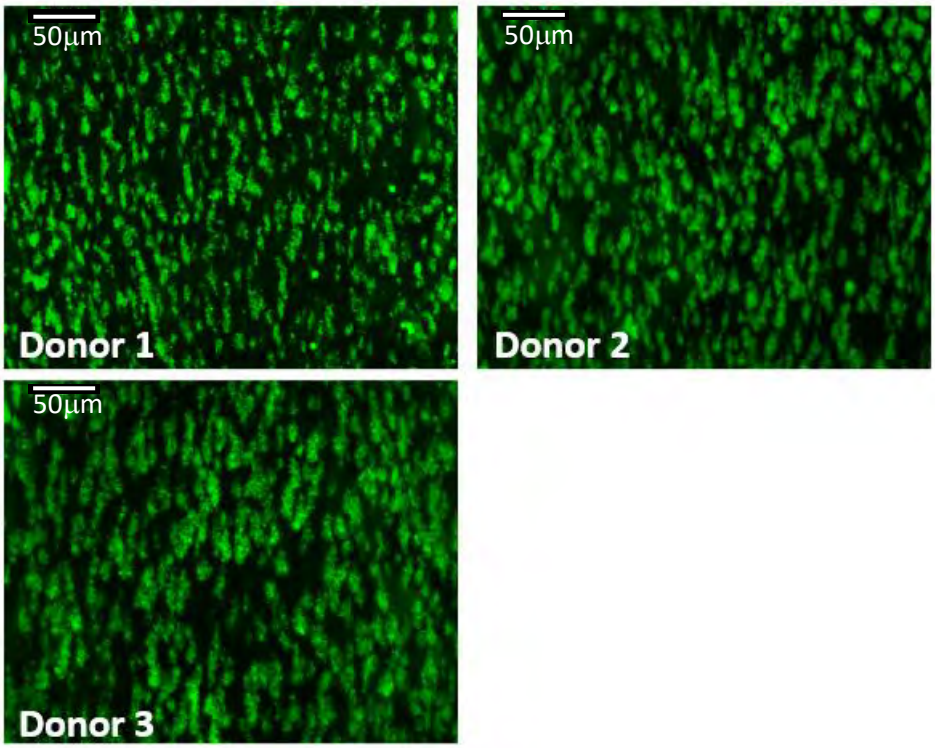


**Figure 4.7 Optimising 0.1 ibidi slides**

Human whole blood labelled with $DIOC_6$ was perfused at a shear rate of 15 dynes/cm$^2$ over immobilised collagen. The Celena® S digital imaging system was used to image thrombus formation on collagen. A total of three donors were used to demonstrate the repeatability of thrombus formation at this shear rate.

### 4.3.8 Optimal cell seeding time for arterial shear rate

The decision to adopt a new slide type for the model meant that the next stage of optimisation was the incorporation of endothelial cells . A potential issue that could arise from the use of the new smaller slides was endothelial cell death, due to poor nutrient exchange. To overcome this potential limitation, a same day cell seeding and model run approach was attempted, seeding the endothelial cells onto the channel slides in the morning and then performing a model run 6-8 hours later. This was investigated using both HUVECs and HCAECs. Confocal microscopy revealed that following whole blood perfusion the confluent cell monolayer was no longer intact in the endothelial compartment of the model and this occurred for both HUVECS and HCAECs (Figure 4.8). As this setup up was causing a loss of endothelial cells following blood perfusion, it was decided that a 24-hour seeding method should be tested, with endothelial cells being seeded onto channels 24 hours prior to a model run. This seeding method also seemed to result in the loss of endothelial cells, with a confluent monolayer no longer being intact (Figure 4.8), in addition, small platelet aggregates could be observed in the spaces between the endothelial cells. It was decided that a longer growth time was needed prior to an experimental run, this time endothelial cells were seeded into channels and allowed to grow for 48 hours prior to a model run. In order to ensure adequate nutrients for the endothelial cells, the cell culture medium was changed every 12 hours in this version of the model. Confocal microscopy demonstrated that a confluent cell monolayer was still intact, following blood perfusion (Figure 4.8).

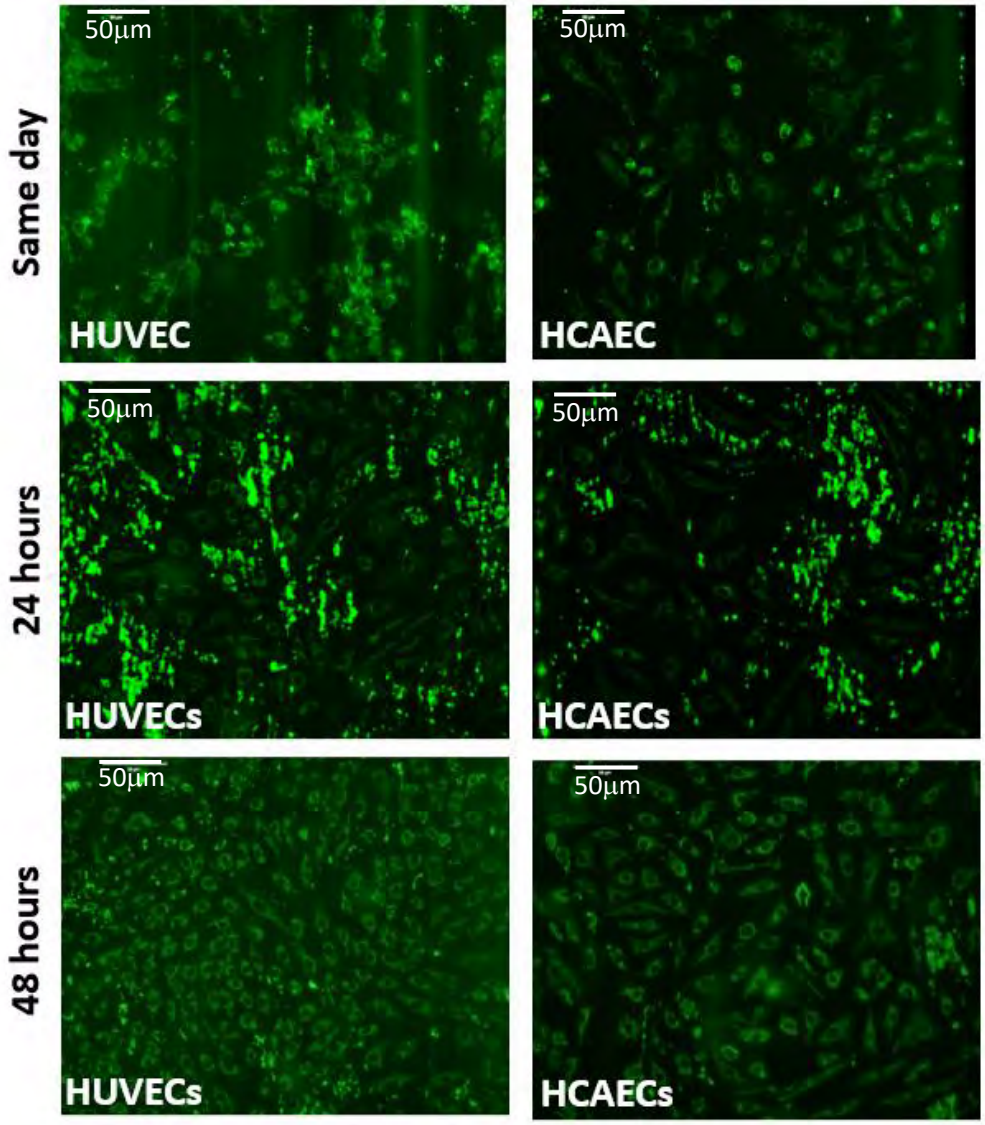


**Figure 4.8 Optimal cell seeding time for arterial shear rate**

HUVECs and HCAECs were seeded onto ibidi 0.1 slides and allowed to adhere and grow for 8 hours, 24 hours and 48 hours. Endothelial cells were fluorescently labelled with $DIOC_6$. Human whole blood was then perfused over the cells at 5 dynes/$cm^2$ before the Celena® S digital imaging system was used to image the endothelial cell compartment and analyse any loss of endothelia cells.

### 4.3.9 Incorporation of HCAECs significantly reduces thrombus size while increasing thrombus number

As the model had now been optimised with an arterial flow rate, the next step was to determine whether the inclusion of HCAECs in a chamber upstream to exposed collagen (100μg/ml) could influence platelet function and thrombus formation, the set up described in Figure 3.4 was used, and blood from five independent donors was perfused through the system at 15 dyne/cm$^2$. A no cell control was used for these experiments, with the upstream chamber containing no cells and the downstream coated with collagen (100μg/ml). Platelet adhesion and thrombus size was analysed (Figure 4.9.A). Results from the experiments demonstrated that the incorporation of HCAECs resulted in a significant reduction in average thrombi size (64.0%, $p<0.01$) (Figure 4.9.B), in addition to a significant increase in average thrombi number (57.1%, $p<0.05$) (Figure 4.9.C). No significant difference in platelet area coverage was observed between the two cell types (Figure 4.9.D).

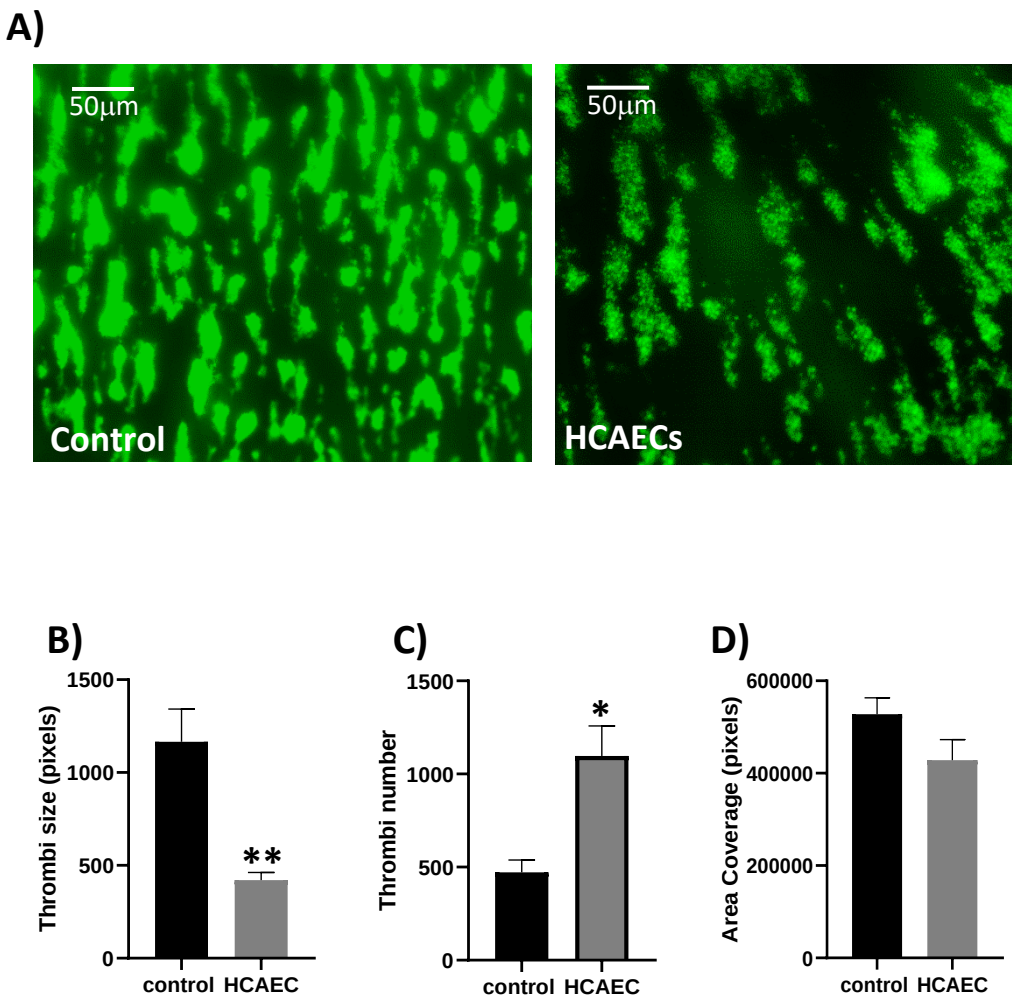


**Figure 4.9 Incorporation of HCAECs significantly reduces thrombus size while increasing thrombus number**

Whole blood labelled with $DIOC_6$ was perfused through HCAEC coated chambers prior to collagen coated chambers and platelet adhesion and thrombus size analysed (A). The presence of HCAECs significantly reduced average thrombi size (B), and increased average thrombi number (C). HCAECs had no significant effect on platelet area coverage. Data represents mean ± SEM; n=5 *p<0.05, **p<0.01 (each n represents an individual donor, with 5 images taken per condition for analysis).

### 4.3.10 Differences in thrombus regulation between HUVECs and HCAECs under arterial shear stress

It was previously demonstrated that incorporation of both HUVECs or HCAECs can positively regulate thrombus formation in the model. A difference in thrombus formation between HUVECs and HCAECs under venous flow was also observed. It was therefore important to assess if there were any differences in thrombus formation between HUVECs and HCAECs under arterial flow conditions. A no cell control was used for these experiments, with the upstream chamber containing no cells and the downstream coated with collagen (100μg/ml). Thrombus formation on immobilised collagen was analysed (Figure 4.10.A). Results from the experiments demonstrated a significant reduction in average thrombi size with HCAECs (63.9%, $p<0.05$) and HUVECs (60.0%, $p<0.05$) (Figure 4.10.B) were present in the model. No significant difference in thrombi number was observed between the three conditions (Figure 4.10.C). The incorporation of HUVECs did significantly reduce platelet area coverage compared to the control (46.3%, $p<0.05$) (Figure 4.10.D), in addition a significant difference between HUVECs and HCAECs was observed ($p<0.01$) (Figure 4.10.D).

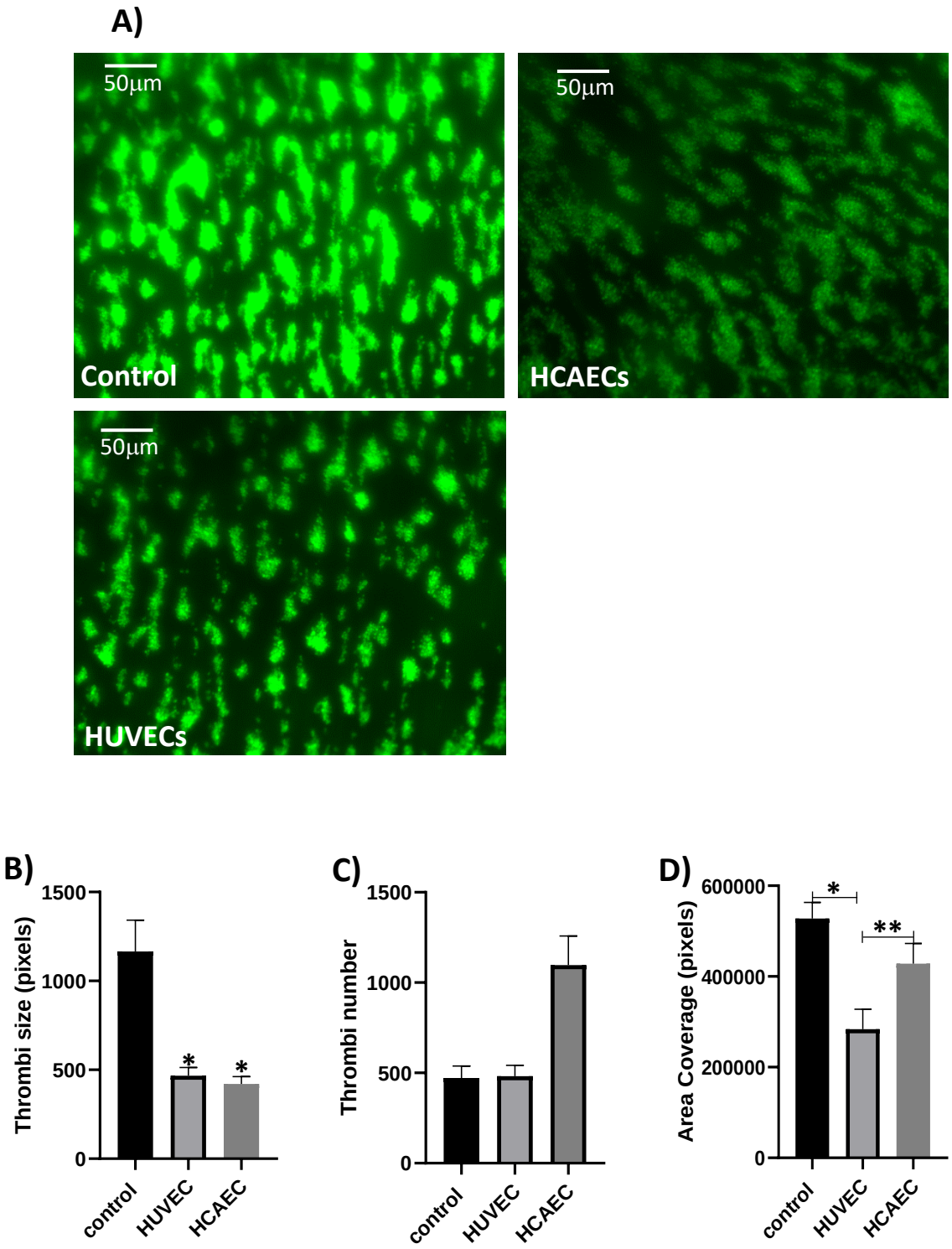


**Figure 4.10 Difference in thrombus regulation between HUVEC and HCAEC under arterial shear stress**

Whole blood labelled with $DIOC_6$ was perfused through HUVEC or HCAEC coated chambers prior to collagen coated chambers and platelet adhesion and thrombus size analysed (A). HCAECs significantly reduced average thrombus size (B), no significant difference in average thrombi number was observed between the three conditions (C). HUVECs significantly reduced platelet area coverage compared to the control, with HCAECs showing an increase compared with HUVECs (D). Data represents mean ± SEM; n=5 *p<0.05, **p<0.01 (each n represents an individual donor, with 5 images taken per condition for analysis).

## 4.4 Discussion

The aim of the research carried out in this chapter was to establish if any significant differences existed between HUVECs and HCAECs in terms of their ability to regulate thrombosis formation. Emerging *in vitro* thrombosis models have begun to incorporate endothelial cells and thus increasing the physiological relevance of these models (Coenen *et al*., 2017). However, this has also introduced a new element of variation, with a wide range of different endothelial cell types being used in these models. This variability between models may impede the ability to standardise these models and could also make comparison of results between research groups unreliable (Coenen *et al*., 2017). The substantial evidence supporting tissue-specific differences between different endothelial cells highlights the need for researchers to use endothelial cells from appropriate vessel beds, in order to accurately model their specific research question (Aird., 2015). Despite this evidence, the majority of emerging *in vitro* thrombosis models utilise HUVECs, likely due to the fact they offer an inexpensive and more easily available option to researchers in addition to being a relatively easy cell type to culture (Lau *et al*., 2021; Coenen *et al*., 2017). Therefore, as part of the model optimisation process it was important to assess the effects of venous endothelial cells versus arterial cells in the *in vitro* thrombosis model.

The venous flow model was used for the initial comparison of HUVECs and HCAECs, this would give initial insights into potential differences between the two cell types in terms of thrombus formation. The model has previously been optimised for accuracy and reproducibility making it a beneficial tool for this first assessment. The results from this experiment demonstrated that both HUVECs and HCAECs significantly reduced average thrombi size, in addition to reducing area coverage. No significant difference in average thrombi number was observed when either cell type was compared to the control, however differences were observed between the two cell types, with an decrease in average thrombi number being observed with HCAECs compared with HUVECs, in addition to a decrease in platelet area coverage. The results from this initial experiment highlighted a potential difference between the two cell types in terms of thrombus formation and therefore it was decided that any differences in expression of key endothelial-derived platelet inhibitors should be

analysed.

In chapter 3, it was shown that TNF-alpha stimulation of HUVECs could induce an activated phenotype in these cells. The potential to incorporate HCAECs into the model meant that it was also important to be able to demonstrate the same activated phenotype in HCAECs. As described previously, a key aspect of endothelial activation observed *in vivo*, is the increased expression of cell adhesion molecules, in particular ICAM-1 and VCAM-1. It was successfully demonstrated, using western blotting, that stimulation of HCAECs with TNF-alpha (10ng/µl) for 24 hours lead to a significant increase in in cell adhesion molecules VCAM-1 and ICAM-1. No significant difference in expression was observed between the two cell types, these results helped confirm that an activated endothelial cell phenotype could be achieved in HCAECs using TNF-alpha stimulation. It was then important to assess the effect of TNF-alpha stimulation on key endothelial mediators, in addition to comparing these results to those observed with HUVECs.

The COX enzymes play a key role in the cardiovascular system, being responsible for prostacyclin and $TXA_2$, two key regulators of platelet activity. The COX-1 enzyme is predominantly responsible for the production of the potent platelet activator, $TXA_2$, with the majority attributed to platelet COX-1 production (Linton and Fazio., 2009). Western blotting revealed no significant difference in COX-1 expression between HUVECs and HCAECs, in addition TNF-alpha stimulation appeared to have no significant effect on the expression of COX-1 in either cell type. Prostacyclin is thought of as the predominant eicosanoid produced by the endothelium and plays a key role in inhibiting platelet adhesion and activation (Linton and Fazio., 2009). COX-2 has been identified as the main producer of endothelial prostacyclin, therefore any changes in COX-2 expression may have a significant effect on platelet activity and thrombus formation (Moncada *et al*., 1977; Fitzgerald and Patrono, 2001). Western blotting demonstrated no significant difference in the protein levels of COX-2 in HUVECs and HCAECs, however real-time PCR revealed an almost 3-fold increase in COX-2 gene expression in HCAECs compared with HUVECs. Some studies have compared differences in prostacyclin production and secretion in venous and arterial cells, producing conflicting results. A study comparing bovine arterial and venous

endothelial cells observed similar amounts of prostacyclin production in both cell types (D'Orleans-Juste *et al*., 1992). In contrast, a study comparing porcine femoral artery endothelial cells with femoral vein endothelial cells showed lower secretion of prostacyclin in venous endothelial cells compared with arterial cells (Geenen *et al*., 2015; Lau *et al*., 2021). These findings support the observations in this study in terms of increased COX-2 gene expression in HCAECs compared with HUVECs. Western blotting demonstrated a significant increase in COX-2 protein levels in HCAECs following TNF-alpha stimulation. As discussed previously, COX-2 is often thought of as the inducible form of COX and has been shown to be induced in response to inflammatory stimulus (Funk and FitzGerald, 2007). The increase in COX-2 in HCAECs helps to demonstrate that TNF-alpha is working correctly in the model and producing inflammatory responses in the endothelial cells which correlates with that observed *in vivo*.

Next, differences in CD39 expression was assessed, CD39 plays a key role in regulating thrombus formation by converting the potent platelet activator ADP into AMP. Western blotting demonstrated no significant difference in protein levels of CD39 between HUVECs and HCAECs. However, real-time PCR revealed a significant decrease in ENTPD1 expression in HCAECs compared to HUVECs. As CD39 plays a key role in platelet regulation it was important to assess if TNF-alpha stimulation was having any effect on CD39 protein levels. Western blotting demonstrated that TNF-alpha stimulation had no significant effect on the protein levels of CD39.

In chapter 3, it was demonstrated that NO had an important role in regulating thrombus formation in the model, with inhibition of eNOS leading to an increase in thrombus formation. Furthermore, it was demonstrated that TNF-alpha stimulation led to a decrease in eNOS expression in HUVECs, which also resulted in an increase in thrombus formation. It was therefore important to assess any difference in eNOS expression between HUVECs and HCAECs. In addition to assessing the effect of TNF-alpha stimulation on eNOS expression in HCAECs. Western blotting revealed no significant differences in phospho and total eNOS protein levels between HUVECs and HCAECs. Real- time PCR however revealed a significant increase in eNOS gene expression in HCAECs compared with HUVECs. There is conflicting evidence in the

literature in terms of the production and release of NO in veins and arteries and the role of the endothelial cells native to these vessels. A study comparing endothelial cell production of NO in porcine arterial endothelial cells versus venous endothelial cells reported similar levels of NO production following stimulation with lipopolysaccharides (Geenen *et al*., 2015). Similar results were observed in a comparison of bovine arterial and venous endothelial cells (D'Orleans- Juste *et al*., 1992). In contrast, a study comparing NO production in canine arterial and venous endothelial cells demonstrated that canine arterial endothelial cells produced and released more NO than venous endothelial cells, in response to flow (Fukaya *et al*., 1996; Lau *et al*., 2021). This supports what was observed with real-time PCR with HCAECs demonstrating a higher expression of eNOS.

Shear stress levels are not uniform throughout the cardiovascular system and vary amongst vessel types, with typically higher shear rates being observed in arterial vessels (5–40 dynes/cm$^2$) compared to venous (1–5 dynes/cm$^2$) (Dela paz *et al*., 2009). As a result, it was essential that similar arterial shear stress levels were achieved in the thrombosis model. It was determined that it would not be possible to use the existing Ibidi 0.4 slides at the increased flow rate as this would make increasing the throughput of the model in the future unfeasible due to the large amount of blood required for modelling multiple conditions. As a result, 0.1 Ibidi slides were chosen for modelling thrombosis at an arterial flow rate, the smaller channel size of these slides allowed the appropriate shear stress to be achieved while using relatively small volumes of blood.

The next stage was the incorporation of HCAECs into the model and culturing endothelial cells on the new slide type. Initial experiments analysed seeding cells the same day as the model run; however, it was demonstrated that blood perfusion this soon after seeding led to the loss of endothelial cells, with cells potentially being sheared off under the increased flow levels. There was an improvement when cells were allowed up to 24 hours to adhere to the slide; however, it was found that 48 hours was optimal for cell adhesion in addition to enabling the possibility of 24 hour TNF-stimulation in the model. The successful incorporation of HCAECs into the thrombus model allowed us to assess the effect of HCAECs on platelet regulation and

thrombus formation. Average thrombus size was significantly reduced when HCAECs were present in the model but interestingly, average thrombi number was significantly increased with HCAECs. This could potentially be due to HCAECs reducing the formation of large platelet aggregates, like those observed in the control, and only allowing predominantly the adhesion of single platelets. In contrast, the control condition appears to have fewer but larger platelet aggregates forming on the collagen.

Finally, it was important to compare HUVECs and HCAECs directly in the model, as previously a significant difference in thrombus formation between HUVECs and HCAECs under venous flow rates has been demonstrated. It was therefore important to assess if these differences persisted under arterial flow. A significant reduction in average thrombi size was observed with HCAECs and HUVECs, however platelet area coverage was significantly increased in HCAECs as compared to HUVECs. This difference may be due to the previously reported differences in key platelet mediators; in particular, the increased eNOS expression in arterial cells. The reduced capacity for NO production in HUVECs may mean that at these high shear rates, not enough NO is released to fully exert its anti-platelet effects. The thrombi that formed when HCAECs are present in the model had a "woolly" phenotype, which may suggest that they are loose aggregates made up of single adhered platelets rather than large platelet aggregates (Unsworth *et al*., 2021). This could provide the reason for the increase in platelet area coverage observed with HCAECs. The differences in thrombus formation observed between HUVECs and HCAECs suggests that arterial cells should be used when modelling arterial thrombosis. Furthermore, these findings support the suggestion that the correct endothelial cell type should be used when modelling different disease types and that HUVECs should not necessarily be used as a "one cell fits all" approach to modelling thrombosis.

In conclusion, arterial endothelial cells were successfully incorporated into the thrombosis model and model runs were performed at a physiologically relevant arterial shear rate. In addition, significant differences in the expression of key platelet mediators was observed between HUVECs and HCAECs. Finally, a difference in the regulation of thrombus formation between the two cell types was demonstrated,

highlighting that the use of tissue- specific endothelial cells was essential for producing a physiologically accurate model of arterial thrombosis.

# 5. Assessment of ACE2/ANG1-7/MAS signalling axis as a potential novel anti-platelet drug target

## 5.1 Introduction

The renin-angiotensin system plays a key role in the cardiovascular system, this hormone system is responsible for regulating blood pressure and controlling electrolyte balance (Santos *et al*., 2019). Renin is produced and released into the circulation from the kidneys in response to a reduction in blood flow. Renin is then responsible for the conversion of angiotensinogen into angiotensin I (ANG) which is then in turn converted into ANG II by the angiotensin-converting enzyme (ACE) (Figure 5.1). ANG II is a potent vasoconstrictor which signals via two receptors, ANG II type 1 (AT1R) and ANG II type 2 (AT2R), to increase blood pressure and restore adequate blood flow (Figure 5.1) (Santos *et al*., 2018). In cardiovascular disease, dysregulation of the renin-angiotensin system is associated with the development hypertension (Szczepanska-sadowska *et al*., 2018). As a result, components of this system present therapeutic targets for the treatment of hypertension with angiotensin receptor inhibitors and ACE inhibitors being utilised to reduce blood pressure (Azizi and Ménard, 2004; Ma *et al*., 2010).

The role of some products of the renin-angiotensin system remained unclear for many years, such as the heptapeptide ANG 1-7 which was previously thought of as an insignificant breakdown product of ANG I and ANG II (Yang *et al*., 1968). Several peptidases can facilitate the conversion ANG I or ANG II into ANG 1-7 (Figure 5.1); however, it was the discovery that the ACE homolog, ACE2, is the predominant enzyme responsible for the conversion of ANG II into ANG 1-7 that increased research interest in this area (Rice *et al*., 2004). In addition, ANG 1-7 was shown to act on the MAS receptor and therefore counteract the activity of ANG II, presenting the ACE2/ANG1-7/MAS signalling axis as a novel therapeutic target. One of the key actions of ANG 1-7 in the vascular system is vasorelaxation, ANG 1-7 achieves this by activating the MAS-1 receptor which stimulates NO production and release which leads to vasodilation. In addition, ANG 1-7 has been shown to potentiate the

vasodilatory effects of bradykinin (Santos *et al*., 2018).

Activation of the ANG II, AT1R and AT2R, appear to have opposing effects (Kuriakose *et al*., 2021). Activation of AT1R initiates a downstream signalling cascade involving multiple molecules including tyrosine kinases, serine threonine kinases and mitogen-activated protein kinases. Activation of AT2R can lead to an increase in NO production which in turn contributes to vasorelaxation and a decrease in vascular tone (Wang *et al*., 2012). ANG II signalling via AT1R leads to several outcomes which are often associated with ANG II such as inflammation and vasoconstriction (Saviao *et al*., 2011). In contrast, by stimulating NO release activation of AT2R appears to oppose the actions of ANG II on ATR1, however the role of AT2R activation in the cardiovascular system remains poorly understood (Kuriakose *et al*., 2021).

ACE2 acts as a negative regulator by facilitating the conversion of ANG II into ANG 1-7, this leads to a decrease in levels of the potent vasoconstrictor ANG II and in turn increases the levels ANG 1-7, which can promote vasodilation via activation of MAS-1 (Figure 5.1) (Mendoza-Torres *et al*., 2015). In the cardiovascular system, ACE2 is expressed by the endothelial cells of arteries and veins (Hamming *et al*, 2004). Several studies have demonstrated the localisation of ACE2 in endothelial cells in multiple vessel beds, with ACE2 mRNA being reported in carotid artery endothelial cells (Sluimer *et al*, 2008), in addition to protein and mRNA expression in umbilical cord endothelial cells (Valdés *et al*., 2006). The role of endothelial ACE2 in the vascular system is yet to be fully identified but current evidence suggests ACE2 plays an important role in stimulating vasodilation, in addition to demonstrating anti-inflammatory effects. ACE2 contributes to vasodilation via the phosphorylation on eNOS which in turns leads to an increase of NO production (Sampaio *et al*., 2007). The anti- inflammatory effects of ACE2 is achieved by opposing the actions of ANG II, in particular the inhibition of ANG II mediated phosphorylation of ERK 1/2 and c-Src (Santos *et al*., 2018).

The activity of the ACE2/ANG1-7/MAS signalling axis in endothelial cells has been shown to promote vasorelaxation and inhibit ANG II-induced inflammation, thus making it an attractive therapeutic target. However, it is important to broaden our view and consider the role of this signalling axis in platelets, as interactions between

endothelial cells and platelets are key to thrombus formation. Therefore, an understanding of the signalling axis in both platelets and endothelial cells will enable us to assess its potential as a novel anti-thrombotic target. The presence of the MAS receptor in platelets was confirmed by *Fraga-Silva et al* in 2008, who utilised western blotting to show the MAS receptor was present in isolated rat platelets (Fraga-Silva *et al*., 2008). It has been shown that ANG 1-7 mediated activation of platelet MAS-1 leads to the induction of NO. It was confirmed that this induction of NO was MAS-1 dependent as the effect of ANG 1-7 on NO stimulation was abolished in MAS deficient mice (Fraga-Silva *et al*., 2008). In addition, to stimulating platelet NO release, ANG 1-7 has also been shown to increase levels of plasma prostacyclin in Bdkrb2$^{-}$/$^{-}$ mice via activation of the AT1R or MAS receptor (Fang *et al*., 2013). As stimulation of the MAS receptor initiates the release of two potent inhibitors of platelet activation, NO and prostacyclin, it presents a potential novel anti-platelet target (Fang *et al*., 2013; Fraga-Silva *et al*., 2008).

In this chapter, the presence of key receptors of the ACE2/ANG1-7/MAS signalling axis in HUVECs and platelets was confirmed. The effect of ANG 1-7 stimulation on the expression of endothelial derived platelet inhibitors was assessed, in addition to the effect of ANG 1-7 stimulation on platelet aggregation. Finally, the *in vitro* thrombosis model was used to demonstrate the effects of ANG 1-7 on thrombus formation.

### 5.1.1 Aims and hypothesis

The principal aims of the work presented in this chapter were to:

1. Confirm the presence of key mediators in the ACE2/ANG1-7/MAS in endothelial cells
2. Assess the effects of ANG1-7 on key endothelial cell regulators of platelet activity
3. Evaluate the effects of ANG 1-7 on platelet aggregation
4. Analyse the effect of ANG 1-7 on thrombus formation in the *in vitro* thrombosis model

**Hypothesis**

ANG 1-7 negatively regulates thrombus formation by stimulating nitric oxide release from platelets and endothelial cells

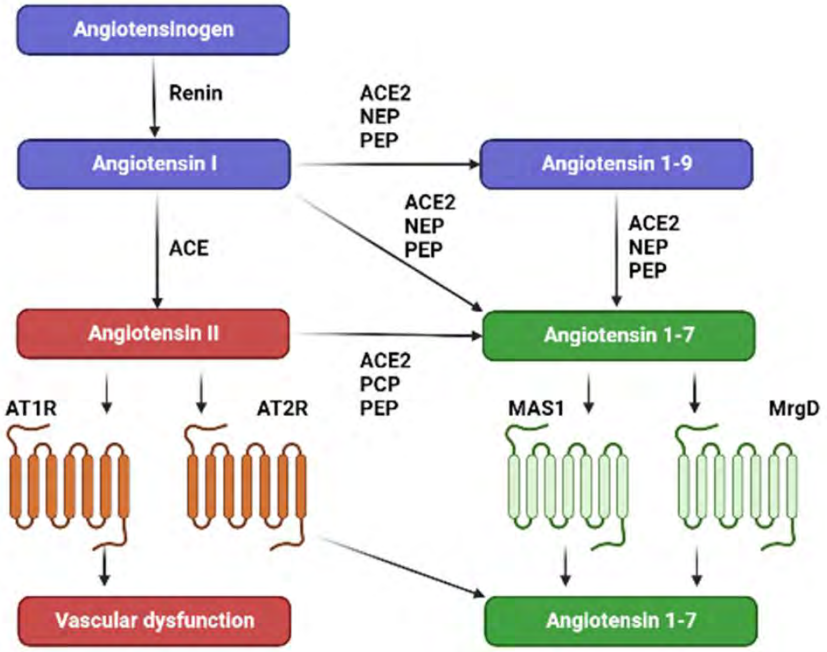


**Figure 5. 1 ACE2/ANG1-7/MAS signalling pathway**

Angiotensinogen is converted into angiotensin (ANG) I by Renin, ANG I is then in turn converted into ANG II by the angiotensin-converting enzyme (ACE). ANG II is a potent vasoconstrictor which signals via two receptors, ANG II type 1 (AT1R) and ANG II type 2 (AT2R), to induce vasoconstriction to increase blood pressure. ANG 1-7 can be formed from ANG I and ANG II by ACE2. ACE2 acts as a negative regulator by facilitating the conversion of ANG II into ANG 1- 7, this leads to a decrease in levels of the potent vasoconstrictor ANG II and in turn increases the levels ANG 1-7, which can promote vasodilation via activation of MAS- 1 and MrgD. NEP, neutral endopeptidase; Mas1, Mas1 receptor; MrgD, Mas-related-G-protein-coupled receptor D; PCP, prolyl carboxypeptidase; PEP, prolyl oligopeptidase; THOP, thimet oligopeptidase. Figure adapted from Kuriakose *et al.* 2021

## 5.2 Summary of *in vitro* model setups used in this chapter

The higher throughput model was utilised for model experiments in this chapter and was setup as described in 2.4.3. Two Ibidi VI$^{0.4}$ µ-slides were connected to each other via siliconized tubing, HUVECs were seeded onto the first µ-slide (plating density 5 x10$^5$/ml) before being incubated for 48 hours at 37ºC with 5% $CO_2$ to allow a confluent monolayer to form. The channels of the second µ-slide were coated with type I collagen fibrils (derived from equine tendons; Labmedics) (100µg/ml) one hour prior to blood perfusion. The first µ-slide was connected to six pairs of reservoirs containing either Tyrodes buffer or human whole blood, via siliconized tubing. Corresponding channels of the two µ-slides were lined up and connected via siliconized tubing. The second µ-slide was connected to a six-syringe withdrawal pump, which enables blood to be perfused through all 6 channels per slide, over endothelial cells before passing over collagen at the same physiological relevant shear stress.

## 5.3 Results

### 5.3.1 Key mediators in the ACE2/ANG 1-7/MAS signalling axis are present in HUVECs

Utilising the thrombosis model enabled the assessment of the effects of stimulating the ACE2/ANG1-7/MAS signalling pathway in platelets and endothelial cells, both separately and in combination. In order to assess the ACE2/ANG1-7/MAS signalling axis as a potential novel therapeutic target in endothelial cells, it was first essential to ensure that key receptors were expressed in HUVECs. As discussed previously, ACE2, AT1R, AT2R and MAS-1 are all important receptors involved in the signalling axis. Western blotting was used to confirm the expression of these receptors in HUVECs which revealed that all four receptors are expressed in HUVECs (Figure 5.2).

,

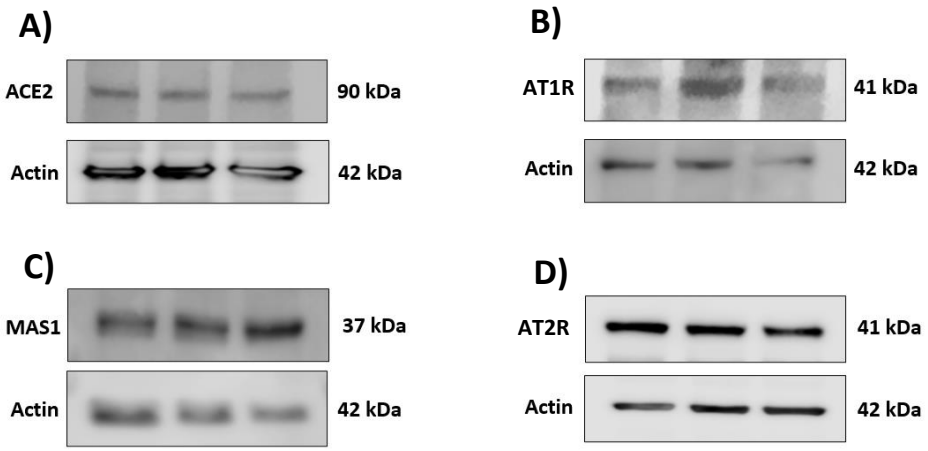


**Figure 5. 2 Key mediators in the ACE2/ANG1-7/MAS signalling axis are present in HUVECs**

HUVECs were cultured for 48 hours to allow a confluent monolayer to form before being lysed for western blotting. Western blotting demonstrated the presence of ACE2 (A), ATR1 (B), MAS-1 (C) and ATR2 (D) in HUVECs. n=3 (each n represents a separate donor).

### 5.3.2 ANG 1-7 and ANG II had no significant effect on key endothelial cell genes

Once the presence of key ACE2/ANG1-7/MAS signalling receptors in HUVECs had been confirmed, the next step was to assess the effects of Angiotensin II and ANG 1-7 on the gene expression of endothelial-derived platelet mediators, separately and in combination. HUVECs were stimulated with Angiotensin II (0.1µM) and ANG 1-7 (0.1µM) or DMSO (0.1%) for 24 hours, cells were then lysed for real-time PCR to assess changes in gene expression. As described previously, COX-1 and COX-2 play a pivotal role in regulating platelet activity via the release of production of both platelet inhibitors and platelet activators, therefore it was important to investigate if there were any changes in the expression of PTGS1 (Figure 5.3.A) and PTGS2 (Figure 5.3.B). In addition, changes in ENTPD (Figure 5.3.C) (CD39) and NOS3 (Figure 5.3.D) (eNOS) were also assessed. Real- time PCR demonstrated no significant changes in gene expression following stimulation with both angiotensin II and ANG 1-7, both separately and in combination.

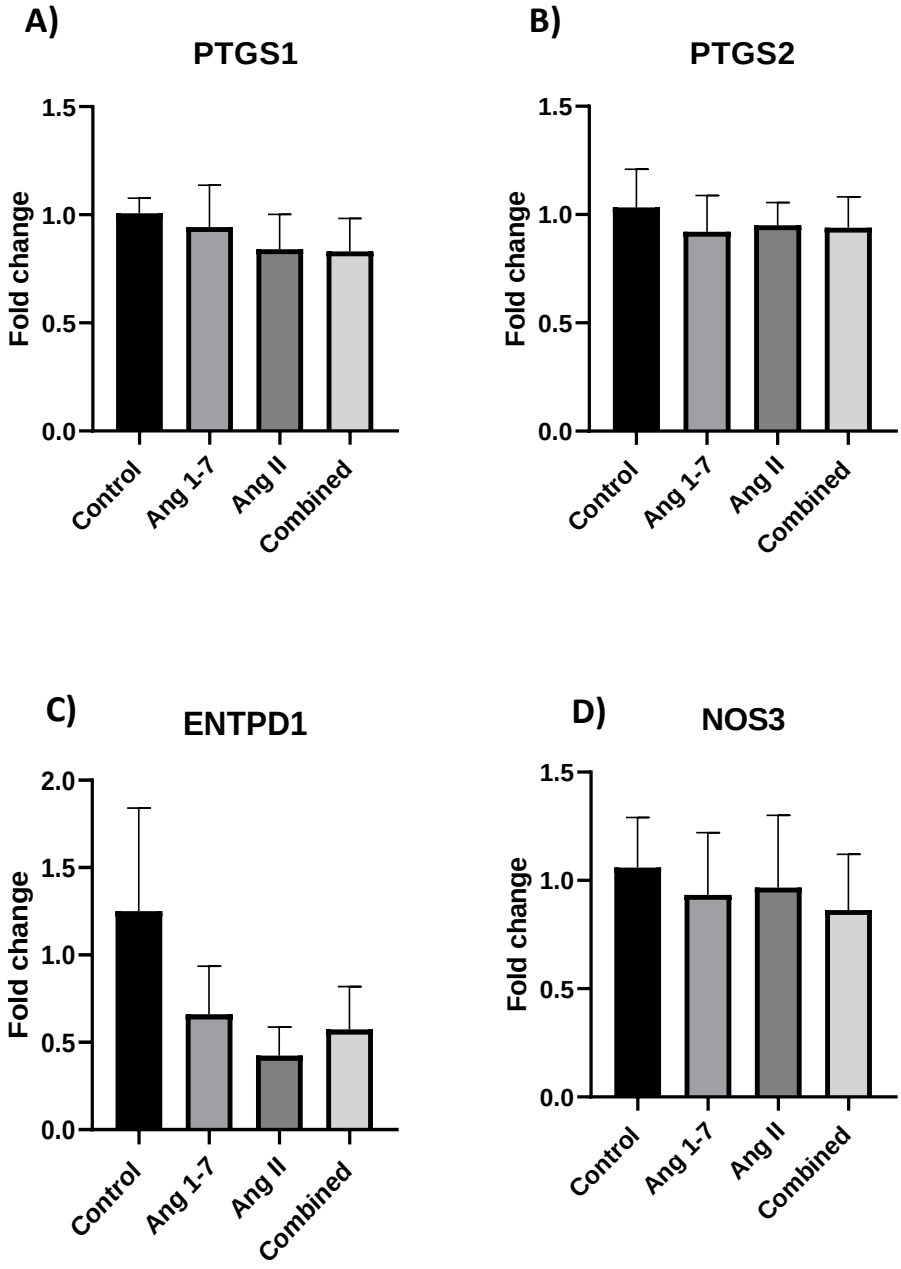


**Figure 5.3 Ang 1-7 and ANG II had no significant effect on key endothelial cell genes**

HUVECs were stimulated with ANG 1-7 (0.1µM) and/or ANG II (0.1µM) for 10 minutes prior to being lysed for real-time PCR. Real-time PCR demonstrated no significant changes in gene expression following stimulation with ANG 1-7 and/or ANG II. n=3 (Each n represents a biological repeat).

### 5.3.3 Key mediators in the ACE2/ANG1-7/MAS signalling axis are present in platelets

Before assessing the effects of targeting the ACE2/ANG1-7/MAS signalling axis in platelets, it was important to confirm the expression of key receptors and mediators. As described previously, MAS-1 has been identified as a key receptor for the anti-thrombotic effect associated with ANG 1-7, therefore it was important to confirm the presence of this receptor in platelets. In addition, to confirming the presence of ATR1 and ATR2 in platelets as they are ANG II receptors and form an integral part of the wider picture in terms of angiotensin signalling. Finally, it was essential to confirm the presence of the ACE2 enzyme as this would indicate the capacity for platelets to produce ANG 1-7 via the conversion of ACE II. Washed platelets were isolated from human whole blood and lysed for protein to allow western blotting to be performed and assess the presence of the previously mentioned proteins. Western blotting confirmed the expression of ACE2 (A), AT1R (B), AT2R (C) and MAS-1 (D) in platelets isolated from human whole blood (Figure 5.4).

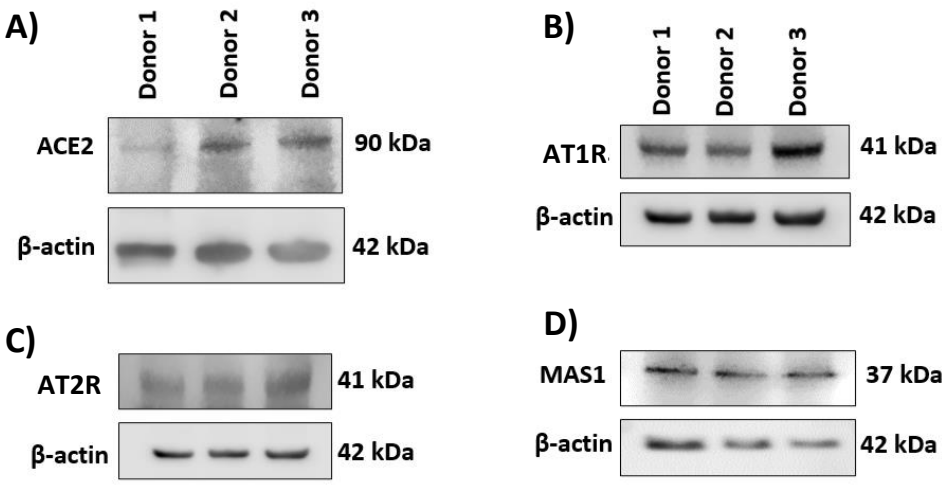


**Figure 5.4 Key mediators in the ACE2/ANG1-7/MAS signalling axis are present in platelets**

Human whole blood was collected from three healthy donors prior to washed platelets being prepared. Platelets were then lysed for western blotting. Western blotting demonstrated the presence of ACE2 (A), AT1R (B), MAS-1 (C) and AT2R (D) in human platelets. n=3 (Each n represents a biological repeat).

### 5.3.4 ANG 1-7 stimulation had no significant effects on platelet aggregation in response to collagen or ADP

Stimulation of platelet MAS-1 may provide a novel anti-platelet target, as ANG 1-7-mediated activation of MAS-1 is thought to induce NO release and therefore exert an anti-thrombotic effect (Fraga-Silva *et al*., 2008). Plate based aggregation was utilised to assess the effect of ANG 1-7 on platelet aggregation. Experiments were performed using two different platelet agonists, collagen and ADP. Collagen-GPVI activation is key in the initial stages of thrombus formation, facilitating the adhesion and activation of platelets (Burkhart *et al.,* 2012). ADP is released from activated platelets and drives the secondary signalling amplification process, recruiting more platelets to the site of the growing thrombus. If any effect on platelet aggregation was observed, the use of two platelet agonists would help identify the signalling pathway that ANG 1-7 may be exerting its effects on and therefore, aid in elucidating the potential mechanisms responsible. A range of ANG 1-7 concentrations (0.001– 10μM) was used to assess the potential effects on platelet aggregation. Platelet rich plasma was incubated in this range of ANG 1-7 concentrations or vehicle control (Tyrodes) (5 μM) for 10 minutes prior to plate agitation; platelet aggregation was then assessed. Plate-based aggregation demonstrated no significant effects on platelet aggregation following stimulation with ANG 1-7 (Figure 5.5).

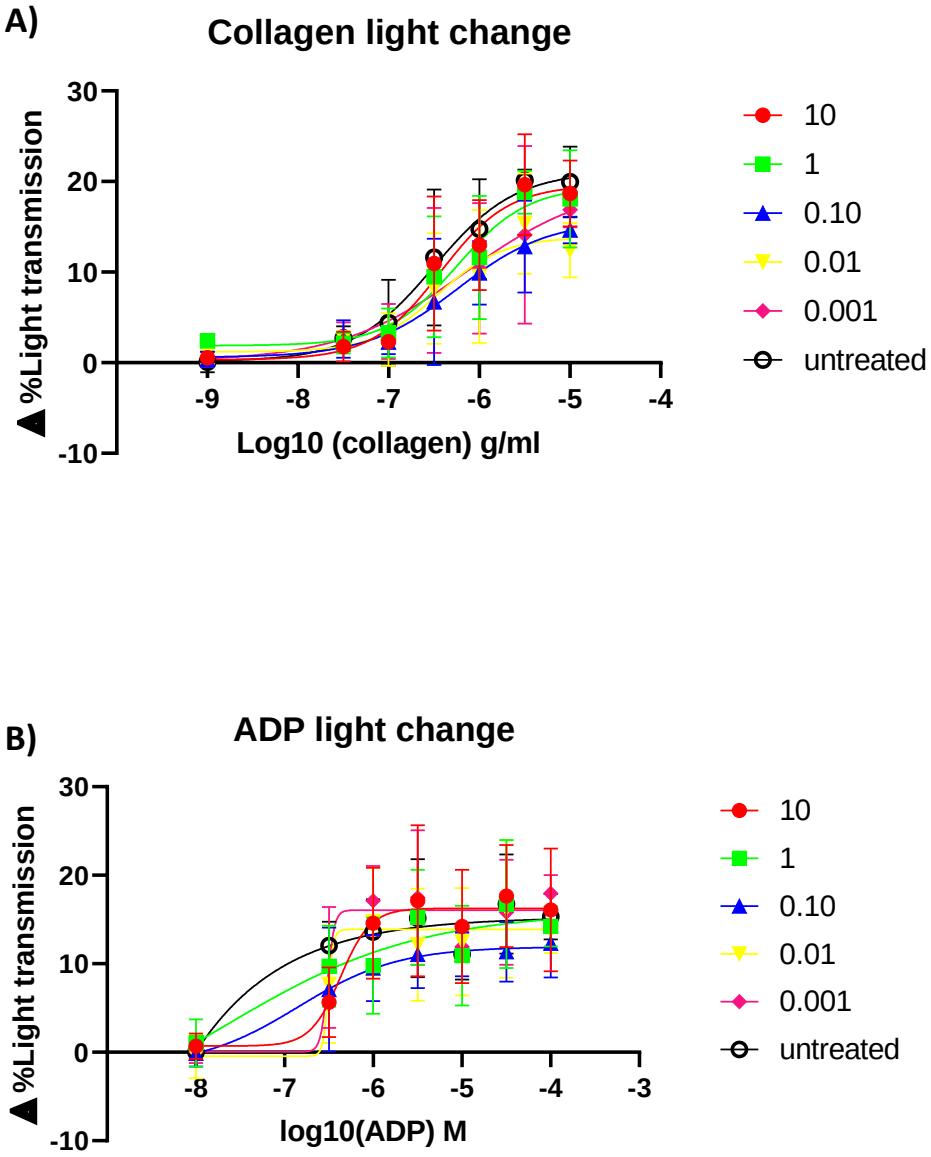


**Figure 5.5 ANG 1-7 stimulation had no significant effects on platelet aggregation in response to collagen or ADP**

Plate based aggregometry assay (PBA) was performed in a 96-well plate. Platelet rich plasma was isolated from human whole blood prior to incubation with a range of ANG 1-7 concentrations (0.001-10µM) for 10 minutes. Following addition of the agonists to the platelet rich plasma, the 96-well plate was placed on a plate shaker at 1200rpm, at 37 ºC for 5 minutes. Finally light transmission was measured using a plate reader. PBA demonstrated no significant changes in platelet aggregation in response to collagen (A) or ADP (B) following ANG 1-7 incubation. n=5 (Each n represents an individual donor).

### 5.3.5 ANG 1-7 had no significant effect on real time aggregation in response to collagen and ADP

No significant effect on platelet aggregation was observed when assessing platelet response to ADP and collagen using PBA. This may be due to the fact that this assay is an end point assay and potentially, not sensitive enough to detect subtle changes in platelet aggregation. As a result, it was decided that real time aggregation should be utilised to enable the assessment of any effect ANG 1-7 stimulation had on platelet aggregation, in real time. Like with the PBA assay, collagen and ADP were used as the platelet agonists in this assay, this would aid elucidating the potential mechanism if an effect was observed with ANG 1-7. A range of ANG 1-7 concentrations (0.1–10μM) was used to assess the potential effects on platelet aggregation. Platelet rich plasma (PRP) was incubated with ANG 1-7 or vehicle control (Tyrodes) (5 μM) at a final concentration of 0.1-10 μM for 5 minutes in siliconized glass cuvettes prior to the addition of agonist (50 μl). The agonists used were collagen (2 μg/ml) (Figure 5.6.A) and ADP (1 μM) (Figure 5.6.B). PRP was stimulated for 5 minutes at 37 °C with continuous stirring (1200 rpm) and aggregation was measured. Real time aggregation revealed no significant difference in platelet aggregation in response to ANG 1-7, with both agonists; collagen (Figure 5.6.C) and ADP (Figure 5.6.D).

**A)**

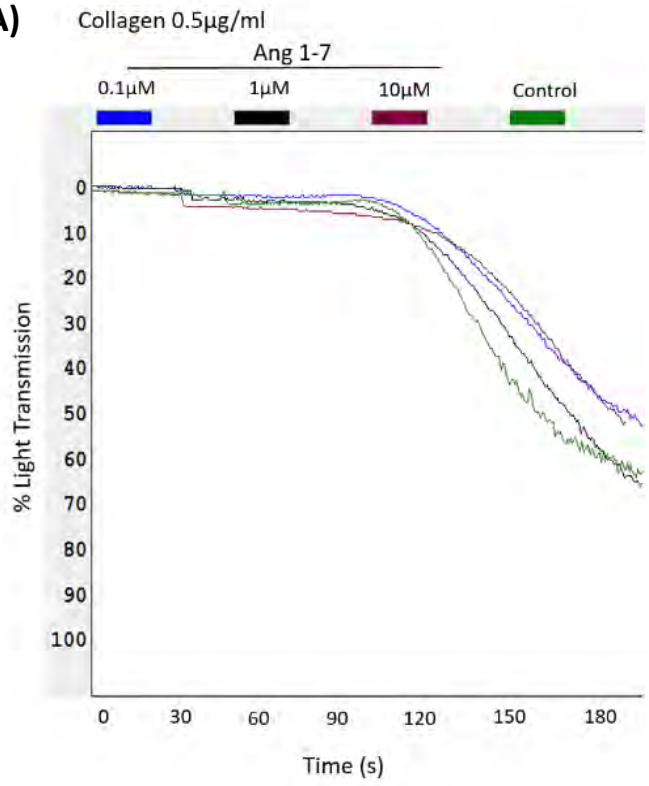
Collagen 0.5µg/ml
Ang 1-7
0.1µM
1µM
10µM
Control
% Light Transmission
0
10
20
30
40
50
60
70
80
90
100
0
30
60
90
120
150
180
Time (s)

**B)**

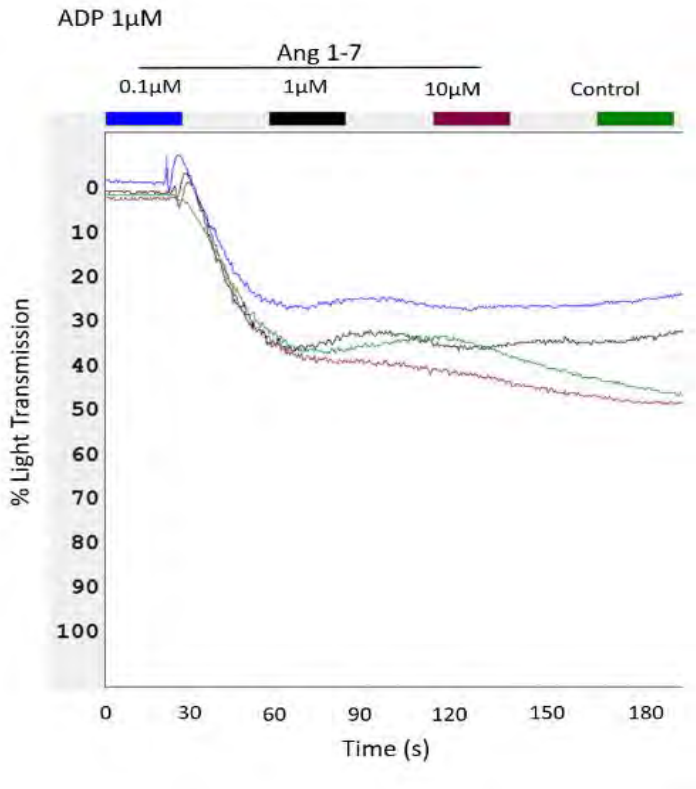
ADP 1µM
Ang 1-7
0.1µM
1µM
10µM
Control
% Light Transmission
0
10
20
30
40
50
60
70
80
90
100
0
30
60
90
120
150
180
Time (s)

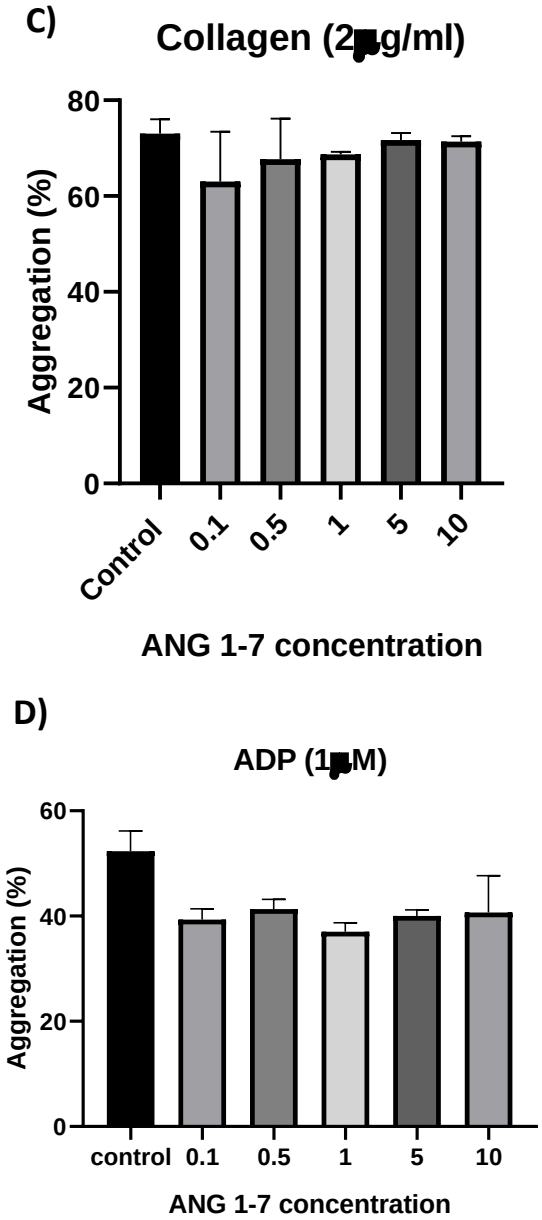


**Figure 5.6 ANG 1-7 had no significant effect on real time aggregation in response to collagen and ADP**

Platelet rich plasma (445 µl) was incubated with Ang1-7 or vehicle control (Tyrodes) (5 µM) at a final concentration of 0.1-10 µM for 5 minutes in siliconized glass cuvettes prior to the addition of agonist (50 µl). The agonists used were collagen (2 µg/ml) (A) and ADP (1 µM) (B). PRP was stimulated for 5 minutes at 37 °C with continuous stirring (1200 rpm) and aggregation measured using a ChronoLog 700 Aggregometer (Labmedics, Oxford) and Aggrolink 8 software. Aggregation was measured as percentage light transmission through the sample, calibrated against platelet poor plasma, taken as 100% light transmission, and non-stimulated PRP taken as 0% light transmission. ANG 1-7 had no effect on collagen (C) or ADP (D) stimulation. Data presented as percentage of aggregation in the presence of Tyrodes-HEPES buffer represents mean ± SEM; n=3 (Each n represents an individual donor).

### 5.3.6 ANG 1-7 had no significant effect on platelet activation

As the presence of key mediators involved in the ACE2/ANG1-7/MAS signalling axis has been confirmed, the next step was to investigate the effect of stimulating this pathway on platelet activation. Flow cytometry was utilised to assess any effects of ANG 1-7 stimulation on platelet activity. Platelet rich plasma was isolated from human whole blood, prior to stimulation with ADP, this would achieve platelet activation and allow us to assess the effects of ANG 1-7 on ADP mediated activation. Following ADP stimulation and incubation in a range of ANG 1-7 concentrations (0.1-10µM) flow cytometry was performed to assess changes in markers of platelet activation; CD63, PAC-1, CD62P and Annexin V. Results from these experiments demonstrated no significant changes in the percentage of cells positive for these markers following treatment with any concentration of ANG 1-7 (Figure 5.7).

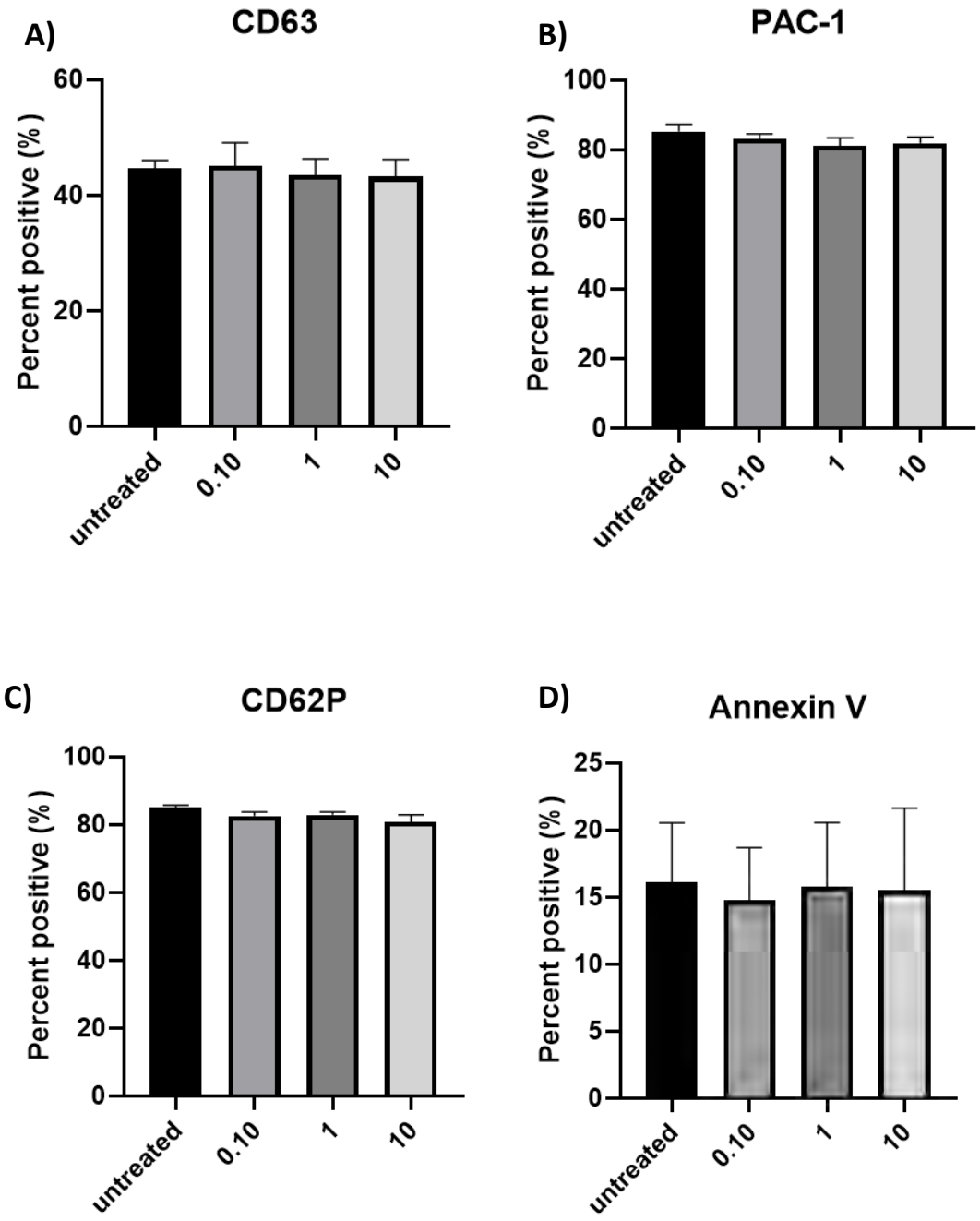


**Figure 5. 7 ANG 1-7 had no significant effect on platelet activation**

Platelet rich plasma (PRP) was prepared from human whole blood and was incubated with a range of ANG1-7 concentrations (0.1–10µM) for 10 minutes, prior to incubation with ADP (10µM) for 5 minutes. Flow cytometry antibodies CD63, PAC-1, CD62P and annexin V were incubated in PRP to allow assessment of platelet activation. Flow cytometry revealed no significant changes in the percentage of cells positive for CD63 (A), PAC-1 (B), CD62P (C) and annexin V (D). n=5 (each n represents an individual donor).

### 5.3.7 The presence of ANG 1-7 in the thrombosis model had no significant effect on thrombus formation

ANG 1-7 stimulation was analysed in the thrombosis model, as this would allow the assessment of the effects of the heptapeptide on endothelial cell regulation of thrombus formation. It was previously demonstrated that ANG 1-7 did not appear to be having any significant effects on the gene expression of key endothelial derived platelet inhibitors, in addition to no significant effect on platelet activation or aggregation. Therefore, it would be interesting to assess if the same results would be observed in the thrombosis model. Using the higher throughput *in vitro* thrombosis model described in section 2.3.4, thrombus formation on immobilised collagen (100μg/ml) was determined in the presence of ANG 1-7. Human whole blood and HUVECs were incubated in ANG 1-7 (0.1-10μM) or vehicle control (Tyrodes) (5 μM) for 10 minutes; thrombus formation on the collagen following perfusion of human whole blood was then assessed (Figure 5.8.A). ANG 1-7 stimulation had no significant effect on average thrombi size (Figure 5.8.B) or area coverage (Figure 5.8.C).

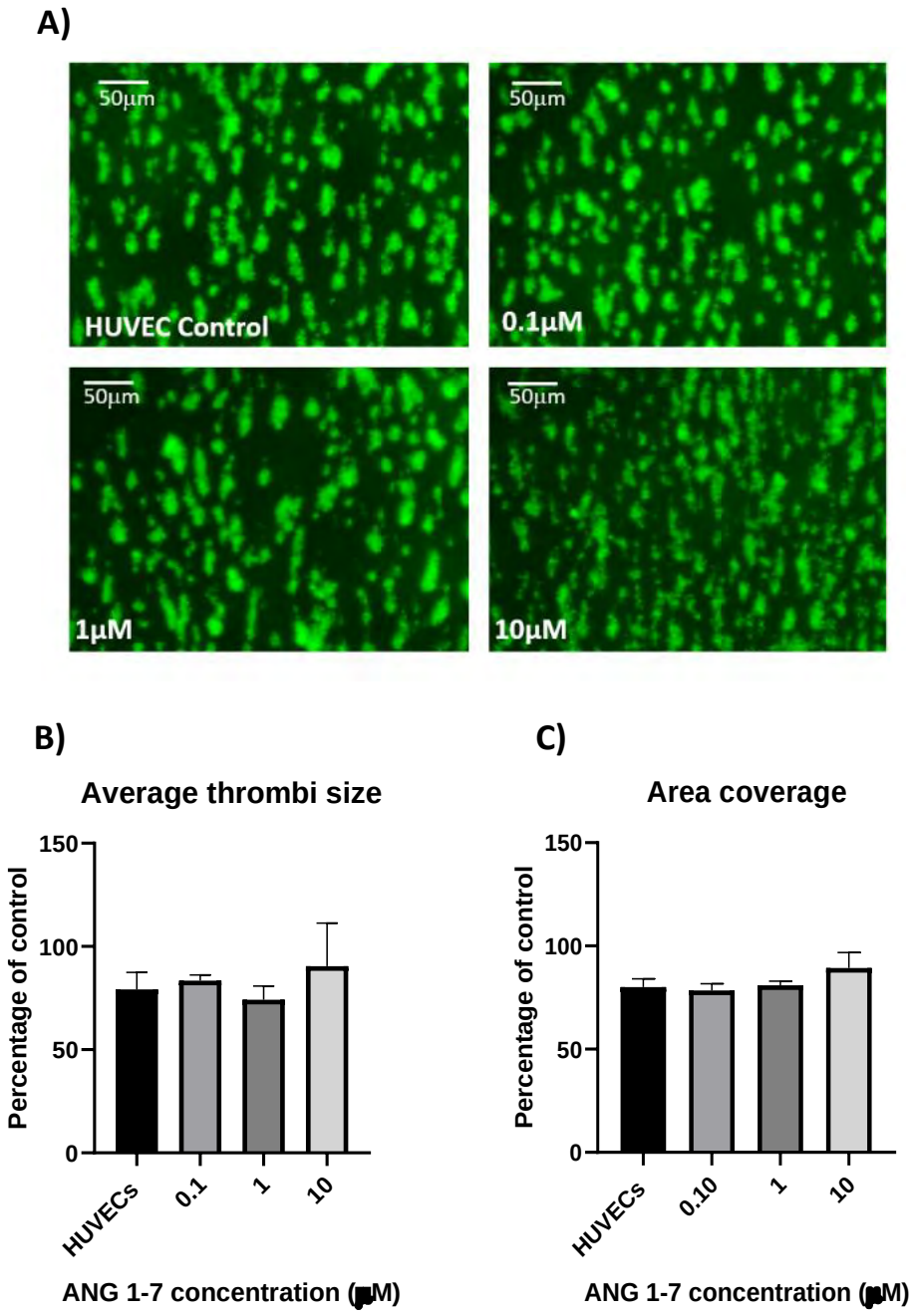


**Figure 5. 8 The presence of ANG 1-7 in our thrombosis model had no significant effect**

Whole blood labelled with $DIOC_6$ was incubated with either vehicle control or ANG 1-7 (0.1-10 µM) prior to perfusion through HUVEC coated chambers, HUVECs were treated with either vehicle control ANG 1-7 (0.1-10 µM) for 30 minutes before blood perfusion. There was no significant difference in average thrombi size (B) or area coverage (C) following any of the treatments. Data represents mean ± SEM; n=3 (each n represents an individual donor, with 5 images taken per condition for analysis).

## 5.4 Discussion

In chapter 3, it was successfully demonstrated that the thrombosis model could be utilised to assess anti-platelet drug efficacy. In addition to the model being a useful tool for analysing the effects of classical anti-platelet therapies, in addition, it was important to highlight how the model could be used to assess potential novel therapeutic targets. The unique setup of the model allows for the assessment of the effects of novel targets on platelets and endothelial cells individually, in addition to in combination, proving a valuable tool for elucidating the exact mechanisms for novel anti-thrombotic effects. The ACE2/ANG1-7/MAS signalling axis has been shown to have anti-thrombotic properties, potentially via the induction of NO both in platelets and endothelial cells (Fang *et al*., 2013; Sampaio *et al*., 2007).

Before assessing the effects of ANG 1-7 stimulation on endothelial cell regulation of thrombus formation, it was first essential to confirm the presence of key components of the signalling axis in HUVECs. As described previously, MAS-1 is the main receptor that ANG 1-7 exerts its anti-thrombotic effects in endothelial cells, it was therefore important to confirm the presence of this receptor. In addition, ACE2 is responsible for the conversion of ANG II into ANG 1-7, therefore it was important to confirm the presence of this important mediator in the signalling axis (Santos *et al*., 2018). ANG 1-7 is often described as having opposing effects to ANG II, therefore it was important to determine if key ANG II receptors, AT1R and AT2R, were present in HUVECs. Western blotting revealed MAS-1, ACE2, AT1R and AT2R were detected in HUVECs. These findings are supported by other studies that have demonstrated the presence of ACE2 and ANG 1-7 in umbilical endothelial cells. *Valdes et al* investigated the distribution of ANG 1-7 and ACE2 in human placentas and demonstrated that both were present in venous and arterial endothelial cells of the umbilical cord (Valdés *et al*., 2006). In addition, a study investigating the expression and role of ANG II receptors in pregnancy induced hypertension the presence of ATR1 and ATR2 mRNA in HUVECs (Takeda-Matsubara *et al*., 2003).

Once the presence of key components in the ACE2/ANG1-7/MAS signalling axis had been confirmed, the next step was to assess the effects of ANG 1-7 stimulation on the expression of endothelial-derived platelet mediators; PTGS1, PTGS2, ENTPD1 and

NOS3. HUVECs were also stimulated with ANG II to assess any changes in the expression of these mediators. Real-time PCR demonstrated no significant changes in any of the mediators following stimulation with ANG II and/or ANG 1-7. A decrease in ENTPD1 was observed with all treatments, this decrease was not statistically significant but further N numbers would improve the power and confidence of the analysis. If ANG 1-7 did indeed decrease ENTPD1 expression it would represent an interesting paradigm with ANG 1-7 potentially having opposing effects on platelet regulation by increasing NO bioavailability (Sampaio *et al*., 2007) but also decreasing ENTPD1 expression.

In order to utilise the model to assess the effects of targeting the ACE2/ANG1-7/MAS signalling axis in endothelial cells and platelets simultaneously, it was important to confirm the expression of ACE2, MAS-2, ATR1 and ATR2 in platelets. Western blotting revealed MAS-1, ACE2, ATR1 and ATR2 were all present in platelets isolated from human whole blood. These findings correlate with other studies that have demonstrated the presence of these receptors in platelets (Fraga-Silva *et al*., 2008; Zhang *et al*., 2020). Having successfully confirmed the presence of key components of the ACE2/ANG1-7/MAS signalling axis the next step was to assess the effect of ANG 1-7 stimulation on platelet activation.

The first assay performed on platelet function was a plate based aggregometry assay (Chan *et al*., 2018) this would allow us to assess the effects of ANG 1-7 stimulation on platelet aggregation. The assay was performed in parallel using two different agonists, collagen and ADP. As described previously, collagen is exposed during vessel wall injury and its binding and activation of platelet GPVI leads to platelet activation and therefore plays key role in the development of a platelet aggregate. Furthermore, ADP is released upon platelet activation and drives further platelet activation and encourages the recruitment of circulating platelets to the growing thrombus, therefore having a key role in the signalling amplification stage of thrombus formation. These two agonists were used in the assay to enable the analysis of the effect of ANG 1-7 on the two different signalling pathways. In addition, collagen is used in the model to mimic the ECM and therefore using collagen in this assay may provide a good predictor for what to expect in the model. The

experiment utilised a range of agonist and ANG 1-7 concentrations and demonstrated no significant changes in platelet aggregation with any concentration of ANG 1-7 used.

It is important to note that the plate-based aggregometry assay is an end-point assay and therefore only gives a snapshot at one point in the aggregation process. There is the potential that ANG 1-7 exerts some effect during the initial stages of platelet activation before being overcome, resulting in aggregate formation. It is not possible to determine this using such an assay and therefore real-time aggregometry was used to assess any effects of ANG 1-7 on platelet aggregation over time. No significant difference in platelet aggregation was observed with any concentration of ANG 1-7. However, despite the lack of statistical significance, the results appear to show a decrease in aggregation in response to ADP, especially at the lowest concentration of 0.1 μM. These results may potentially be underpowered and further N numbers would aid in increasing the power and confidence of these results.

Thrombus formation is a multi-phased process, with initial platelet activation being the first step in the formation of a stable platelet aggregate. Therefore, there was the potential that ANG 1-7 may not inhibit the whole aggregation process but could still be exerting an effect on platelet activation. Flow cytometry was chosen to assess the effects of ANG 1- 7 on platelet activation, this would allow the assessment of any changes in the levels of platelet activation markers following stimulation with ANG 1-7. CD63 was used as it has previously been shown as a marker for platelet activation, with the expression of CD63 increasing on the surface of platelets following granule secretion (Sharda and Flaumenhaft, 2018). Therefore, assessment of changes in CD63 would allow us to determine if ANG 1-7 was having any effects on granule secretion. The PAC-1 antibody detects activation of integrin $\alpha_{IIb}\beta_3$ (Lu and Malinauskas, 2010), utilisation of this antibody would tell us if ANG 1-7 was exerting any effect on this signalling pathway. Platelet activation is associated with an increased surface expression of CD62P (Lu and Malinauskas, 2010) and therefore provides an additional marker of platelet activation. For completeness, annexin V was also used, the use of these four markers of platelet activation enabled the assessment of the effects of ANG 1-7 on platelet activation and could help to

elucidate any potential mechanisms for these effects. The results from the flow cytometry experiments showed no significant changes in any of the markers of platelet activation following treatment with ANG 1-7.

As the thrombosis model uses human whole blood and endothelial cells it enables the assessment of both platelet activity and endothelial cell regulation of thrombus formation simultaneously. As a result, the model was utlised to assess the effects of ANG 1-7 on thrombus formation by incubating both blood and endothelial cells in a range of ANG 1-7 concentrations (0.1-10 µM). This would enable us to determine if the ACE2/ANG1-7/MAS signalling pathway presented a novel anti-thrombotic target. No significant changes in thrombus formation were observed when ANG 1-7 was incubated in whole blood and endothelial cells. This would suggest that ANG 1-7 was not potentiating NO release in the model. Although no significant changes were observed, these results correlate with what was demonstrated previously with established aggregation assays, highlighting how the model can accurately assess thrombus formation, with the added advantage of being able to assess any effects of endothelial cell regulation.

An anti-thrombotic effect with ANG 1-7 has been demonstrated previously in experiments using rat and mouse models. Thrombus weight significantly decreased following infusion of ANG 1-7 at 10 pmol/kg/min (Fraga-Silva *et al*., 2008). The study used a range of concentrations and found that this effect was dose-dependent and that the antithrombotic effect actually decreased at higher concentrations, with the highest concentration of $10^3$ pmol/kg/min having no significant effect on thrombus weight (Fraga-Silva *et al*., 2008). These findings suggested that ANG 1-7 may actually have opposing effects at different concentrations and also highlights that ANG 1-7 may only exert its antithrombotic effect when used in the picomolar range (Fraga-Silva *et al*., 2008). This has been further demonstrated by other studies that report contrasting effects of ANG 1-7 on platelet aggregation. One such study investigating platelet dysfunction on liposaccharide treated Wistar rats reported that 1 mg/kg intravenous infusion of ANG 1-7 had no significant effect on platelet aggregation in response to ADP (Tsai *et al*., 2021). This study used a similar plate based aggregometry assay to assess platelet aggregation in response to ADP in platelet rich

plasma isolated from Wistar rats. It is therefore interesting to note that the study reported similar finding to us in terms of ADP mediated platelet aggregation, it therefore raises the question whether the different effects on platelet aggregation reported with ANG 1-7 are due to concentration choice, assay choice or a combination of multiple factors.

# 6. General Discussion

## 6.1 Project overview

Currently, there is not a gold standard, physiological relevant *in vitro* thrombosis model, despite the emergence of several thrombosis models recently, many are associated with a range of limitations, which need to be overcome in order to achieve an accessible and reproducible thrombosis model. A major limitation associated with emerging models is the lack of endothelial cells and therefore the inability to assess the contribution of the endothelium in thrombus formation. As a result, this project sought to develop a physiologically relevant *in vitro* thrombosis model by combining human endothelial cells with human whole blood to faithfully model atherothrombosis. The development of this model has demonstrated a number of novel findings:

- Endothelial cells can negatively regulate thrombus formation when incorporated into an *in vitro* model
- TNF-alpha stimulation abolishes the anti-platelet effects of endothelial cells
- DAPT efficacy is dependent on endothelial cell function
- Venous and arterial endothelial cells differ in their regulation of thrombus formation

## 6.2 An endothelialised model allows for the assessment of endothelial cell regulation of thrombus formation

Endothelial cells play a key role in the regulation of thrombus formation via the release of several platelet inhibitors, such as NO and prostacyclin. As a result, any model that aims to accurately model thrombosis should incorporate endothelial cells; however, many of the current *in vitro* models are devoid of endothelial cells and those that do incorporate them, suffer from other limitations. In the present study, endothelial cells were successfully incorporated into a thrombosis model and their ability to negatively regulate platelet activity was demonstrated. Several other research

groups have begun to incorporate endothelial cells into their "vessel on a chip" models, interestingly not all of these models include a confluent monolayer of cells (Brouns *et al*., 2020). Brouns *et al* have developed an endothelialised model with Ibidi micro-slides coated with collagen and tissue factor and endothelial cells grown to a density of 40-60% on top of this coating. This model aims to replicate the vessel environment, with exposed collagen and tissue factor surrounded by endothelial cells, allowing for the assessment of the hemostatic control of endothelial cells (Brouns *et al*., 2020). The study found that the presence of endothelial cells in the model led to a delay in coagulation, in addition to a reduction in platelet deposition. These findings correlate with the data presented in this study where a reduction in thrombus size and platelet area coverage was observed when endothelial cells were present in the model, thus contributing to the growing evidence that supports the incorporation of endothelial cells into any model which wishes to faithfully replicate arterial thrombosis.

## 6.3 TNF-alpha stimulation can achieve an activated and dysfunctional phenotype in endothelial cells

The presence of an activated and dysfunctional endothelium is a key component of atherothrombosis, therefore it is essential that this environment is closely replicated when developing an *in vitro* thrombosis model. Western blotting was successfully used to demonstrate the presence of activated endothelial cells in the model, this was confirmed by the increase in cell adhesion molecules (Teasdale *et al*., 2017; Xia *et al*., 1998). Endothelial dysfunction is often described as an imbalance between vasoconstriction and vasodilation, this imbalance is caused by a reduction in the bioavailability of NO (Sun *et al*., 2020). Western blotting and real-time PCR were used to confirm that TNF-alpha stimulation of HUVECs led to a decrease in eNOS expression, suggesting a dysfunctional endothelial cell phenotype was being achieved in the model.

TNF-alpha stimulation has been utilised in several emerging endothelialised *in vitro* models (Jain *et al*., 2016; Lagadec *et al*., 2003; da Costa *et al*., 2007) with varying results being reported in terms of endothelial cell activation and the regulation of

thrombus formation. In one such study, Jain *et al* used a microfluidic device lined with fixed endothelial cells to assess thrombus formation. The study confirmed that TNF-alpha stimulation caused an increase in cell adhesion molecules ICAM-1 and VCAM-1 in a dose dependent manner. The study also demonstrated that this increase in adhesion cell molecules was associated with an increase in platelet adhesion to the surface of the endothelial cells. Although the study supports some aspects of this current study, most notably TNF-alpha increasing cell adhesion molecules and increasing platelet adhesion, the use of fixed endothelial cells is a major limitation of this study. Endothelial cells contribute to platelet regulation via the release of platelet inhibitors such as NO and prostacylin, in addition to the release of platelet activators, such as TXA2. A fixed endothelium would no longer be functioning correctly and releasing these key signalling molecules, in contrast this study has demonstrated that endothelial cells incorporated into a thrombosis model can regulate thrombus formation, potentially through the release of NO. Therefore, the use of living endothelial cells in the model gives it an advantage over a fixed cell model.

As discussed previously, endothelial dysfunction was mimicked in the model via TNF-alpha stimulation of endothelial cells. These results correlate with results reported in a *in vivo* study by Gao *et al* which used type 2 diabetes (T2D) and T2D null for TNF mice to demonstrate the role of TNF-alpha in T2D-induced endothelial cell dysfunction. The study showed that NO mediated vasodilation was greater in the T2D null for TNF mice compared with the T2D control mice, indicating TNF-alpha plays a key role in endothelial cell dysfunction in T2D, potentially by attenuating the activity of NO. These findings support the use of TNF-alpha to achieve endothelial dysfunction in the model by reducing eNOS expression in endothelial cells.

## 6.4 Endothelial dysfunction may impact anti-platelet drug efficacy

DAPT is the standard of care for the secondary prevention of coronary artery disease, combining the cyclooxygenase inhibitor aspirin with a $P2Y_{12}$ antagonist to prevent platelet activation and the generation of platelet signalling amplification (Degrauwe *et al*., 2017; Chan *et al*., 2015). Recent evidence has emerged to suggest a synergistic

relationship between $P2Y_{12}$ blockade and the endothelial-derived mediators, prostacyclin and NO (Armstrong *et al*., 2020; Chan *et al*., 2015). This suggests a patient's response to DAPT will be dependent on their level of $P2Y_{12}$ inhibition, in addition to their levels of NO and prostacyclin (Chan *et al*., 2015). It is therefore possible that endothelial dysfunction could have an impact on a patient's response to DAPT, with a decrease in NO levels potentially leading to a decrease in the effectiveness of DAPT. This issue is further compounded by recent findings that suggest no additive effect on platelet inhibition is observed when aspirin is used in combination with strong $P2Y_{12}$ inhibitors, such as prasugrel and ticagrelor (Leadbetter *et al*., 2011; Warner *et al*., 2016). Furthermore, there is evidence to suggest combining aspirin with these strong $P2Y_{12}$ could actually lead to a reduction in anti-thrombotic efficacy, partially due to aspirin's effect on the endothelial-derived platelet inhibitor, prostacyclin (Warner *et al*., 2010). This study has demonstrated that when TNF-alpha stimulated endothelial cells are incorporated into the model, the therapeutic effects of DAPT on thrombus formation are abolished. It was also previously shown that TNF-alpha stimulation leads to a reduction in eNOS expression, these findings support the link between NO bioavailability and the efficacy of DAPT drugs. Furthermore, these findings suggest that endothelial dysfunction may severely limit the effectiveness of this therapy and should be considered when exploring treatment options. There is a growing call for a more personalised approach to treating cardiovascular disease, with the suggestion that endothelial function tests should be performed in order to ensure that the right drug is given to the correct patient based on their individual vascular health (Matsuzawa *et al*., 2014). The findings reported in this study further highlight the impact of endothelial dysfunction on DAPT efficacy and support the need for assessment of endothelial mediator production in cardiovascular patients prior to initiation of therapy.

## 6.5 Appropriate endothelial cells should be used to answer specific research questions

Despite evidence indicating distinctive heterogeneity between endothelial cells from different vessel bed locations, HUVECs remain the predominant cell type of choice

for many of the current *in vitro* thrombosis models. In this present study, a difference in the expression of key endothelial cell mediators between HUVECs and HCAECs was demonstrated, in addition a significant difference in thrombus regulation between the two cell types was observed. Many of the emerging *in vitro* models utilise HUVECs as the endothelial cell of choice, most likely due to their cost, however the findings from this project suggest this may not provide an accurate predictor of *in vivo* interactions and that tissue specific cells should be used depending on the research group's area of interest. Many reported studies have chosen to optimise alternative aspects of their models while using endothelial cells from the incorrect vessel bed. For example, Costa *et al* have reported a 3D-printed microfluidic model of arterial thrombosis but have chosen to use HUVECs instead of arterial cells in their model setup. The study combined human thoracic computed tomography angiography (CTA) scan images with 3D modelling technology to produce 3D vessel "chips" which accurately replicate the vessel shape observed *in vivo* (Costa *et al*., 2017). HUVECs were then cultured on vessel chips for 48 hours, until a confluent monolayer had formed. Despite this model using the latest 3D printing technology to produce vessel chips that accurately replicate the architecture of arterial vessels, the model is limited by the use of venous cells rather than arterial cells. It was demonstrated in chapter five that HCAECs have a higher expression of NOS3 and PTGS2, in addition to a lower expression of ENTPD1, compared with HUVECs. Furthermore, this study observed a significant difference in thrombus formation between the cell types, therefore it is essential that thrombosis models incorporate the correct cell type for their area of interest, such as using arterial cells for modelling arterial thrombosis, in order to produce a physiologically relevant thrombosis model.

## 6.6 Further investigation into ACE2/ANG1-7/MAS signalling axis as a novel therapeutic target is needed

This study was unable to confirm any effect of ANG 1-7 stimulation on the gene expression of endothelial-derived platelet mediators. In addition, platelet aggregation assays and the utilisation of the thrombosis model demonstrated no significant effects on platelet aggregation or thrombus formation. Despite findings of

this study, the pathway remains an interesting and potentially novel antithrombotic target based on evidence in the literature. There are several reports in the literature of ANG 1-7 stimulating NO release, from both endothelial cells and platelets (Fang *et al*., 2013, Fraga silva *et al*., 2008). As NO is potent inhibitor of platelet activation, it was expected that some effects on thrombus formation would be observed and this would correlate with findings of these other research groups. A non-significant decrease in ADP induced platelet aggregation in response to ANG 1-7 (0.1 µM) was observed at the lowest concentration in the experimental range. Some studies have reported the effects on NO release in the picomolar range (Fraga-Silva *et al*., 2008), therefore future work should assess this concentration range to further assess ACE2/ANG1-7/MAS as an antithrombotic target.

## 6.7 Limitations and future directions

In this present study, a endothelialised *in vitro* thrombosis model that allowed for the assessment of endothelial cell regulation of thrombus formation was successfully developed. Despite demonstrating that the model faithfully mimicked many aspects of human atherothrombosis, in addition to showing the sensitivity of the model to changes to the endothelial cell compartment, the model is not without limitations. Here these limitations will be addressed and ways these can be improved upon in the future to optimise the current model and achieve a physiological relevant model of human atherothrombosis will be explored.

As outlined in the methods in chapter two, the blood collected from healthy donors was collected in citrated vacutainers, the presence of which is needed to prevent the blood from clotting upon collection. The presence of anticoagulants in the whole blood used in the experiments means that the coagulation cascade was being inhibited and therefore was not fully contributing to thrombus formation. As described previously, the coagulation cascade plays an essential role in secondary haemostasis via the production of thrombin and fibrin, the latter of the two being important for strengthening and stabilising the platelet plug (Palta *et al*., 2014). As the model uses citrated blood, it is possible bigger thrombi are unable to form as the lack of fibrin production means many aggregates may be loose and unstable and could potentially experience loss of platelets due to the high shear rate observed in

the model. The focus of this project was endothelial cell regulation of platelets and therefore assessment of this was possible with citrated blood, especially as coagulation was not the focus of this study. However, many groups have utilised the ability to recalcify blood prior to model experiments therefore enabling coagulation to occur. This should be the next step in the optimisation of this model, future research should aim to use recalcified blood which would allow for the assessment of the interactions between platelets, endothelial cells and clotting factors in thrombus formation.

In the development of this thrombosis model, TNF- alpha stimulation was successfully used to achieve endothelial activation. TNF-alpha was chosen as it has been shown to be involved in the progression atherosclerosis, with increases in TNF-alpha levels in the blood and increased TNF-alpha production localised to atherosclerotic plaques being observed in patients with cardiovascular disease (Fatkhullina *et al*., 2016). However, it is important to note that TNF-alpha is not the only proinflammatory cytokine involved in the development of an atherosclerotic plaque (Fatkhulina *et al*., 2016). Interferon gamma (IFN-γ) is produced by $CD4^+$ cells, $CD8^+$ cells and natural killer cells and levels of the cytokine has been shown to be elevated in atherosclerotic plaques (Young *et al*., 2002). IFN-γ has been shown to be play a key role in mediating the uptake of oxidized LDL by macrophages (Wuttge *et al*., 2004). The interleukin class of cytokines has also been shown to contribute to the development of atherosclerosis via several mechanisms, including promoting the infiltration of monocytes into the tunica intima of arterial vessels (Smith *et al*., 2010). The model could be improved by using additional cytokines when stimulating the endothelial cells and that a cocktail of multiple cytokines may aid in accurately replicating an atherothrombotic vessel environment.

It has been well established that upon plaque rupture circulating platelets bind to exposed collagen and become activated; this is initial platelet adhesion and activation is the critical first step in the formation of a stable platelet plug. In addition, of all the different collagen types present in atherosclerotic plaque, type I collagen has been shown to make up around 60% of the plaque content (Katsuda *et al*., 1992). For these reasons, collagen was used in this model to replicate the exposure of ECM

proteins following plaque rupture. Platelet adhesion to collagen in the model, in addition to the formation of platelet aggregates was successfully demonstrated. Although collagen is exposed upon plaque rupture, it is not the only exposed ECM protein nor is it the only ECM protein to promote vessel occlusion upon plaque rupture.

In addition to the presence of collagen in atherosclerotic plaques a number of additional ECM proteins, known as proteoglycans have been identified as contributors to the pathogenesis of atherosclerosis. Proteoglycans have been shown to have a range of functions, including contributing to lipid retention, stabilising collagen and mediating cell-cell and cell-matrix interactions (Nielsen *et al*., 2020). Changes in these proteins have been associated with plaque instability, for example the levels of biglycan and lumican has been shown to be increased in unstable plaques, these findings have led to the suggestion that proteoglycan expression could be utilised as a marker of plaque stability (Hansmeier *et al*., 2018). In addition, a difference in the accumulation of proteoglycans has been reported between plaques susceptible to rupture compared to those susceptible to erosion (Kolodgie et a., 2003). It has yet to be fully establishing what role, if any, these proteins might have in promoting platelet adhesion, activation and clot stabilisation during the formation of a platelet plug. However, the model developed during this project could be further improved by testing a range of different ECM proteins compositions and assessing the effects of these on thrombus formation. This would also allow for the model to be used for the assessment of plaque rupture or plaque erosion, as the correct ECM composition could be incorporated into the model to assess the desired disease state.

Through the comparison of HUVECs with HCAECs, this study was able to demonstrate that endothelial cells from different vessel beds differ in their regulation of thrombus formation. With this knowledge, the model was optimised by determining the HCAECs should be used instead of HUVECs when modelling arterial thrombosis. Despite this optimisation of the endothelial cell compartment, a limitation with this compartment still exists, primarily that the endothelial cells used in the model were cultured under static conditions. It has been previously shown by Noris *et al* that

HUVECs cultured under physiological relevant shear rates release more NO than cells cultured under static conditions (Noris *et al*., 1995). The study demonstrated that, using a cone and plate apparatus, laminar shear stress stimulates NO synthesis in HUVECs, after 1 hour exposure to laminar flow at 8 dyne/cm$^2$ a non-significant increase in NO synthesis was observed. After culturing the cells under this shear stress for six hours a significant increase in NOS was observed compared with static cultured cells. Furthermore, Noris *et al* observed a 100% increase in eNOS mRNA following exposure to shear stress, indicating that culturing HUVECs under laminar shear stress increases eNOS gene expression, resulting in increased NO synthesis. These findings correlated with those reported in other studies, such as Ashpole *et al*, that have cultured HUVECs under physiological shear stress. Ashpole *et al* observed a significant increase in NO production in HUVECs cultured under a shear stress of 10 dyne/cm$^2$ for 24 hours compared with HUVECs cultured at 0.1 dyne/cm$^2$. During this study, it was demonstrated that NO from the endothelial cells incorporated into the model may be responsible for positively regulating thrombus formation. Therefore, a further optimisation of the model would be to culture endothelial cells under physiological relevant shear stress prior to experiments and analyse if any differences in thrombus formation exist when flow cultured cells are incorporated into the model, compared with static cultured cells. This optimisation step could be achieved relatively simply as the manufacturer (Ibidi) of the slides used in the model also make a flow system that is compatible with these slides. Using this commercially available system ensured that the model was still easily accessible and reproducible for other researchers that wish to adopt the model.

## 6.8 Conclusions

In conclusion, this study developed and optimised an *in vitro* thrombosis model that enables the assessment of endothelial cell regulation of thrombus formation. This study has demonstrated that when endothelial cells are incorporated into a thrombosis model they have a significant effect on thrombus formation on collagen. This study identified TNF-alpha as an appropriate stimulus for achieving endothelial dysfunction and activation, enabling it to be used to optimise the model in terms of replicating an atherothrombotic vessel environment. This project also provided

evidence that supports the growing theory that endothelial mediators are key to DAPT efficacy and the impact of endothelial dysfunction on inter-patient variability. Finally, this project demonstrated the difference between HUVECs and HCAECs in terms of their expression of platelet mediators and their ability to regulate thrombus formation. Taken together, the results present in this thesis support the incorporation of endothelial cells into physiological relevant *in vitro* thrombosis models. In addition to highlighting the need for research groups to use endothelial cells from the correct tissue bed to answer their specific research question.

# References


Ajjan, R.A., Standeven, K.F., Khanbhai, M., Phoenix, F., Gersh, K.C., Weisel, J.W., Kearney, M.T., Ariëns, R.A.S., Grant, P.J., 2009. Effects of Aspirin on Clot Structure and Fibrinolysis Using a Novel In Vitro Cellular System. ATVB 29, 712–717. https://doi.org/10.1161/ATVBAHA.109.183707

Al-Zakwani, I., Al-Lawati, J., Alsheikh-Ali, A.A., Almahmeed, W., Rashed, W., Al-Mulla, A., Zubaid, M., 2020. Impact of Dual versus Single Antiplatelet Therapy on Major Cardiovascular Outcomes in Patients with Acute Coronary Syndrome in the Arabian Gulf. Med Princ Pract 29, 181–187. https://doi.org/10.1159/000503438

Ardlie, N.G., McGuiness, J.A., Garrett, J.J., 1985. Effect on human platelets of catecholamines at levels achieved in the circulation. Atherosclerosis 58, 251–259. https://doi.org/10.1016/0021-9150(85)90070-X

Azizi, M., Ménard, J., 2004. Combined Blockade of the Renin-Angiotensin System With Angiotensin-Converting Enzyme Inhibitors and Angiotensin II Type 1 Receptor Antagonists. Circulation 109, 2492–2499. https://doi.org/10.1161/01.CIR.0000131449.94713.AD

Banz, Y., Beldi, G., Wu, Y., Atkinson, B., Usheva, A., Robson, S.C., 2008. CD39 is incorporated into plasma microparticles where it maintains functional properties and impacts endothelial activation: CD39 and Microparticles. British Journal of Haematology 142, 627–637. https://doi.org/10.1111/j.1365-2141.2008.07230.x

Bennett, J.S., 2006. Platelet-Fibrinogen Interactions. Annals of the New York Academy of Sciences 936, 340–354. https://doi.org/10.1111/j.1749-6632.2001.tb03521.x

Bentzon, J.F., Otsuka, F., Virmani, R., Falk, E., 2014. Mechanisms of Plaque Formation and Rupture. Circ Res 114, 1852–1866. https://doi.org/10.1161/CIRCRESAHA.114.302721

Blair, P., Flaumenhaft, R., 2009. Platelet alpha-granules: basic biology and clinical correlates. Blood Rev. 23, 177–189. https://doi.org/10.1016/j.blre.2009.04.001

Bledzka, K., Smyth, S.S., Plow, E.F., 2013. Integrin αIIbβ3: From Discovery to Efficacious Therapeutic Target. Circ Res 112, 1189–1200. https://doi.org/10.1161/CIRCRESAHA.112.300570

Born, G.V., 1962. Aggregation of blood platelets by adenosine diphosphate and its reversal. Nature 194, 927–929. https://doi.org/10.1038/194927b0

Bradford, H.N., Pixley, R.A., Colman, R.W., 2000. Human Factor XII Binding to the Glycoprotein Ib-IX-V Complex Inhibits Thrombin-induced Platelet Aggregation. Journal of Biological Chemistry 275, 22756–22763. https://doi.org/10.1074/jbc.M002591200

Brouns, L.N., Provenzle, I., van Geffen, J., van der Meijden, P.E.J., Heemskerk, J.W.M., 2020. Localized endothelial-based control of platelet aggregation and coagulation under flow: A proof-of-principle vessel-on-a-chip study. Journal of thrombosis and haemostasis. 18, 931-941. https://doi.org/10.1111/jth.14719

Bunting, S., Widmer, R., Lipari, T., Rangell, L., Steinmetz, H., Carver-Moore, K., Moore, M.W., Keller, G.-A., de Sauvage, F.J., 1997. Normal Platelets and Megakaryocytes Are Produced In Vivo in the Absence of Thrombopoietin. Blood 90, 3423–3429. https://doi.org/10.1182/blood.V90.9.3423

Burkhart, J.M., Vaudel, M., Gambaryan, S., Radau, S., Walter, U., Martens, L., Geiger, J., Sickmann, A., Zahedi, R.P., 2012. The first comprehensive and quantitative analysis of human platelet protein composition allows the comparative analysis of structural and functional pathways. Blood 120, e73–e82. https://doi.org/10.1182/blood-2012-04-416594

Bye, A.P., Unsworth, A.J., Gibbins, J.M., 2016. Platelet signaling: a complex interplay between inhibitory and activatory networks. J Thromb Haemost 14, 918–930. https://doi.org/10.1111/jth.13302

Cerrito, E., Lazzaro, M.P., Gaudio, E., Arminio, P., Aloisi, G., 1993. 5HT2-receptors and serotonin release: Their role in human platelet aggregation. Life Sciences 53, 209–215. https://doi.org/10.1016/0024-3205(93)90671-O

Chan, M.V., Armstrong, P.C., Warner, T.D., 2018. 96-well plate-based aggregometry. Platelets 29, 650–655. https://doi.org/10.1080/09537104.2018.1445838

Chan, M.V., Knowles, R.B.M., Lundberg, M.H., Tucker, A.T., Mohamed, N.A., Kirkby, N.S., Armstrong, P.C.J., Mitchell, J.A., Warner, T.D., 2016. P2Y $_{12}$ receptor blockade synergizes strongly with nitric oxide and prostacyclin to inhibit platelet activation: NO and PGI $_{2}$ synergize with P2Y $_{12}$ receptor blockade. Br J Clin Pharmacol 81, 621–633. https://doi.org/10.1111/bcp.12826

Chen, Y.-C., Huang, A.L., Kyaw, T.S., Bobik, A., Peter, K., 2016. Atherosclerotic Plaque Rupture: Identifying the Straw That Breaks the Camel's Back. ATVB 36. https://doi.org/10.1161/ATVBAHA.116.307993

Chistiakov, D.A., Sobenin, I.A., Orekhov, A.N., 2013. Vascular Extracellular Matrix in Atherosclerosis. Cardiology in Review 21, 270–288. https://doi.org/10.1097/CRD.0b013e31828c5ced

Clark, C.B., Zhang, Y., Martin, S.M., Ray Davies, L., Xu, L., Kregel, K.C., Miller, F.J., Buettner, G.R., Kerber, R.E., 2003. The nitric oxide synthase inhibitor NG-nitro-l-arginine decreases defibrillation-induced free radical generation. Resuscitation 57, 101–108. https://doi.org/10.1016/S0300-9572(02)00413-6

Clemetson, K., Clemetson, J., 2007. Collagen Receptors as Potential Targets for Novel Anti-Platelet Agents. CPD 13, 2673–2683. https://doi.org/10.2174/138161207781662894

Coenen, D.M., Mastenbroek, T.G., Cosemans, J.M.E.M., 2017. Platelet interaction with activated endothelium: mechanistic insights from microfluidics. Blood 130, 2819–2828. https://doi.org/10.1182/blood-2017-04-780825

Cramer, E., Savidge, G., Vainchenker, W., Berndt, M., Pidard, D., Caen, J., Masse, J., Breton-Gorius, J., 1990. Alpha-granule pool of glycoprotein IIb-IIIa in normal and pathologic platelets and megakaryocytes. Blood 75, 1220–1227. https://doi.org/10.1182/blood.V75.6.1220.1220

Cramer, E.M., Norol, F., Guichard, J., Breton-Gorius, J., Vainchenker, W., Massé, J.M., Debili, N., 1997. Ultrastructure of platelet formation by human megakaryocytes cultured with the Mpl ligand. Blood 89, 2336–2346.

Danenberg, H.D., Szalai, A.J., Swaminathan, R.V., Peng, L., Chen, Z., Seifert, P., Fay, W.P., Simon, D.I., Edelman, E.R., 2003. Increased thrombosis after arterial injury in human C-reactive protein-transgenic mice. Circulation 108, 512–515. https://doi.org/10.1161/01.CIR.0000085568.13915.1E

Dardik, R., Savion, N., Kaufmann, Y., Varon, D., 1998. Thrombin promotes platelet-mediated melanoma cell adhesion to endothelial cells under flow conditions: role of platelet glycoproteins P-selectin and GPIIb-IIIA. Br. J. Cancer 77, 2069–2075. https://doi.org/10.1038/bjc.1998.349

Davignon, J., Ganz, P., 2004. Role of Endothelial Dysfunction in Atherosclerosis. Circulation 109. https://doi.org/10.1161/01.CIR.0000131515.03336.f8

Day, R.O., Graham, G.G., 2004. The vascular effects of COX-2 selective inhibitors. Aust Prescr 27, 142–145. https://doi.org/10.18773/austprescr.2004.119

Day, S.M., Reeve, J.L., Myers, D.D., Fay, W.P., 2004. Murine thrombosis models. Thromb. Haemost. 92, 486–494.

De Candia, E., 2012. Mechanisms of platelet activation by thrombin: A short history. Thrombosis Research 129, 250–256. https://doi.org/10.1016/j.thromres.2011.11.001

Dela-Paz, N.G., D'Amore, P.A., 2009. Arterial versus venous endothelial cells. Cell and Tissue Research 335, 5–16. https://doi.org/10.1007/s00441-008-0706-5.

de Witt, S.M., Swieringa, F., Cavill, R., Lamers, M.M.E., van Kruchten, R., Mastenbroek, T., Baaten, C., Coort, S., Pugh, N., Schulz, A., Scharrer, I., Jurk, K., Zieger, B., Clemetson, K.J., Farndale, R.W., Heemskerk, J.W.M., Cosemans, J.M.E.M., 2014. Identification of platelet function defects by multi-parameter assessment of thrombus formation. Nature Communications 5, 4257. https://doi.org/10.1038/ncomms5257

Degrauwe, S., Pilgrim, T., Aminian, A., Noble, S., Meier, P., Iglesias, J.F., 2017. Dual antiplatelet therapy for secondary prevention of coronary artery disease. Open Heart 4, e000651. https://doi.org/10.1136/openhrt-2017-000651

DeWitt, D.L., Day, J.S., Sonnenburg, W.K., Smith, W.L., 1983. Concentrations of prostaglandin endoperoxide synthase and prostaglandin I2 synthase in the endothelium and smooth muscle of bovine aorta. J. Clin. Invest. 72, 1882–1888. https://doi.org/10.1172/JCI111151

Dyer, L., Patterson, C., 2010. Development of the Endothelium: An Emphasis on Heterogeneity. Semin Thromb Hemost 36, 227–235. https://doi.org/10.1055/s-0030-1253446

Eltzschig, H.K., Köhler, D., Eckle, T., Kong, T., Robson, S.C., Colgan, S.P., 2009. Central role of Sp1-regulated CD39 in hypoxia/ischemia protection. Blood 113, 224–232. https://doi.org/10.1182/blood-2008-06-165746

Emeis, J., 1995. The Control of tPA and PAI-1 Secretion from the Vessel Wall. Vascular Medicine Review vmr–6, 153–166. https://doi.org/10.1177/1358863X9500600208

Estevez, B., Du, X., 2017. New Concepts and Mechanisms of Platelet Activation Signaling. Physiology 32, 162–177. https://doi.org/10.1152/physiol.00020.2016

Ezumi, Y., Shindoh, K., Tsuji, M., Takayama, H., 1998. Physical and Functional Association of the Src Family Kinases Fyn and Lyn with the Collagen Receptor Glycoprotein VI-Fc Receptor  Chain Complex on Human Platelets 10.

Fabre, J.E., Nguyen, M., Latour, A., Keifer, J.A., Audoly, L.P., Coffman, T.M., Koller, B.H., 1999. Decreased platelet aggregation, increased bleeding time and resistance to thromboembolism in P2Y1-deficient mice. Nat. Med. 5, 1199–1202. https://doi.org/10.1038/13522

Falati, S., Gross, P., Merrill-Skoloff, G., Furie, B.C., Furie, B., 2002. Real-time in vivo imaging of platelets, tissue factor and fibrin during arterial thrombus formation in the mouse. Nat. Med. 8, 1175–1181. https://doi.org/10.1038/nm782

Fang, C., Stavrou, E., Schmaier, A.A., Grobe, N., Morris, M., Chen, A., Nieman, M.T., Adams, G.N., LaRusch, G., Zhou, Y., Bilodeau, M.L., Mahdi, F., Warnock, M., Schmaier, A.H., 2013. Angiotensin 1-7 and Mas decrease thrombosis in Bdkrb2−/− mice by increasing NO and prostacyclin to reduce platelet spreading and glycoprotein VI activation. Blood 121, 3023–3032. https://doi.org/10.1182/blood-2012-09-459156

Farrehi, P.M., Ozaki, C.K., Carmeliet, P., Fay, W.P., 1998. Regulation of arterial thrombolysis by plasminogen activator inhibitor-1 in mice. Circulation 97, 1002–1008. https://doi.org/10.1161/01.cir.97.10.1002

Fatkhullina, A.R., Peshkova, I.O., Koltsova, E.K., 2016. The role of cytokines in the development of atherosclerosis. Biochemistry Moscow 81, 1358–1370. https://doi.org/10.1134/S0006297916110134

Félétou, M., Huang, Y., Vanhoutte, P.M., 2011. Endothelium-mediated control of vascular tone: COX-1 and COX-2 products: COX-1, COX-2 and endothelial dysfunction. British Journal of Pharmacology 164, 894–912. https://doi.org/10.1111/j.1476-5381.2011.01276.x

Flaumenhaft, R., Tanaka, E., Graham, G.J., De Grand, A.M., Laurence, R.G., Hoshino, K., Hajjar, R.J., Frangioni, J.V., 2007. Localization and quantification of platelet-rich thrombi in large blood vessels with near-infrared fluorescence imaging. Circulation 115, 84–93. https://doi.org/10.1161/CIRCULATIONAHA.106.643908

Fontana, P., Berdagué, P., Castelli, C., Nolli, S., Barazer, I., Fabbro-Peray, P., Schved, J.-F., Bounameaux, H., Mach, F., De Moerloose, P., Reny, J.-L., 2010. Clinical predictors of dual aspirin and clopidogrel poor responsiveness in stable cardiovascular patients from the ADRIE study: Predictors of dual antiplatelet poor responsiveness. Journal of Thrombosis and Haemostasis 8, 2614–2623. https://doi.org/10.1111/j.1538-7836.2010.04063.x

Fraga-Silva, R.A., Pinheiro, S.V.B., Gonçalves, A.C.C., Alenina, N., Bader, M., Souza Santos, R.A., 2008. The Antithrombotic Effect of Angiotensin-(1-7) Involves Mas-Mediated NO Release from Platelets. Mol Med 14, 28–35. https://doi.org/10.2119/2007-00073.Fraga-Silva

Fritsma, G.A., 2015. Platelet Structure and Function. American Society for Clinical Laboratory Science 28, 125–131. https://doi.org/10.29074/ascls.28.2.125

Funk, C.D., FitzGerald, G.A., 2007. COX-2 Inhibitors and Cardiovascular Risk 50, 10.

Gachet, C., 2006. Regulation of platelet functions by P2 receptors. Annu. Rev. Pharmacol. Toxicol. 46, 277–300. https://doi.org/10.1146/annurev.pharmtox.46.120604.141207

Gachet, C., 2001. Identification, characterization, and inhibition of the platelet ADP receptors. Int. J. Hematol. 74, 375–381. https://doi.org/10.1007/BF02982079

Gale, A.J., 2011. Current Understanding of Hemostasis. Toxicol Pathol 39, 273–280. https://doi.org/10.1177/0192623310389474

Geddings, J.E., Mackman, N., 2014. Recently Identified Factors that Regulate Hemostasis and Thrombosis. Thromb Haemost 111, 570–574. https://doi.org/10.1160/TH13-10-0812

Gibbins, J.M., 2004. Platelet adhesion signalling and the regulation of thrombus formation. Journal of Cell Science 117, 3415–3425. https://doi.org/10.1242/jcs.01325

Gimbrone, M.A., 2017. Endothelial Cell Dysfunction and the Pathobiology of Atherosclerosis 37.

Gori, A.M., Marcucci, R., Migliorini, A., Valenti, R., Moschi, G., Paniccia, R., Buonamici, P., Gensini, G.F., Vergara, R., Abbate, R., Antoniucci, D., 2008. Incidence and Clinical Impact of Dual Nonresponsiveness to Aspirin and Clopidogrel in Patients With Drug-Eluting Stents. Journal of the American College of Cardiology 52, 734–739. https://doi.org/10.1016/j.jacc.2008.05.032

Hackeng, T.M., Sere, K.M., Tans, G., Rosing, J., 2006. Protein S stimulates inhibition of the tissue factor pathway by tissue factor pathway inhibitor. Proceedings of the National Academy of Sciences 103, 3106–3111. https://doi.org/10.1073/pnas.0504240103

Hadi, H.A., Suwaidi, J.A., 2007. Endothelial dysfunction in diabetes mellitus. Vascular Health and Risk Management 24.

Hamilos, M., Petousis, S., Parthenakis, F., 2018. Interaction between platelets and endothelium: from pathophysiology to new therapeutic options. Cardiovascular Diagnosis and Therapy 8, 13.

Harker, L.A., Roskos, L.K., Marzec, U.M., Carter, R.A., Cherry, J.K., Sundell, B., Cheung, E.N., Terry, D., Sheridan, W., 2000. Effects of megakaryocyte growth and development factor on platelet production, platelet life span, and platelet function in healthy human volunteers. Blood 95, 2514–2522.

Harrison, P., Cramer, E.M., 1993. Platelet alpha-granules. Blood Rev. 7, 52–62. https://doi.org/10.1016/0268-960x(93)90024-x

Helenius, M.H., Vattulainen, S., Orcholski, M., Aho, J., Komulainen, A., Taimen, P., Wang, L., de Jesus Perez, V.A., Koskenvuo, J.W., Alastalo, T.-P., 2015. Suppression of endothelial CD39/ENTPD1 is associated with pulmonary vascular remodeling in pulmonary arterial hypertension. American Journal of Physiology-Lung Cellular and Molecular Physiology 308, L1046–L1057. https://doi.org/10.1152/ajplung.00340.2014

Hellem, A.J., 1960. The adhesiveness of human blood platelets in vitro. Scand. J. Clin. Lab. Invest. 12 Suppl, 1–117.

Henke, P.K., Pearce, C.G., Moaveni, D.M., Moore, A.J., Lynch, E.M., Longo, C., Varma, M., Dewyer, N.A., Deatrick, K.B., Upchurch, G.R., Wakefield, T.W., Hogaboam, C., Kunkel, S.L., 2006. Targeted Deletion of CCR2 Impairs Deep Vein Thombosis Resolution in a Mouse Model. The Journal of Immunology 177, 3388–3397. https://doi.org/10.4049/jimmunol.177.5.3388

Heuberger, D.M., Schuepbach, R.A., 2019. Protease-activated receptors (PARs): mechanisms of action and potential therapeutic modulators in PAR-driven inflammatory diseases. Thrombosis J 17, 4. https://doi.org/10.1186/s12959-019-0194-8

Holinstat, M., 2017. Normal platelet function. Cancer Metastasis Rev 36, 195–198. https://doi.org/10.1007/s10555-017-9677-x

Hollopeter, G., Jantzen, H.-M., Vincent, D., Li, G., England, L., Ramakrishnan, V., Yang, R.-B., Nurden, P., Nurden, A., Julius, D., Conley, P.B., 2001. Identification of the platelet ADP receptor targeted by antithrombotic drugs. Nature 409, 202–207. https://doi.org/10.1038/35051599

Horii, K., Kahn, M.L., Herr, A.B., 2006. Structural basis for platelet collagen responses by the immune-type receptor glycoprotein VI. Blood 108, 936–942. https://doi.org/10.1182/blood-2006-01-010215

Hou, Y., 2015. Platelets in hemostasis and thrombosis: Novel mechanisms of fibrinogen-independent platelet aggregation and fibronectinmediated protein wave of hemostasis. J Biomed Res. https://doi.org/10.7555/JBR.29.20150121

Huang, J., Li, X., Shi, X., Zhu, M., Wang, J., Huang, S., Huang, X., Wang, H., Li, L., Deng, H., Zhou, Y., Mao, J., Long, Z., Ma, Z., Ye, W., Pan, J., Xi, X., Jin, J., 2019. Platelet integrin αIIbβ3: signal transduction, regulation, and its therapeutic targeting. J Hematol Oncol 12, 26. https://doi.org/10.1186/s13045-019-0709-6

Hyman, M.C., Petrovic-Djergovic, D., Visovatti, S.H., Liao, H., Yanamadala, S., Bouïs, D., Su, E.J., Lawrence, D.A., Broekman, M.J., Marcus, A.J., Pinsky, D.J., 2009. Self-regulation of inflammatory cell trafficking in mice by the leukocyte surface apyrase CD39. J. Clin. Invest. 119, 1136–1149. https://doi.org/10.1172/JCI36433

Imseis, H.M., 1997. Tumour Necrosis Factor-a Induces Cyclo-oxygenase-2 Gene Expression in First Trimester Trophoblasts: Suppression by Glucocorticoids and NSAIDs 521–526.

Inoue, O., Suzuki-Inoue, K., Dean, W.L., Frampton, J., Watson, S.P., 2003. Integrin α2β1 mediates outside-in regulation of platelet spreading on collagen through activation of Src kinases and PLCγ2. Journal of Cell Biology 160, 769–780. https://doi.org/10.1083/jcb.200208043

Ishii, H., Salem, H., Bell, C., Laposata, E., Majerus, P., 1986. Thrombomodulin, an endothelial anticoagulant protein, is absent from the human brain. Blood 67, 362–365. https://doi.org/10.1182/blood.V67.2.362.362

Italiano, J.E., Shivdasani, R.A., 2003. Megakaryocytes and beyond: the birth of platelets: *Megakaryocytes and beyond*. Journal of Thrombosis and Haemostasis 1, 1174–1182. https://doi.org/10.1046/j.1538-7836.2003.00290.x

Jackson, S.P., Nesbitt, W.S., Westein, E., 2009. Dynamics of platelet thrombus formation. Journal of Thrombosis and Haemostasis 7, 17–20. https://doi.org/10.1111/j.1538-7836.2009.03401.x

Jin, J., Daniel, J.L., Kunapuli, S.P., 1998. Molecular basis for ADP-induced platelet activation. II. The P2Y1 receptor mediates ADP-induced intracellular calcium mobilization and shape change in platelets. J. Biol. Chem. 273, 2030–2034. https://doi.org/10.1074/jbc.273.4.2030

Jung, S.M., Moroi, M., Soejima, K., Nakagaki, T., Miura, Y., Berndt, M.C., Gardiner, E.E., Howes, J.-M., Pugh, N., Bihan, D., Watson, S.P., Farndale, R.W., 2012. Constitutive Dimerization of Glycoprotein VI (GPVI) in Resting Platelets Is Essential for Binding to Collagen and Activation in Flowing Blood. Journal of Biological Chemistry 287, 30000–30013. https://doi.org/10.1074/jbc.M112.359125

Kahn, M.L., Zheng, Y.-W., Huang, W., Bigornia, V., Zeng, D., Moff, S., Farese, R.V., Tam, C., Coughlin, S.R., 1998. A dual thrombin receptor system for platelet activation. Nature 394, 690–694. https://doi.org/10.1038/29325

Kanthi, Y.M., Sutton, N.R., Pinsky, D.J., 2014. CD39: Interface Between Vascular Thrombosis and Inflammation. Curr Atheroscler Rep 16, 425. https://doi.org/10.1007/s11883-014-0425-1

Kato, K., Kanaji, T., Russell, S., Kunicki, T.J., Furihata, K., Kanaji, S., Marchese, P., Reininger, A., Ruggeri, Z.M., Ware, J., 2003. The contribution of glycoprotein VI to stable platelet adhesion and thrombus formation illustrated by targeted gene deletion. Blood 102, 1701–1707. https://doi.org/10.1182/blood-2003-03-0717

Katsuda, S., Kaji, T., 2003. Atherosclerosis and Extracellular Matrix. J Atheroscler Thromb 10, 267–274. https://doi.org/10.5551/jat.10.267

Kauskot, A., Hoylaerts, M.F., 2012. Platelet Receptors, in: Gresele, P., Born, G.V.R., Patrono, C., Page, C.P. (Eds.), Antiplatelet Agents, Handbook of Experimental Pharmacology. Springer Berlin Heidelberg, Berlin, Heidelberg, pp. 23–57. https://doi.org/10.1007/978-3-642-29423-5_2

Kim, S., Kunapuli, S.P., 2011. P2Y12 receptor in platelet activation. Platelets 22, 54–58. https://doi.org/10.3109/09537104.2010.497231

Kirkby, N.S., Lundberg, M.H., Chan, M.V., Vojnovic, I., Solomon, A.B., Emerson, M., Mitchell, J.A., Warner, T.D., 2013. Blockade of the purinergic P2Y $_{12}$ receptor greatly increases the platelet inhibitory actions of nitric oxide. Proc. Natl. Acad. Sci. U.S.A. 110, 15782–15787. https://doi.org/10.1073/pnas.1218880110

Kunapuli, S.P., Ding, Z., Dorsam, R.T., Kim, S., Murugappan, S., Quinton, T.M., 2003. ADP receptors--targets for developing antithrombotic agents. Curr. Pharm. Des. 9, 2303–2316. https://doi.org/10.2174/1381612033453947

Kuriakose, J., Montezano, A.C., Touyz, R.M., 2021. ACE2/Ang-(1-7)/Mas1 axis and the vascular system: vasoprotection to COVID-19-associated vascular disease. Clinical Science 135, 387–407. https://doi.org/10.1042/CS20200480

Kurz, K.D., Main, B.W., Sandusky, G.E., 1990. Rat model of arterial thrombosis induced by ferric chloride. Thromb. Res. 60, 269–280. https://doi.org/10.1016/0049-3848(90)90106-m

Lee, J., Song, K.H., Kim, T., Doh, J., 2018. Endothelial Cell Focal Adhesion Regulates Transendothelial Migration and Subendothelial Crawling of T Cells. Front. Immunol. 9, 48. https://doi.org/10.3389/fimmu.2018.00048

Li, Z., Delaney, M.K., O'Brien, K.A., Du, X., 2010. Signaling During Platelet Adhesion and Activation. ATVB 30, 2341–2349. https://doi.org/10.1161/ATVBAHA.110.207522

Lin, C.-C., Hsiao, L.-D., Chien, C.-S., Lee, C.-W., Hsieh, J.-T., Yang, C.-M., 2004. Tumor necrosis factor-α-induced cyclooxygenase-2 expression in human tracheal smooth muscle cells: involvement of p42/p44 and p38 mitogen-activated protein kinases and nuclear factor-κB. Cellular Signalling 16, 597–607. https://doi.org/10.1016/j.cellsig.2003.10.002

Lindner, V., Fingerle, J., Reidy, M.A., 1993. Mouse model of arterial injury. Circ. Res. 73, 792–796. https://doi.org/10.1161/01.res.73.5.792

Lu, Q., Malinauskas, R.A., 2010. Comparison of Two Platelet Activation Markers Using Flow Cytometry After In Vitro Shear Stress Exposure of Whole Human Blood: COMPARISON OF TWO PLATELET ACTIVATION MARKERS USING FLOW CYTOMETRY. Artificial Organs no-no. https://doi.org/10.1111/j.1525-1594.2010.01051.x

Luo, W., Liu, B., Zhou, Y., 2016. The endothelial cyclooxygenase pathway: Insights from mouse arteries. European Journal of Pharmacology 780, 148–158. https://doi.org/10.1016/j.ejphar.2016.03.043

Ma, T.K., Kam, K.K., Yan, B.P., Lam, Y.-Y., 2010. Renin-angiotensin-aldosterone system blockade for cardiovascular diseases: current status: RAAS blockade. British Journal of Pharmacology 160, 1273–1292. https://doi.org/10.1111/j.1476-5381.2010.00750.x

Machlus, K.R., Italiano, J.E., 2013. The incredible journey: From megakaryocyte development to platelet formation. Journal of Cell Biology 201, 785–796. https://doi.org/10.1083/jcb.201304054

Maffrand, J.P., Bernat, A., Delebassée, D., Defreyn, G., Cazenave, J.P., Gordon, J.L., 1988. ADP plays a key role in thrombogenesis in rats. Thromb. Haemost. 59, 225–230.

Maliszewski, C.R., Delespesse, G.J., Schoenborn, M.A., Fanslow, W.C., Nakajima, T., Baker, E., Poindexter, K., Birks, C., n.d. The CD39 lymphoid cell activation antigen. Molecular cloning and structural characterization. 11.

Martin, J.F., Trowbridge, E.A., Salmon, G.L., Slater, D.N., 1982. The relationship between platelet and megakaryocyte volumes. Thromb. Res. 28, 447–459. https://doi.org/10.1016/0049-3848(82)90162-1

Massberg, S., Brand, K., Grüner, S., Page, S., Müller, E., Müller, I., Bergmeier, W., Richter, T., Lorenz, M., Konrad, I., Nieswandt, B., Gawaz, M., 2002. A Critical Role of Platelet Adhesion in the Initiation of Atherosclerotic Lesion Formation. Journal of Experimental Medicine 196, 887–896. https://doi.org/10.1084/jem.20012044

Mayer, B., Schmid, M., Klatt, P., Schmidt, K., 1993. Reversible inactivation of endothelial nitric oxide synthase by $N^{G}$-nitro-L-arginine. FEBS Letters 333, 203–206. https://doi.org/10.1016/0014-5793(93)80405-J

McNicol, A., Israels, S.J., 1999. Platelet Dense Granules: Structure, Function and Implications for Haemostasis. Thrombosis Research 95, 1–18. https://doi.org/10.1016/S0049-3848(99)00015-8

Mellion, B., Ignarro, L., Ohlstein, E., Pontecorvo, E., Hyman, A., Kadowitz, P., 1981. Evidence for the inhibitory role of guanosine 3', 5'-monophosphate in ADP-induced human platelet aggregation in the presence of nitric oxide and related vasodilators. Blood 57, 946–955. https://doi.org/10.1182/blood.V57.5.946.946

Mendoza-Torres, E., Oyarzún, A., Mondaca-Ruff, D., Azocar, A., Castro, P.F., Jalil, J.E., Chiong, M., Lavandero, S., Ocaranza, M.P., 2015. ACE2 and vasoactive peptides: novel players in cardiovascular/renal remodeling and hypertension. Therapeutic Advances in Cardiovascular Disease 9, 217–237. https://doi.org/10.1177/1753944715597623

Miura, Y., Takahashi, T., Jung, S.M., Moroi, M., 2002. Analysis of the Interaction of Platelet Collagen Receptor Glycoprotein VI (GPVI) with Collagen. Journal of Biological Chemistry 277, 46197–46204. https://doi.org/10.1074/jbc.M204029200

Moroi, M., Jung, S., Shinmyozu, K., Tomiyama, Y., Ordinas, A., Diaz-Ricart, M., 1996. Analysis of platelet adhesion to a collagen-coated surface under flow conditions: the involvement of glycoprotein VI in the platelet adhesion. Blood 88, 2081–2092. https://doi.org/10.1182/blood.V88.6.2081.bloodjournal8862081

Moroi, M., Jung, S.M., Okuma, M., Shinmyozu, K., 1989. A patient with platelets deficient in glycoprotein VI that lack both collagen-induced aggregation and adhesion. J. Clin. Invest. 84, 1440–1445. https://doi.org/10.1172/JCI114318

Nayer, A., Asif, A., 2013. Idiopathic membranous nephropathy and anti-phospholipase A2 receptor antibodies. Journal of Nephropathology 2, 214–216.

Obergfell, A., Eto, K., Mocsai, A., Buensuceso, C., Moores, S.L., Brugge, J.S., Lowell, C.A., Shattil, S.J., 2002. Coordinate interactions of Csk, Src, and Syk kinases with αIIbβ3 initiate integrin signaling to the cytoskeleton. Journal of Cell Biology 157, 265–275. https://doi.org/10.1083/jcb.200112113

Offermanns, S., Laugwitz, K.L., Spicher, K., Schultz, G., 1994. G proteins of the G12 family are activated via thromboxane A2 and thrombin receptors in human platelets. Proceedings of the National Academy of Sciences 91, 504–508. https://doi.org/10.1073/pnas.91.2.504

Orosz, Z., Csiszar, A., Labinskyy, N., Smith, K., Kaminski, P.M., Ferdinandy, P., Wolin, M.S., Rivera, A., Ungvari, Z., 2007. Cigarette smoke-induced proinflammatory alterations in the endothelial phenotype: role of NAD(P)H oxidase activation 292, 10.

Palta, S., Saroa, R., Palta, A., 2014. Overview of the coagulation system. Indian J Anaesth 58, 515–523. https://doi.org/10.4103/0019-5049.144643

Pasquet, J.-M., Gross, B., Quek, L., Asazuma, N., Zhang, W., Sommers, C.L., Schweighoffer, E., Tybulewicz, V., Judd, B., Lee, J.R., Koretzky, G., Love, P.E., Samelson, L.E., Watson, S.P., 1999. LAT Is Required for Tyrosine Phosphorylation of Phospholipase C□2 and Platelet Activation by the Collagen Receptor GPVI. MOL. CELL. BIOL. 19, 9.

Paul, B.Z.S., Jin, J., Kunapuli, S.P., 1999. Molecular Mechanism of Thromboxane A2-induced Platelet Aggregation. Journal of Biological Chemistry 274, 29108–29114. https://doi.org/10.1074/jbc.274.41.29108

Petrich, B.G., Marchese, P., Ruggeri, Z.M., Spiess, S., Weichert, R.A.M., Ye, F., Tiedt, R., Skoda, R.C., Monkley, S.J., Critchley, D.R., Ginsberg, M.H., 2007. Talin is required for integrin-mediated platelet function in hemostasis and thrombosis. Journal of Experimental Medicine 204, 3103–3111. https://doi.org/10.1084/jem.20071800

Peyvandi, F., Garagiola, I., Baronciani, L., 2011. Role of von Willebrand factor in the haemostasis. Blood Transfusion s3–s8. https://doi.org/10.2450/2011.002S

Pinsky, D.J., Broekman, M.J., Peschon, J.J., Stocking, K.L., Fujita, T., Ramasamy, R., Connolly, E.S., Huang, J., Kiss, S., Zhang, Y., Choudhri, T.F., McTaggart, R.A., Liao, H., Drosopoulos, J.H.F., Price, V.L., Marcus, A.J., Maliszewski, C.R., 2002. Elucidation of the thromboregulatory role of CD39/ectoapyrase in the ischemic brain. J. Clin. Invest. 109, 1031–1040. https://doi.org/10.1172/JCI0210649

Puri, R.N., Colman, R.W., 1997. ADP-induced platelet activation. Crit. Rev. Biochem. Mol. Biol. 32, 437–502. https://doi.org/10.3109/10409239709082000

Quek, L.S., Pasquet, J.-M., Hers, I., Cornall, R., Knight, G., Barnes, M., Hibbs, M.L., Dunn, A.R., Lowell, C.A., Watson, S.P., 2000. Fyn and Lyn phosphorylate the Fc receptor γ chain downstream of glycoprotein VI in murine platelets, and Lyn regulates a novel feedback pathway. Blood 96, 4246–4253. https://doi.org/10.1182/blood.V96.13.4246

Ricciotti, E., FitzGerald, G.A., 2011. Prostaglandins and Inflammation. ATVB 31, 986–1000. https://doi.org/10.1161/ATVBAHA.110.207449

Ricciotti, E., Yu, Y., Grosser, T., FitzGerald, G.A., 2013. COX-2, the dominant source of prostacyclin. Proc. Natl. Acad. Sci. U.S.A. 110. https://doi.org/10.1073/pnas.1219073110

Rice, G.I., Thomas, D.A., Grant, P.J., Turner, A.J., Hooper, N.M., 2004. Evaluation of angiotensin-converting enzyme (ACE), its homologue ACE2 and neprilysin in angiotensin peptide metabolism. Biochemical Journal 383, 45–51. https://doi.org/10.1042/BJ20040634

Richardson, J.L., Shivdasani, R.A., Boers, C., Hartwig, J.H., Italiano, J.E., 2005. Mechanisms of organelle transport and capture along proplatelets during platelet production. Blood 106, 4066–4075. https://doi.org/10.1182/blood-2005-06-2206

Rijken, D.C., Lijnen, H.R., 2009. New insights into the molecular mechanisms of the fibrinolytic system. Journal of Thrombosis and Haemostasis 7, 4–13. https://doi.org/10.1111/j.1538-7836.2008.03220.x

Roque, M., Fallon, J.T., Badimon, J.J., Zhang, W.X., Taubman, M.B., Reis, E.D., 2000. Mouse model of femoral artery denudation injury associated with the rapid accumulation of adhesion molecules on the luminal surface and recruitment of neutrophils. Arterioscler. Thromb. Vasc. Biol. 20, 335–342. https://doi.org/10.1161/01.atv.20.2.335

Rouzer, C.A., Marnett, L.J., 2009. Cyclooxygenases: structural and functional insights. Journal of Lipid Research 50, S29–S34. https://doi.org/10.1194/jlr.R800042-JLR200

Sampaio, W.O., Souza dos Santos, R.A., Faria-Silva, R., da Mata Machado, L.T., Schiffrin, E.L., Touyz, R.M., 2007. Angiotensin-(1-7) Through Receptor Mas Mediates Endothelial Nitric

Oxide Synthase Activation via Akt-Dependent Pathways. Hypertension 49, 185–192. https://doi.org/10.1161/01.HYP.0000251865.35728.2f

Sangkuhl, K., Shuldiner, A.R., Klein, T.E., Altman, R.B., 2011. Platelet aggregation pathway. Pharmacogenetics and Genomics 21, 516–521. https://doi.org/10.1097/FPC.0b013e3283406323

Santoro, S.A., Staatz, W.D., Baranski, K.J., 1991. Distinct determinants on collagen support a2,1 integrin-mediated platelet adhesion and platelet activation. CELL REGULATION 2, 9.

Santos, R.A.S., Oudit, G.Y., Verano-Braga, T., Canta, G., Steckelings, U.M., Bader, M., 2019. The renin-angiotensin system: going beyond the classical paradigms. American Journal of Physiology-Heart and Circulatory Physiology 316, H958–H970. https://doi.org/10.1152/ajpheart.00723.2018

Santos, R.A.S., Sampaio, W.O., Alzamora, A.C., Motta-Santos, D., Alenina, N., Bader, M., Campagnole-Santos, M.J., 2018. The ACE2/Angiotensin-(1–7)/MAS Axis of the Renin-Angiotensin System: Focus on Angiotensin-(1–7). Physiological Reviews 98, 505–553. https://doi.org/10.1152/physrev.00023.2016

Schlachterman, A., Schuettrumpf, J., Liu, J.-H., Furlan Freguia, C., Freguia, C.F., Toso, R., Poncz, M., Camire, R.M., Arruda, V.R., 2005. Factor V Leiden improves in vivo hemostasis in murine hemophilia models. J. Thromb. Haemost. 3, 2730–2737. https://doi.org/10.1111/j.1538-7836.2005.01639.x

Selvadurai, M.V., Hamilton, J.R., 2018. Structure and function of the open canalicular system – the platelet's specialized internal membrane network. Platelets 29, 319–325. https://doi.org/10.1080/09537104.2018.1431388

Sharda, A., Flaumenhaft, R., 2018. The life cycle of platelet granules. F1000Res 7, 236. https://doi.org/10.12688/f1000research.13283.1

Siljander, P.R.-M., Hamaia, S., Peachey, A.R., Slatter, D.A., Smethurst, P.A., Ouwehand, W.H., Knight, C.G., Farndale, R.W., 2004. Integrin Activation State Determines Selectivity for Novel Recognition Sites in Fibrillar Collagens. Journal of Biological Chemistry 279, 47763–47772. https://doi.org/10.1074/jbc.M404685200

Smyth, E.M., 2010a. Thromboxane and the thromboxane receptor in cardiovascular disease. Clinical Lipidology 5, 209–219. https://doi.org/10.2217/clp.10.11

Smyth, E.M., 2010b. Thromboxane and the thromboxane receptor in cardiovascular disease. Clinical Lipidology 5, 209–219. https://doi.org/10.2217/clp.10.11

Smyth, S.S., Reis, E.D., Väänänen, H., Zhang, W., Coller, B.S., 2001. Variable protection of beta 3-integrin--deficient mice from thrombosis initiated by different mechanisms. Blood 98, 1055–1062. https://doi.org/10.1182/blood.v98.4.1055

Stockschlaeder, M., Schneppenheim, R., Budde, U., 2014. Update on von Willebrand factor multimers: focus on high-molecular-weight multimers and their role in hemostasis. Blood Coagulation & Fibrinolysis 25, 206–216. https://doi.org/10.1097/MBC.0000000000000065

Stroka, K.M., Vaitkus, J.A., Aranda-Espinoza, H., 2012. Endothelial cells undergo morphological, biomechanical, and dynamic changes in response to tumor necrosis factor-α. Eur Biophys J 41, 939–947. https://doi.org/10.1007/s00249-012-0851-3

Takeda-Matsubara, Y., Matsubara, K., Ochi, H., Ito, M., Iwai, M., Horiuchi, M., n.d. Expression of Endothelial Angiotensin II Receptor mRNA in Pregnancy-Induced Hypertension 16, 7.

Tanahashi, N., Fukuuchi, Y., Tomita, M., Tomita, Y., Inoue, K., Satoh, H., Abe, T., 2001. Adhesion of adenosine diphosphate-activated platelets to human brain microvascular endothelial cells under flow in vitro is mediated via GPIIb/IIIa. Neurosci. Lett. 301, 33–36. https://doi.org/10.1016/s0304-3940(01)01608-1

Tang, E.H.C., Vanhoutte, P.M., 2008. Gene expression changes of prostanoid synthases in endothelial cells and prostanoid receptors in vascular smooth muscle cells caused by aging and hypertension. Physiological Genomics 32, 409–418. https://doi.org/10.1152/physiolgenomics.00136.2007

Teasdale, J.E., Hazell, G.G.J., Peachey, A.M.G., Sala-Newby, G.B., Hindmarch, C.C.T., McKay, T.R., Bond, M., Newby, A.C., White, S.J., 2017. Cigarette smoke extract profoundly suppresses TNFα-mediated proinflammatory gene expression through upregulation of ATF3 in human coronary artery endothelial cells. Sci Rep 7, 39945. https://doi.org/10.1038/srep39945

Thon, J.N., Montalvo, A., Patel-Hett, S., Devine, M.T., Richardson, J.L., Ehrlicher, A., Larson, M.K., Hoffmeister, K., Hartwig, J.H., Italiano, J.E., 2010. Cytoskeletal mechanics of proplatelet maturation and platelet release. Journal of Cell Biology 191, 861–874. https://doi.org/10.1083/jcb.201006102

Thondapu, V., Mamon, C., Poon, E.K.W., Kurihara, O., Kim, H.O., Russo, M., Araki, M., Shinohara, H., Yamamoto, E., Dijkstra, J., Tacey, M., Lee, H., Ooi, A., Barlis, P., Jang, I.-K., 2021. High spatial endothelial shear stress gradient independently predicts site of acute coronary plaque rupture and erosion. Cardiovascular Research 117, 1974–1985. https://doi.org/10.1093/cvr/cvaa251

Tricot, O., Mallat, Z., Heymes, C., Belmin, J., Lesèche, G., Tedgui, A., 2000. Relation Between Endothelial Cell Apoptosis and Blood Flow Direction in Human Atherosclerotic Plaques. Circulation 101, 2450–2453. https://doi.org/10.1161/01.CIR.101.21.2450

Tsai, H.-J., Shih, C.-C., Chang, K.-Y., Liao, M.-H., Liaw, W.-J., Wu, C.-C., Tsao, C.-M., 2021. Angiotensin-(1–7) treatment blocks lipopolysaccharide-induced organ damage, platelet dysfunction, and IL-6 and nitric oxide production in rats. Sci Rep 11, 610. https://doi.org/10.1038/s41598-020-79902-x

Tulasne, D., Judd, B.A., Johansen, M., Asazuma, N., Best, D., Brown, E.J., Kahn, M., Koretzky, G.A., Watson, S.P., 2001. C-terminal peptide of thrombospondin-1 induces platelet aggregation through the Fc receptor γ-chain–associated signaling pathway and by agglutination. Blood 98, 3346–3352. https://doi.org/10.1182/blood.V98.12.3346

Valdés, G., Neves, L.A.A., Anton, L., Corthorn, J., Chacón, C., Germain, A.M., Merrill, D.C., Ferrario, C.M., Sarao, R., Penninger, J., Brosnihan, K.B., 2006. Distribution of Angiotensin-(1-7) and ACE2 in Human Placentas of Normal and Pathological Pregnancies. Placenta 27, 200–207. https://doi.org/10.1016/j.placenta.2005.02.015

van Hinsbergh, V.W.M., 2012. Endothelium—role in regulation of coagulation and inflammation. Semin Immunopathol 34, 93–106. https://doi.org/10.1007/s00281-011-0285-5

van Hinsbergh, V.W.M., 2001. The endothelium: vascular control of haemostasis. European Journal of Obstetrics & Gynecology and Reproductive Biology, Proceedings of the Third Symposium of the Wim Schellekens Foundation "Thrombophilia and Reproduction" 95, 198–201. https://doi.org/10.1016/S0301-2115(00)00490-5

Vergallo, R., Papafaklis, M.I., D'Amario, D., Michalis, L.K., Crea, F., Porto, I., 2019. Coronary plaque erosion developing in an area of high endothelial shear stress: insights from serial optical coherence tomography imaging. Coronary Artery Disease 30, 74–75. https://doi.org/10.1097/MCA.0000000000000673

Wang, G., Coleman, C.G., Glass, M.J., Zhou, P., Yu, Q., Park, L., Anrather, J., Pickel, V.M., Iadecola, C., 2012. Angiotensin II type 2 receptor-coupled nitric oxide production modulates free radical availability and voltage-gated $Ca^{2+}$ currents in NTS neurons. American Journal of Physiology-Regulatory, Integrative and Comparative Physiology 302, R1076–R1083. https://doi.org/10.1152/ajpregu.00571.2011

Wang, X., Xu, L., 2005. An optimized murine model of ferric chloride-induced arterial thrombosis for thrombosis research. Thromb. Res. 115, 95–100. https://doi.org/10.1016/j.thromres.2004.07.009

Watanabe, D., Hashimoto, S., Ishiai, M., Matsushita, M., Baba, Y., Kishimoto, T., Kurosaki, T., Tsukada, S., 2001. Four Tyrosine Residues in Phospholipase C-γ2, Identified as Btk-dependent Phosphorylation Sites, Are Required for B Cell Antigen Receptor-coupled Calcium Signaling. Journal of Biological Chemistry 276, 38595–38601. https://doi.org/10.1074/jbc.M103675200

Westrick, R.J., Winn, M.E., Eitzman, D.T., 2007. Murine models of vascular thrombosis (Eitzman series). Arterioscler. Thromb. Vasc. Biol. 27, 2079–2093. https://doi.org/10.1161/ATVBAHA.107.142810

White, S.J., Newby, A.C., Johnson, T.W., 2016. Endothelial erosion of plaques as a substrate for coronary thrombosis. Thromb Haemost 115, 509–519. https://doi.org/10.1160/th15-09-0765

Whiteheart, S.W., 2017. Fueling platelets: Where does the glucose come from? Arterioscler Thromb Vasc Biol 37, 1592–1594. https://doi.org/10.1161/ATVBAHA.117.309841

Wilson, S.J., Newby, D.E., Dawson, D., Irving, J., Berry, C., 2017. Duration of dual antiplatelet therapy in acute coronary syndrome. Heart 103, 573–580. https://doi.org/10.1136/heartjnl-2016-309871

Wonerow, P., Obergfell, A., Wilde, J.I., Bobe, R., Asazuma, N., Brdička, T., Leo, A., Schraven, B., Hořejší, V., Shattil, S.J., Watson, S.P., 2002. Differential role of glycolipid-enriched membrane domains in glycoprotein VI- and integrin-mediated phospholipase Cγ2 regulation in platelets. Biochemical Journal 364, 755–765. https://doi.org/10.1042/bj20020128

Xia, P., Gamble, J.R., Rye, K.-A., Wang, L., Hii, C.S.T., Cockerill, P., Khew-Goodall, Y., Bert, A.G., Barter, P.J., Vadas, M.A., 1998. Tumor necrosis factor-␣ induces adhesion molecule expression through the sphingosine kinase pathway. Cell Biology 6.

Yau, J.W., Teoh, H., Verma, S., 2015. Endothelial cell control of thrombosis. BMC Cardiovasc Disord 15, 130. https://doi.org/10.1186/s12872-015-0124-z

Zhang, Si, Liu, Y., Wang, X., Yang, L., Li, H., Wang, Y., Liu, M., Zhao, X., Xie, Y., Yang, Y., Zhang, Shenghui, Fan, Z., Dong, J., Yuan, Z., Ding, Z., Zhang, Y., Hu, L., 2020. SARS-CoV-2 binds platelet ACE2 to enhance thrombosis in COVID-19. J Hematol Oncol 13, 120. https://doi.org/10.1186/s13045-020-00954-7